IN THE UNITED STATES PATENT AND TRADEMARK OFFICE

Applicant	: Hubert Köster, Ph.D. *et al.*	Art Unit	: 1639
Serial No.	: 10/760,085	Examiner	: Sue Xu Liu
Filed	: January 16, 2004	Conf. No.	: 8019
Cust. No.	: 77202		

Title : CAPTURE COMPOUNDS, COLLECTIONS THEREOF AND METHODS FOR ANALYZING THE PROTEOME AND COMPLEX COMPOSITIONS

Commissioner for Patents
P.O. Box 1450
Alexandria, VA 22313-1450

DECLARATION PURSUANT TO 37 C.F.R. §1.132

Sir:

I, **HUBERT KÖSTER**, declare as follows:

1. Qualifications

a. I obtained my Vordiplom (equivalent to a Bachelors) in Chemistry in 1963 and my Diplomchemiker (equivalent to a Masters) in Chemistry in 1966, both from the University of Hamburg, in Hamburg, Germany. In 1968, I obtained my Doctorate from the Technical University in Braunschweig, Germany based on work performed at the Max-Planck-Institute in Göttingen, Germany. I later became an Assistant Professor at the University of Hamburg in 1969, and became a tenured Professor in 1982 for Organic Chemistry and Biochemistry. I initiated the formation of Germany's first biotech company in 1981, Biosyntech, and have founded or co-founded a total of four biotech companies, primarily around my own inventions: Biosyntech in Hamburg, Germany, Milligen/Biosearch, Bedford/Burlington, MA, Sequenom, San Diego, CA/Hamburg and HK Pharmaceuticals, Inc. in San Diego, CA. At Biosyntech I was Chairman of the Scientific Advisory Board and Chief Technical Officer, at Milligen/Biosearch Vice President Science & Technology; at Sequenom I held the position first of Chief Scientific Officer and Chairman of the Scientific Advisory Board and later President and Chief Executive Officer and director of the Board. At HK Pharmaceuticals I was Chairman, president and CEO and director of the Board. I am currently the Managing Director of caprotec GmbH in Berlin, Germany, which succeeded HK Pharmaceuticals, Inc..

b. At Biosyntech I developed DNA Synthesizers and invented what today is state-of-the-art in DNA synthesis chemistry (inorganic polymeric supports and beta-cyanoethylphosphoamidites), at Milligen/Biosearch I was responsible for the development of systems for chemical synthesis of DNA and peptides as well as protein sequencing and DNA sequencing. At Sequenom we developed high throughput and highly accurate systems for

genotyping (SNP analysis) and allelotyping based on my inventions using mass spectrometry and at HK Pharmaceuticals/caprotec technologies for the analysis of complex protein mixtures (proteome analysis). I have about 120 scientific publications and I am author/inventor in more than 60 issued patents.

2. I am a joint inventor of the technology on which the above-captioned application is based, and I have reviewed the Office Action, mailed on July 28, 2009. The application describes and the claims are directed to methods, which are among those that caprotec has commercialized under the name Capture Compound Mass Spectrometry (CCMS), for identifying and studying small molecule-protein interactions.

3. As described in the response to the Office Action provided herewith, the claims are directed to methods for identifying targeted and non-targeted protein molecules with which small molecules, such as drugs, interact. This is achieved by providing a capture compound that contains a capture function, particularly an activatable group that forms covalent bonds with amino acid side chains (designated X), and that presents the small molecule (designated Y), such as the drug, a function for immobilization or sorting (designated Q). X, Y and Q are presented on a core, designated Z. As described in the application, the capture compounds can include additional components, such as a solubility function to increase or alter solubility as desired.

Capture compounds, including capture compounds whose capture function is activatable, for covalently capturing biomolecules are known (see, *e.g.*, the response with which this Declaration is provided). They, however, have not heretofore been used to present a small molecule whose interactions are to be assess in methods as claimed in this application. This application employs the capture compounds to present the small molecule (Y), such as a drug) in order to assess its interactions. Known capture compounds (with X, Z and Q groups) can be modified to present a drug, as described in the application, for use in this method. In addition, capture compounds for use in the method can be prepared as described in detail in the application.

4. To help appreciate the methods claimed in this application, a study, done under my direction at my company caprotec, is described below. This study has been published as (Fischer *et al.* Toxicol Sci. 2010 Jan;113(1):243-53. Epub 2009 Sep 26). This study provides a practical application of the claimed methods, which should aid in appreciating the methods and their power and elegance. As described in the application, drugs interact with their intended target protein, but also interact with other protein molecules (non-targets). For

drugs, non-targets can be involved with or responsible for undesirable side-effects. The claimed methods provide a way to identify, not only targets of small molecules, such as drugs, if not known, but also, non-targets.

In the study described herein, technology described in the application (referred to as CCMS herein) was used to elucidate the molecular basis for the difference in the toxicological profiles between the drugs Tolcapone and Entacapone. The results show that the claimed methods can unravel the set of proteins that interact with the drugs Tolcapone and Entacapone, respectively. Capture Compounds containing these two drugs capture the target protein COMT. Tolcapone, however, additionally binds to essential proteins in relevant pathways such as fatty acid ß-oxidation and oxidative phosphorylation. The results demonstrate that CCMS is a powerful tool for the generic identification of a drugs mode of action as well as non-target protein interactions.

The drugs Tolcapone and Entacapone are potent inhibitors of catechol-O-methyl transferase (COMT) for the treatment of Parkinson's disease (see, *e.g.*, Schapira et al., Neurology 55, S65-68; discussion S69-71 (2000)). Although these two drugs are similar, and even structurally identical with respect to the COMT binding moiety, they show a number of pharmacological differences and thus different clinical effectiveness (Deane *et al.*, Cochrane Database Syst Rev, CD004554 (2004)). A recent Cochrane meta-analysis of 14 studies in 2566 patients found both drugs to be statistically superior to placebo in increasing "on" time and decreasing „off" time and an approximately twice as long therapeutic effect of Tolcapone. This difference is reflected by the pharmacological profile, where Tolcapone is characterized by greater bioavailability and higher COMT affinity. Tolcapone increases the half-life of the dopamine precursor levodopa by 80 % vs. 40 % for Entacapone (Factor, Neurotherapeutics 5, 164-180 (2008)). A significant number of patients treated with Tolcapone show disturbed levels of liver enzymes and in 1998 three patient fatalities attributed to Tolcapone induced hepatotoxicity were reported (Deane et al. Cochrane Database Syst Rev, CD004554 (2004)).

Hence for these drugs, the target is COMT; any other molecules to with which these molecules interact are non-targets. Differences in non-targets with which these drugs interact elucidate the toxicity of Tolcapone compared to Entacapone. As described below, capture compounds that present each of these drugs (and each of these drugs in different orientations) were prepared. We incubated the capture compounds with protein fractions obtained from rat liver as well as lysates of the human hepatocyte cell line HepG2 to assess

isolate and identify protein molecules with which Tolcapone and Entacapone interact. Application of the CCMS technology reproducibly and unambiguously demonstrated that, in addition binding to COMT (the target protein), Tolcapone interacts with a large number of proteins carrying out essential functions in the respiratory chain, fatty acid ß-oxidation and bile acid synthesis. In the liver, fatty acids are metabolized by ß-oxidation in mitochondria and peroxisomes and by omega-oxidation in microsomes (drug non-targets) with which Entacapone does not interact. Peroxisomal beta-oxidation is responsible for the metabolism of very-long-chain-fatty acids. Impairment of correct peroxisomal function may lead to the accumulation of long-fatty acids or of hydrogen peroxide through the peroxisomal oxidative reactions. Both mechanisms contribute to hepatotoxicity and thus can explain the phenotype of Tolcapone side-effects.

5. The study, results and discussion

Materials and Methods

Chemical synthesis of Entacapone and Tolcapone Capture Compounds

Structures of final compounds are shown in Figure 2, below. The schema for synthesis also are set forth below. Referring to the schemes below, the compounds were synthesized using standard chemical synthetic methods as follows.

General. Unless otherwise noted, all reactions were performed in dried glassware under argon. Commercially available reagents and solvents were used as received without further purification. Column chromatography was carried out by using Geduran® Si 60 silica gel from Merck. MPLC purification was performed on a Buechi system (Buechi control unit C-620; 2 Buechi pump modules C-605; column - omnifit (230 x 15 mm); stationary phase - LiChroprep RP-select B 25-40 µm; Buechi UV photometer C-635; Buechi fraction collector C-660; mobile phase A: 0,1% AcOH Millipore grade; mobile phase B: acetonitrile prepsolv grade). LCT was carried out on a Waters system (HPLC pump Waters 1525; autosampler CTC HTS PAL; column oven Techlab K7 (40°C); diode array detector Waters 2998 (200 – 600 nm); MS detector Waters LCT time of flight mass spectrometer equipped with an electrospray ion source). LCT method A: column - Phenomenex Mercury MS (20 x 2 mm); stationary phase - Phenomenex Synergi Fusion RP, 2,5 µm; guard column Phenomenex Security Guard - Synergi Fusion RP; flow 0,4 mL/min; mobile phase A: 0,1% HCOOH Millipore grade; mobile phase B: acetonitrile LCMS grade; 10% B to 40% B in 9 min; 40% B to 100% B in 2 min; 100% B for 4 min. Accurate mass spectrometric analysis was performed on an LTQ Orbitrap XL mass spectrometer (Thermo Electron, Bremen, Germany)

utilizing a nanoelectrospray ion source (Proxeon Biosystems A/S, Denmark). For the analysis a 5 μM solution of the corresponding sample in water/acetonitrile (50/50, 0.1 % formic acid) was directly injected via the syringe pump with a flow rate of 1 μl/min. The singly-charged polydimethylcyclosiloxane background ion (Si(CH3)2O)6H+ (m/z 445.120025) generated during the electrospray process from ambient air was used as lock mass for real time internal recalibration. Further mass spectrometric settings were as follows: spray voltage was set to 1.7 kV, temperature of the heated transfer capillary was set to 200 °C. MS spectra (from m/z 400–2000) were acquired in the orbitrap with a resolution of r= 60,000 at m/z 400 (after accumulation to a target value of 500,000 charges in the linear ion trap). Proton nuclear magnetic resonance (1H NMR) spectra and carbon nuclear magnetic resonance (13C NMR) spectra were recorded on an Avance 400 (400 MHz) from Bruker. Chemical shifts are reported in ppm relative to CHCl3 (δ 7.27) for 1H NMR and the central resonance of CDCl3 (δ 77.0) for 13C NMR. The synthesis of the scaffolds is published elsewhere (ChemBioChem accepted). DCC = N,N'-Dicyclohexylcarbodiimide; DIC = N,N′-Diisopropylcarbodiimide; DIPEA = N,N-Diisopropylethylamine; DMA = N,N-Dimethylacetamide; DMF = N,N-Dimethylformamide; EDC = N-(3-Dimethylaminopropyl)-N′-ethylcarbodiimide; HATU = O-(7-Azabenzotriazol-1-yl)-N,N,N’-tetramethyluronium hexafluoro-phosphate; HOBt = 1-Hydroxybenzotriazole; DMAP = 4-Dimethylaminopyridine; TEA = Triethylamine; TFA = Trifluoroacetic acid; cHex = Cyclohexane.

General procedure "phenol-substitution." Under an atmosphere of argon, a solution of the mentioned phenol in dry DMF (0.1 M) was treated with NaH (2.2 eq) and stirred for 10 min. A highly concentrated solution of the corresponding bromide (1.2 eq) in dry DMF was added dropwise and the reaction mixture was stirred for 17 h at 23 °C. If LCT analysis showed incomplete conversion, additionally NaH (1.1 eq) was added and the reaction mixture was stirred for 10 min before additionally bromide (0.6 eq) was added. Stirring was continued for additionally 17 h at 23 °C, then the reaction was quenched with water and HCl solution (2 M) and extracted with DCM. The solvents were removed under reduced pressure and the crude product was purified by column chromatography.

General procedure "Boc deprotection." A suspension of the mentioned Boc-protected amine in DCM (0.2 M) was treated with TFA (DCM/TFA, 3/1 v/v) at 0 °C. The reaction mixture was allowed to warm gradually to 23 °C and was stirred for 30 min. The solvent and TFA was intensively removed under reduced pressure. The crude product generally was used without further purification or was purified by MPLC in special cases.

General procedure "HATU mediated amide coupling". Under an atmosphere of argon, a solution of the mentioned amine (mostly as TFA-salt) in dry DMF (0.05 M) was treated with a highly concentrated solution of B1- or B2-Scaffold respectively (1.0 eq) in dry DMF and DIPEA (5 eq). After being stirred for 10 min, HATU (1.2 eq) was added and the reaction mixture was stirred for 17 h at 23 °C with exclusion of light. The solvent was removed under reduced pressure and the crude product was purified by MPLC.

General procedure "DIC/DMAP mediated amide coupling." Under an atmosphere of argon, a solution of the mentioned amine (mostly as TFA-salt) in dry DMA (0.02 M) was treated with B1- or B2-Scaffold respectively (1 eq), Triethylamine (2 eq), DMAP (2 eq), HOBt (2 eq) and 1,3-Diisopropylcarbodiimide (5 eq). The reaction mixture was stirred for 2-3 d at 23 °C with exclusion of light. The solvent was removed under reduced pressure and the crude product was purified by MPLC.

Compound 2. Starting from commercial available Tolcapone 1 (compound 1) and according to general procedure "phenol-substitution", title compound 2 (39.4 mg, 52%) could be observed after column chromatography (cHex/EtOAc, 2:1 to 1:2) as a yellow solid. 1H NMR (CDCl3): δ 11.03 (br s, 1H), 8.14 (d, J = 1.7 Hz, 1H), 7.69 (d, J = 1.7 Hz, 1H), 7.67 (d, J = 8.0 Hz, 2H), 7.32 (d, J = 8.0 Hz, 2H), 5.09 (br s, 1H), 4.19 (t, J = 5.0 Hz, 2H), 3.63 (m, 1H), 2.46 (s, 3H), 1.45 (s, 9H). LCT method A.

Compound 3. Starting from commercial available Tolcapone 1 and according to general procedure "phenol-substitution", title compound 3 (69.2 mg, 85%) could be observed after column chromatography (cHex/EtOAc, 2:1) as a yellow solid.

Compound 4. Starting from commercial available Tolcapone 1 and according to general procedure "phenol-substitution", crude compound 4 was observed after filtration over silica as a yellow solid and was used for the next step without further purification.

Compound 5. Starting from compound 2 and according to general procedure "Boc deprotection", title compound 5 (31.9 mg, 88%) could be observed after column chromatography (DCM/MeOH, 100:1 to 5:1) as a yellow solid.

Compound 6. Starting from compound 3 and according to general procedure "Boc deprotection", crude compound 5 could be observed as a yellow, solid product and was used without further purification.

Compound 7. Starting from crude compound 4 and according to general procedure "Boc deprotection", title compound 7 (57.9 mg, 44% over 2 steps) could be observed as an orange solid after MPLC.

Compound 8. Starting from compound 5 and according to general procedure "DIC/DMAP mediated amide coupling", title compound 8 (5 mg, 40%) could be observed as a yellow solid after MPLC.

Compound 9. Starting from crude 6 and according to general procedure "DIC/DMAP mediated amide coupling", title compound 9 (8.3 mg, 30%) could be observed as a yellow solid after MPLC.

Compound 10. Starting from crude 6 and according to general procedure "HATU mediated amide coupling", title compound 10 (8 mg, 29%) could be observed as a yellow solid after MPLC.

Compound 11. Starting from compound 7 and according to general procedure "DIC/DMAP mediated amide coupling", title compound 11 (10.0 mg, 36%) could be observed as a yellow solid after MPLC.

Compound 12. Entacapone 12 was prepared according to literature. Analytical data was consistent to those reported.

Compound 14. Under an atmosphere of argon, a solution of Entacapone 12 (76 mg, 0.25 mmol) in dry DMF (0.6 mL) was treated with NaH (13.1 mg, 0.55 mmol) and stirred for 10 min. A solution of tert-butyl 2-bromoethylcarbamate (100 mg, 0.45 mmol) in dry DMF (0.1 mL) was added dropwise and the reaction mixture was stirred for 17 h at 23 °C. As LCT analysis showed incomplete conversion, additionally NaH (6.6 mg, 0.28 mmol) was added, the mixture was stirred for 10 min, and tert-butyl 2-bromoethylcarbamate (50 mg, 0.23 mmol) was added. The reaction mixture was stirred for additionally 5 h at 23 °C, quenched with water (60 µL) and the crude product was filtered over silica. The solvents were removed under reduced pressure to complete dryness and the crude product was dissolved in DCM (2.5 mL). TFA (1 mL) was added at 0 °C, the reaction mixture was stirred for 10 min, was then allowed to warm gradually to 23 °C and was stirred for additionally 30 min. The solvent and TFA was removed under reduced pressure and the crude product was purified by MPLC to yield title compound 14 (17.7 mg, 15%) as an orange solid.

Compound 15. Starting from compound 14 and according to general procedure "DIC/DMAP mediated amide coupling", title compound 15 (3.4 mg, 25%) could be observed as a yellow oil after MPLC.

Compound 16. Starting from compound 14 and according to general procedure "HATU mediated amide coupling", title compound 16 (3.7 mg, 27%) could be observed as an orange oil after MPLC.

Compound 17. Under an atmosphere of argon, a solution of commercial available 4-Bromo-N-methylbenzylamine (500 mg, 2.5 mmol) in dry DCM (12.5 mL) was treated with TEA (0.42 mL, 3 mmol) and Boc2O (654 mg, 3.0 mmol) at 0 °C. The reaction mixture was stirred for 1 h at 0 °C, was allowed to warm gradually to 23 °C and stirred additionally 2 h. The crude product was portioned between water and DCM. The organic solvent was removed under reduced pressure and the crude product was purified by column chromatography (cHex/EtOAc, 20:1 to 2:1) to give title compound 17 (716 mg, 95%) as a clear, colorless oil.

Compound 19. Under an atmosphere of Argon, a solution of n-BuLi (1.55 ml, 1.6 M in hexanes, 2.48 mmol) was added dropwise to a solution of compound 17 (679 mg, 2,26 mmol) in dry THF (7 mL) at -78 °C. The solution was stirred for 30 min at -78 °C. Then, a solution of aldehyde 18 (522 mg, 2.15 mmol) in dry THF (3 mL) was added dropwise that the temperature did not rise over -70 °C. The reaction mixture was stirred for 30 min at -78 °C, gradually warmed to 23 °C and stirred additionally 30 min. The reaction was quenched with water (20 mL), extracted with DCM and the solvents were removed under reduced pressure. The crude product was purified by column chromatography (cHex/EtOAc, 20:1 to 3:1) to give the title compound (296 mg, 30%) as a colorless oil.

Compound 20. Sodium tert-butoxide (83 mg, 0.86 mmol) was added to a solution of alcohol 19 (266 mg, 0.57 mmol) in Toluene (2.9 mL) under argon. Cyclohexanone (364 µL, 3.51 mmol) was added dropwise under stirring and the reaction mixture was stirred for 1.5 h at 120 °C. Then, 20 mL water were added, the layers were separated, and the water layer was extracted with EtOAc. The combined organic layers were washed with brine, dried over MgSO4 and the solvents were removed under reduced pressure. The crude product was dissolved in dry MeOH under argon and treated with Ammonium formate (181 mg, 2.87 mmol) and Palladium (7.1 mg, 10% on carbon, 0.067 mmol). The reaction mixture was stirred for 2.5 h under reflux. After cooling to 23 °C, the crude product was filtered over a pad of Celite®, the filter cake was washed with MeOH and the solvent was removed under reduced pressure. The crude product was purified by column chromatography (cHex/EtOAc, 20:1 to 2:1) to give title compound 20 (137 mg, 64%) as a colorless oil.

Compound 21. At 18 °C, a solution of compound 20 (73 mg, 0.2 mmol) in AcOH (0.4 mL) was treated with nitric acid (15 µl, 0.22 mmol) and stirred for 2 h at 23 °C. Then, DCM (5 mL) and water (5 mL) were added, the layers were separated and the water layer was extracted with DCM. The organic layers were combined, the solvent was removed under

reduced pressure and the crude product was purified by column chromatography (DCM/MeOH, 100:1) to give title compound 21 (54.9 mg, 67%) as a yellow solid.

Compound 22. At -78 °C a solution of Boron tribromide (84 µl, 1.0 M in DCM, 0.084 mmol) was added dropwise to a solution of compound 21 (10 mg, 0.024 mmol) in dry DCM (0.25 mL) under argon. The reaction mixture was stirred for 10 min at -78 °C and additionally 17 h at 23 °C. The solvent was removed under reduced pressure to complete dryness, MeOH was added carefully and the solution was stirred for 5 min. The solvent was removed under reduced pressure and the crude product was suspended in dry DCM (0.2 mL). At 0 °C BocGly (4.2 mg, 0.024 mmol), DCC (5.94 mg, 0.029 mmol), DMAP (0.3 mg, 2.4 µmol) and TEA (17 µl, 0.12 mmol) were added. The reaction mixture was stirred for 2 h at 0 °C and additionally 17 h at 23 °C. As LCT analysis showed incomplete conversion, BocGly (2.1 mg, 0.012 mmol), HATU (5.48 mg, 0.014 mmol) and dry DMA (0.2 mL) were added. The reaction mixture was stirred for 3 h at 23 °C. The solvents were removed under reduced pressure and the crude product was purified by MPLC ~~()~~ to give title compound 22 (4.1 mg, 37%) as a red oil.

Compound 23. At -78 °C a solution of Boron tribromide (84 µl, 1.0 M in DCM, 0.084 mmol) was added dropwise to a solution of compound 21 (10 mg, 0.024 mmol) in dry DCM (0.25 mL) under argon. The reaction mixture was stirred for 10 min at -78 °C and additionally 17 h at 23 °C. The solvent was removed under reduced pressure to complete dryness, MeOH was added carefully and the solution was stirred for 5 min. The solvent was removed under reduced pressure and a portion of crude product (10.6 mg, 0.035 mmol) was suspended in dry DMF (0.5 mL). At 0 °C 6-(Boc-amino)hexanoic acid (8.9 mg, 0.039 mmol), DIPEA (30.5 µL mg, 0.175 mmol) and HATU (16.0 mg, 0.12 mmol) were added. The reaction mixture was stirred for 2 h at 0 °C and additionally 17 h at 23 °C. The solvent was removed under reduced pressure and the crude product was purified by MPLC to give title compound 23 (7.7 mg, 43%) as a red oil.

Compound 24. Starting from compound 22 and according to general procedures "Boc deprotection" and "HATU mediated amide coupling", title compound 24 (3 mg, 32%) could be observed as a red solid after MPLC.

Compound 25. Starting from compound 22 and according to general procedures "Boc deprotection" and "HATU mediated amide coupling", title compound 25 (7 mg, 43%) could be observed as a red solid after MPLC.

Compound 28. At 0 °C, N-Ethylethylenediamine (2.0 g, 22.7 mmol) was added dropwise to a solution of HCl in MeOH (18.2 mL, 1.25 M) under argon. The solution was allowed to warm gradually to 23 °C and was stirred for 15 min. Water was added and stirred for 30 min. A solution of Boc2O (4.95 g, 22.7 mmol) in MeOH (15 mL) was added dropwise and the reaction mixture was stirred for additionally 1 h. The solvent was removed under reduced pressure, NaOH solution (60 mL, 2 N) was added and the crude product was extracted with DCM (3 x 100 mL). The combined organic layers were washed with brine, dried over $MgSO_4$ and the solvent was removed under reduced pressure to yield a crude product (3.98 g, 93 %) as colorless needles. The crude product (2.0 g, 10.6 mmol) was added to a solution of Cyanoacetic acid (0.9 g, 10.6 mmol) in dry DCM (100 mL). At 0 °C the solution was treated with EDC (2.44 g, 12.7 mmol) and DMAP (32 mg, 0.27 mmol) and stirred for 2 h at 0 °C and additionally 17 h at 23 °C. Water was added and the crude product was extracted with DCM (3 x 100 mL). The combined organic layers were washed with HCl solution (1 M) and brine, dried over MgSO4 and the solvent was removed under reduced pressure. The crude product was purified by column chromatography (cHex/EtOAc, 1:1 to 1:2) to give title compound 28 (2.11 g, 78%) as a colorless oil (rotamers or regioisomers).

Compound 29. Under an atmosphere of argon, a solution of Nitrovanillin (5.0 g, 25.36 mmol) in dry pyridine (13 mL) was treated with AlCl3 (4.06 g, 30.43 mmol) at 0 °C. The reaction mixture was stirred for 3 h at 50 °C. After cooling to 0 °C, HClconc (15 mL) was added and the crude product was extracted with EtOAc. The organic layers were combined, washed with brine, dried over MgSO4 and the solvents were removed under reduced pressure. The crude product was purified by recrystallization from cHex/EtOAc (4:1) to give a clean batch of title compound 29 (2.86 g, 62%) and a second batch mainly containing the title compound (1,66 g) as a yellow-orange solid.

Compound 30. A solution of compound 28 (67 mg, 0.26 mmol) in a solvent mixture of Toluene and cHex (0.35 mL, 1:1 (v/v)) was treated with aldehyde 29 (36.6 mg, 0.2 mmol) and piperidine (2.0 µL, 0.02 mmol). The reaction mixture was stirred for 3 h at 90 °C. Then, the solvent was removed with a stream of nitrogen at 90 °C and the crude product was purified by MPLC to yield title compound 30 (57 mg, 68%) as an orange oil.

Compound 31. Starting from compound 30 and according to general procedures "Boc deprotection" and "DIC/DMAP mediated amide coupling" title compound 31 (8.1 mg, 18%) could be observed as a yellow oil after MPLC.

Compound 32. Starting from compound 30 and according to general procedures "Boc deprotection" and "HATU mediated amide coupling" title compound 32 (13.2 mg, 51%) could be observed as a an orange oil after MPLC.

Analysis of the Capture Compounds by mass spectrometry and NMR confirmed the identity and structure of the final reaction products. Purity of the compounds was determined by 1H-NMR and was found to be greater than 95 %.

Computational methods

Preparation of Molecular Structures: Atomic coordinates for the ternary complex between COMT, the cosubstrate S-adenosyl-methionine, and the inhibitor BIA3-335 was obtained from the Protein Data Bank (PDB, www.rcsb.org) file 1H1D. The magnesium ion was considered covalently bound to Asp141 and Asp169. The side chain of Lys144 was modeled in the neutral form. The structure was minimized with the molecular modeling package SYBYL8.1 (Tripos Inc., St. Louis, USA) using the Tripos force field, Gasteiger-Marsili charges and the Powell gradient algorithm. The backbone, the magnesium ion, and its coordination atoms (O1 in Asp141, O2 in Asp169, OD1 in Asn170, the oxygen of HOH53, and both oxygens in the catechol moiety of the ligand) were frozen during minimization. Molecular docking: In order to reduce the rotational degrees of freedom and to focus on the interactions of the selectivity and the reactivity functions with the protein, the Capture Compounds were modelled without the polyethyleneglycol linker and the biotin moiety. Unrestrained flexible docking between COMT and Tcp-Bz-CC was performed with Surflex-Dock5 included in the SYBYL Package using the default settings. The co-crystallized ligand was extracted and the protomol was generated based on the ligand. Twenty poses were sampled.

The results were investigated for the correct binding of the catechol moiety in the binding pocket and the positioning of the crosslinking unit in vicinity of the protein surface, especially close to polar side chains. The polyethyleneglycole linker and the biotin moiety (based on the PDB file with the accession number 1STP) were added manually and minimized using standard procedures.

COMT affinity assay

Bioanalytical services for the determination of KD values were provided by MDS Pharma Services Inc (Peitou Taipei, Taiwan).

scaffold (100 µM) with 50 µL of Dynabeads® MyOneTM Streptavidin C1, (Invitrogen, Karlsruhe, Germany) at room temperature for 5 min. After washing twice with wash buffer (WB, containing 50 mM Tris HCl, pH 7.5, 1 mM EDTA, 1 M NaCl, 0.5 µM octyl-ß-D-glucopyranoside) the respective magnetic capture beads were added to the reaction mix and rotated at 4 °C for ca 3 hrs with protection from light. Subsequently, the reaction mixture was irradiated using the device for irradiation from caprotec sold as caproBox^{TM} (wavelength 310 nm, irradiance Ie≥10 mW/cm^2) for 20 min with mixing at intervals of 2.5 min. After UV light exposure, the beads were collected using the caprotec device called caproMagTM, a device for the handling of magnetic beads (caprotec bioanalytics GmbH, Berlin, Germany), and washed first six times with 200 µL WB (caprotec bioanalytics GmbH, Berlin, Germany), and then twice with ultrapure water. Until further analysis beads were stored at 4 °C in ultrapure water.

For capture experiments using fractions of rat liver, the initial protein amounts in the capture reactions were 0.4 mg for mitochondrial or microsomal, and 1.4 mg in case of the cytosolic fraction, respectively. Capture buffer and WB were supplemented with 0.1 % n dodecyl-ß-maltoside (Glycon, Luckenwalde, Germany).

Western Blot

After separation by SDS-PAGE captured proteins were transferred to a nitrocellulose membrane (Whatman, Kent, UK). Proteins were stained with Ponceau red (Sigma, Steinheim, Germany) to control the blotting efficiency (data not shown). The membrane was blocked for 1 h at room temperature with a solution of 5 % (w/v) skimmed milk powder in Tris buffered saline (20 mM Tris HCl, pH 7.5, 150 mM NaCl (TBS), supplemented with 0.1 % (v/v) Tween 20 (TBS T)). Incubation with the primary antibody was performed for 1 h at room temperature or over night at 4 °C followed by three wash steps in TBS T and incubation with the secondary antibody for 1 h at room temperature. Antibodies were diluted in 5 % skimmed milk powder in TBS T as follows: anti-COMT 1:2,500, secondary anti-goat antibody conjugated to horseradish peroxidase 1:2,000. After three washes in TBS-T and one wash in TBS membranes were treated using Pierce ECL Western Blotting Substrate (Thermo Fisher Scientific, Schwerte, Germany) according to the manufacturer's instructions. Hyperfilm ECL films (GE Healthcare, München, Germany) were used to detect the chemoluminescence. In case of blots for the detection of biotinylated proteins streptavidin-horseradish peroxidase was used instead of a first antibody at a dilution of 1:1,000 in 5 % skimmed milk powder in

TBS T and Blots developed directly after washing three times with TBS-T and once with TBS.

In solution digest

For analysis of the complex protein mixture obtained after capture experiments, the washed beads were resuspended in 10 µl 50 mM ammonium bicarbonate and 1 µl trypsin (0.5 µg/µl) (sequencing grade, Roche, Mannheim, Germany) for 16 h at 37 °C on a thermoshaker (Eppendorf, Hamburg, Germany). Subsequently, tryptic peptides were desalted using Stage Tips® (Proxeon Biosystems A/S, Odense, Denmark) and eluted with methanol according to the manufacturer's instructions. The eluate was evaporated to dryness in a miVac DNA vacuum centrifuge (Genevac®, UK) and stored at -20 °C until mass spectrometric analysis.

In-gel digestion

For subsequent analysis by SDS-PAGE, the beads with captured proteins were resuspended in 7 µl Laemmli buffer and heated to 95 °C for 5 min. Gels were stained using the FireSilver® Kit (Proteome Factory, Berlin, Germany) according to the manufacturer's instructions and washed twice for 10 min with LC-MS grade water. Gel bands were excised, cut into small pieces, and washed twice with each 100 µl water and 100 µl 50 % ethanol (v/v). Gel bands were shrunk with 50 µl 100 % ethanol for approximately 5 min. Subsequently, the washing and shrinking steps were repeated. Protein digestion was carried out by rehydration of bands for 20 min on ice with 12.5 ng/µl of trypsin solution in 50 mM NH_4HCO_3 and subsequent incubation for 16 h at 37 °C. The extraction of peptides was carried out in two consecutive steps by incubating the gel pieces with 50 % acetonitril (ACN) with 2.5 % formic acid (FA) for 15 min. The pooled supernatants were then dried in a miVac DNA vacuum centrifuge (Genevac®). Desalting, elution, evaporation and storage of tryptic peptides were performed as described for in-solution digested samples.

Nano LC-MS/MS

The protein digest was redissolved in 5 µl of 5 % FA. Subsequently, peptides were loaded onto a nanoflow Biosphere C18 pre-column (5 µm, 120 Å, 20 x 0.1 mm, nanoseparations, Netherlands) coupled to a nanoflow Biosphere C18 analytical column (5 µm, 120 Å, 105 x 0.075 mm). The experiments were performed on an Easy-nLC™ liquid chromatography system (Proxeon Biosystems A/S, Odense, Denmark) connected to an LTQ Orbitrap XL mass spectrometer (Thermo Electron, Bremen, Germany) using a nano-electrospray ion source (Proxeon Biosystems A/S, Odense, Denmark). For the analysis of in-solution digest samples peptides were eluted during an 80-min linear gradient from 5 %

ACN/0.1 % FA to 40 % ACN/0.1 % FA followed by an additional 2 min to 100 % ACN/0.1 % FA and remaining at 100 % for another 8 min with a controlled flow rate of 300 nl/min. For the analysis of extracted gel bands a linear 40-min gradient increasing from 5 % ACN/0.1 % FA to 40 %ACN/0.1 % FA followed by an additional 2 min to 100 % ACN/0.1 % FA and remaining at 100 % for another 8 min with a controlled flow rate of 300 nl/min.

The mass spectrometric analysis was performed in the data-dependent mode to automatically switch between orbitrap-MS and LTQ-MS/MS (MS2) acquisition. The mass spectrometer duty cycle was controlled by setting the IT automatic gain control. Survey full scan MS spectra (from m/z 400–2000) were acquired in the orbitrap with a resolution of r= 60,000 at m/z 400 (after accumulation to a target value of 500,000 charges in the linear ion trap). The most intense ions (up to five, depending on signal intensity) were sequentially isolated for fragmentation in the linear ion trap using collision- induced dissociation (CID) at a target value of 10,000 charges. The resulting fragment ions were recorded in LTQ.
For accurate mass measurements in the MS mode the singly-charged polydimethylyclo-iloxane background ion (Si(CH3)2O)6H+ (m/z 445.120025) generated during the electrospray process from ambient air was used as lock mass for real time internal recalibration. Target ions already mass selected for CID were dynamically excluded for the duration of 60 s. Charge state screening and rejection of ions for CID with unassigned charge were set. Further mass spectrometric settings were as follows: spray voltage was set to 1.7 kV, temperature of the heated transfer capillary was set to 200 °C, and relative normalized collision energy was 35 % for MS2. The minimal signal required for MS2 was 500 counts. An activation q = 0.25 and an activation time of 30 ms was applied for MS2 acquisitions. After each analysis of an in-solution digest sample the system was washed by performing at least one linear gradient that was used for the respective peptide separation.

Peptide identification via database search

Proteins were identified by automated database searching against the UniProtKB/Swiss-Prot (release 56.5) database using SEQUEST implemented in Bioworks 3.3.1 SP1 (Thermo Fisher Scientific, Schwerte, Germany). Specific search parameters used in the SEQUEST analyses were 5 ppm precursor tolerance, 1 amu fragment ions tolerance, and full trypsin specificity allowing for up to 2 missed cleavages. Phosphorylation at serine, threonine, and tyrosine, oxidation of methionines, deamidation at asparagines and glutamine, acetylation at lysine and serine, formylation at lysine, and methylation at arginine, lysine,

serine, threonine and asparagine were allowed as variable modifications. No fixed modifications were used in the database search.

The SEQUEST peptide identifications were required to satisfy minimum XCorr values of 2, 2.5, and 3 for singly, doubly, and triply charged peptides, a minimum ΔCn of 0.1, and a peptide probability ≥0.001. Peptides with a greater score than this were accepted for analysis without further validation. The estimated percentage of false discovery peptide identifications was determined using the reversed protein database approach and was <1 %.

Results

Capture Compounds

Tolcapone and Entacapone are potent inhibitors of catechol-O-methyl transferase (COMT) for the treatment of Parkinson's disease. The catechol groups of these drugs compete with dopamine for coordination of the catechol moiety with the magnesium ion in the COMT binding pocket (Bonifacio *et al.*, CNS Drug Rev 13, 352-379 (2007)). The drugs have shown significant hepatoxicity limiting their therapeutic utility. In particular, Tolcapone was temporarily withdrawn, due to the drug's implication in fulminant liver failure and the consequent death of 3 patients; now monitoring of liver enzymes is mandatory during drug treatment (Unger *et al.*, Eur Neurol 60, 122-126 (2008). In order to investigate the molecular mechanisms underlying the cause of hepatoxicity we prepared Capture Compounds containing Tolcapone and Entacapone as selectivity functions (Y groups), respectively (Figure 2). Different moieties of a drug may form different interactions with cellular proteins inducing different pharmacogenic responses. Thus, we choose two points of attachment for each drug to the scaffold (Figure 2). In one set we used the catechol responsible for the interaction with COMT as the attachment point (Figure 2. 2, 3, 4: Tcp-Ct-CC and 6: Ecp-Ct-CC), and in addition we linked the drugs at the opposite end via the benzylic or the amino group, respectively (Figure 2. 5: Tcp-Bz-CC and 7: Ecp-Am-CC). As a result, different pharmacophoric elements of Entacapone and Tolcapone were presented to the complex protein mixtures tested. As a control the Capture Compound without selectivity group (scaffold) was used. "...each drug to the scaffold (Figure 2). The design of the Capture Compounds was carried out with the aim that for one attachment position the Capture Compound functionalities should not interfere with the interaction between the drug and it's target COMT. For Entacapone, the Capture Compound with attachment via the amino group should be able to bind COMT as does the original drug. To verify the quality of our molecular design we commissioned standard affinity measurements between one of the

Capture Compounds and the purified target protein COMT. Published K_D values for the affinity of the drug Entacapone to COMT vary by one order of magnitude between 0.3 nM and 10nM). The KD of the Entacapone Capture Compound Ecp-Am-CC was determined to be 430 nM. These results demonstrate that although the attachment of the Capture Compound scaffold may lead to a slight reduction of affinity Entacapone still effectively binds COMT, demonstrating that the pharmacophoric potential of the drug is retained within the Capture Compound.

Validation of the CCMS approach with soluble rat liver proteins

We first tested our Capture Compounds in the cytosolic fraction of rat liver, which shows a reduced protein complexity compared to whole cell lysates. UV irradiation induces a covalent bond between the reactivity function of the Capture Compound and the protein interacting with the drug. As the Capture Compound contains a biotin moiety (sorting function), interacting proteins become biotinylated during the capture process and can not only be isolated by streptavidin beads but also detected in an anti-biotin (e.g. streptavidin) Western Blot (Figure 4A), demonstrating the covalent bond to the Capture Compound. By SDS-PAGE (Figure 4B) all isolated proteins were visualized. The comparison of silver stained SDS-PAGE and anti-biotin Western Blot clearly demonstrated that the isolated proteins were covalently bound. Western Blots directed against the COMT protein (Figure 4C) demonstrated that the target is indeed captured and – comparing Figure 4 A and C – covalently bound. Analysis of the respective samples by mass spectrometry in addition to Western Blots demonstrated the unambiguous and reproducible isolation and identification of the known drug target COMT with the Capture Compounds containing the free catechol moiety (Tcp-Bz-CC and Ecp-Am-CC) Table 1), while, as expected, compounds with attachment at the opposite end (Tcp-Ct-CC and Ecp-Ct-CC) did not bind COMT. These, however, presented different pharmacophoric elements of the drugs to the protein mixture, and allowed capturing of proteins that interacted with these elements of the drugs.

Notably, the Capture Compounds interacted with bile salt sulfotransferase (ST2A1) and alcohol sulfotransferase A (ST2A2), independently of the attachment point. ST2A1 and ST2A2 belong to the group of cytosolic sulfotransferases, phase II detoxification enzymes involved in the biotransformation of a wide variety of structurally diverse endo- and xenobiotics, including many therapeutic agents and endogenous steroids. Binding of all four Capture Compounds to these enzymes is in accord with the rather unspecific role of the sulfotranferases in detoxification processes (Nowell *et al.*,. Oncogene 25, 1673-1678 (2006)).

As the scaffold control did not show this interaction, this indicates that the binding of sulfotranfarases is specific and might be triggered by toxicologically relevant events.

The Capture Compounds with free catechol moieties exposed to the cytosol showed, apart from the sulfotransferases, strong and specific interaction only with the target protein COMT. Those Capture Compounds with attachment via the catechol group (Tcp-Ct-CC1 and Ecp-Ct-CC1) revealed additional interacting proteins in the cell lysate. Notably, for the Tolcapone Capture Compound Tcp-Ct-CC1, additional peroxisomal proteins were captured. Peroxisomal acyl-coenzyme A oxidase 3 (ACOX3) and peroxisomal multifunctional enzyme type 2 (DBH4 also MFP-2 or MFE-2) play essential roles in fatty acid β-oxidation. The phenotypical data (Yu *et al.*. Curr Mol Med 3, 561-572 (2003); Huyghe, S. *et al.* Am J Pathol 168, 1321-1334 (2006); and Baes, M., *et al.*, J Biol Chem 275, 16329-16336 (2000)) associated with the two captured peroxisomal enzymes, indicate that Tolcapone related side-effects may be due, in part, to the interaction of these enzymes with Tolcapone. Moreover, these results show that CCMS can identify the molecular basis of drug side-effects.

Tolcapone as decoupling reagent of the respiratory chain

In order to reveal the mode of hepatotoxic action of Tolcapone and Entacapone in the human liver, we performed capture experiments in whole cell lysates of the human hepatocyte cell line HepG2. As the chemical structure of Entacapone and Tolcapone at the catecholic site is identical and the experiments using cytosolic rat liver fractions indicated that Tolcapone attached via the catecholic group captures relevant drug non-targets, we employed compounds with this attachment point. To generate a comprehensive coverage of drug-protein interactions we designed two additional Capture Compounds differing in the linker length between the drug molecule and the reactivity group (Tcp-Ct-CC2 and –CC3 Figure2A).

Capture experiments in HepG2 whole cell lysates revealed that Tolcapone Capture compounds, independent of linker length, interacted with a large number of different proteins in the cell, while Entacapone Capture Compounds showed relatively few interactions independent of attachment point. Even fewer proteins were found when capturing was performed with the scaffold control (Figure 5A). LC-MS/MS analysis of the respective complex protein mixtures led to the identification of the Tolcapone and Entacapone interaction partners. Proteins identified in the control experiment with scaffold were excluded from further analysis. We established the overlap between the captured proteins to classify the interaction partners of the respective drugs. The Tolcapone compounds captured a total of

124 proteins; with the Entacapone Capture Compounds, however, only **20** proteins were captured (Figure 3). While some proteins were captured exclusively by one Capture Compound, the majority of proteins was captured independent of the linker length, and, thus, considered as interaction partners with highest confidence. For an overall functional classification of the proteins we performed Gene Ontology annotation via BioMart of the ENSEMBL Genome Browser (www.ensembl.org, build 52 NCBI63) according to Cellular Component Terms.

For Entacapone Capture Compounds, twenty proteins were specifically captured and their cellular distribution showed no distinctive features regarding toxic side effects. For Tolcapone, a considerably large proportion of the 124 captured proteins were assigned to the mitochondria (Figures 3 and 5B) and, in particular, within the mitochondrial membrane. To gain deeper insight into the role of the captured proteins in metabolism, we performed out a KEGG Pathway (Aoki *et al.* Curr Protoc Bioinformatics Chapter 1, Unit 1 12 (2005)) analysis via the Database for Annotation, Visualization and Integrated Discovery (DAVID, V6, 2008 david.abcc.ncifcrf.gov/; Dennis *et al.* DAVID: Database for Annotation, Visualization, and Integrated Discovery. Genome Biol 4, P3 (2003)). We found that the captured proteins are essential components of the respiratory chain, the bile acid synthesis, and peroxisomal fatty acid ß-oxidation (summarized in Figure 3). Enzymes functioning in bile acid synthesis and peroxisomal fatty acid ß-oxidation are in accord with the results obtained from the soluble fraction of rat liver. In particular, the human homolog of ACOX3 was again reproducibly captured, confirming a possible disturbance of fatty acid ß-oxidation by Tolcapone in humans. Notably, the captured mitochondrial proteins contained subunits from each of the complex in the respiratory chain (Figure 5C), for example, eight subunits of ATP synthase. While nearly all subunits were captured by two or three of the Tolcapone capture compounds none were isolated by Entacapone Capture Compounds. The comparison to the structurally similar but far less toxic drug Entacapone indicates that the observed Tolcapone-protein interactions likely are the cause of toxicity.

Detailed analysis of proteins interacting with Tolcapone in rat liver mitochondria and microsomal fractions

To investigate the interaction partners of Tolcapone in mitochondria and peroxisomes in detail, we carried out capture experiments in the mitochondria and microsomal fractions of rat liver. In both preparations, we again found that Tolcapone Capture Compounds capture significantly more proteins than the respective Entacapone compounds. Consistent with the

results described above, we identified key-enzymes of fatty acid ß-oxidation, such as peroxisomal multifunctional enzyme type2, peroxisomal acyl-coenzyme A oxidase 3, and the long-chain-fatty-acid-CoA ligase 1 which is found both in the mitochondrial and peroxisomal membrane as specific interaction partners of Tolcapone with the potential to induce side-effects (see, Table 2, below).

Discussion

Application of CCMS technology reproducibly and unambiguously demonstrated that besides binding COMT, Tolcapone interacts with a large number of proteins carrying out essential functions in the respiratory chain, fatty acid ß-oxidation and bile acid synthesis. In the liver, fatty acids are metabolized by ß-oxidation in mitochondria and peroxisomes and by omega-oxidation in microsomes. Peroxisomal beta-oxidation is responsible for the metabolism of very-long-chain-fatty acids. Impairment of correct peroxisomal function may lead to the accumulation of long-fatty acids or of hydrogen peroxide through the peroxisomal oxidative reactions. Both mechanisms contribute to hepatotoxicity and thus can explain the phenotype of Tolcapone side-effects.

Peroxisomal acyl-coenzyme A oxidase 3 (ACOX3) belongs to the family of fatty acyl-CoA oxidases. Recently, it has been shown that mice lacking fatty acyl-CoA oxidases developed steatohepatitis, demonstrating the importance of this class of enzymes for proper liver function (Yu *et al.* Curr Mol Med 3, 561-572 (2003). Peroxisomal multifunctional enzyme type 2 (MFP-2, also D-bifunctional protein, DHB4) plays a central role in peroxisomal ß-oxidation as it handles most, if not all, peroxisomal ß-oxidation substrates (Huyghe *et al.* Biochim Biophys Acta 1761, 973-994 (2006)).. In humans, deficiency of this enzyme causes a severe developmental syndrome with abnormalities in several organs leading to death within the first year of life (Huyghe et al. Biochim Biophys Acta 1761, 973-994 (2006)). Accumulation of branched-long-chain fatty acids and very-long-chain fatty acids as well as a disturbed synthesis of bile acids were documented for these patients. Moreover, lack or mutations of DHB4 are a cause of D-bifunctional protein deficiency (DBPD). The clinical manifestations of this deficiency is similar to those of disorders of peroxisomal assembly, including X-linked adrenoleukodystrophy, Zellweger cerebrohepatorenal syndrome, and neonatal adrenoleukodystrophy (Watkins *et al.* J Clin Invest 83, 771-777 (1989); Wanders *et al.*, J Inherit Metab Dis 13, 375-379 (1990)). Premature death is observed in one third of MFP-2 knockout mice accompanied by more severe aberrations in bile acid metabolism and excessive accumulation of very-long-chain

fatty acids in brain and liver (Huyghe, S. et al. Am J Pathol 168, 1321-1334 (2006); and Baes, M., et al., J Biol Chem 275, 16329-16336 (2000)).

Besides interference with fatty acid ß-oxidation, our results show that Tolcapone inserts into the inner mitochondrial membranes and interacts with components of the respiratory chain. A molecular mechanism in which Tolcapone compromises the function of the respiratory chain is in accordance with cell physiological data reporting a decrease of membrane potential in the presence of Tolcapone (Haasio *et al.*, Eur J Pharmacol 453, 21-26 (2002) similar to the *bona fide* decoupling agent 2,4-dinitrophenol. A toxicological study (Haasio *et al.* J Neural Transm 109, 1391-1401 (2002)) in which rats were treated either with Entacapone or Tolcapone reported that no treatment related findings were observed in Entacapone-treated rats. Animals treated with Tolcapone showed increased respiration, decreased activity and drowsiness, and elevation of the rectal body temperature.

The results presented herein provide a molecular basis for the reported clinical and cell physiological observations. Mitochondria and peroxisomes in the liver were identified as the cellular compartments mainly affected during Tolcapone treatment. Indeed, the malfunction of the respiratory chain, fatty acid ß-oxidation or bile acid synthesis alone would likely lead to hepatotoxicity (Pessayre *et al.*. Cell Biol Toxicol 15, 367-373 (1999); Jaeschke *et al.*, Toxicol Sci 65, 166-176 (2002)).

* * *

I further declare that all statements made herein of my own knowledge are true and that all statements made on information and belief are believed to be true; and further, that these statements were made with knowledge that willful false statements and the like so made are punishable by fine or imprisonment, or both, under section 1001 of Title 18 of the United States Code, and that such willful false statements may jeopardize the validity of the application or any patent resulting therefrom.

Signature _____ Berlin, February 3, 2010
Hubert Köster Date:

Figure and Table Legends

Figure 1. Schematic depiction of Capture Compounds (A) and the capture process (B). Capture Compounds are trifunctional probes: based on affinity a selectivity function (the drug, red) interacts with the proteins in a biological sample in equilibrium, a reactivity function (orange) irreversibly forms a covalent bond, and a sorting function (yellow) allows the captured protein(s) to be isolated for mass spectrometric analysis.

Figure 2. Chemical structures of Tolcapone (Tcp) and Entacapone (Ecp) Capture Compounds. 1) The scaffold without selectivity function was used as a control. Tolcapone Capture Compounds with attachment via the catechol group and with free benzylic function (2 to 4, Tcp-Ct-CC). Tolcapone Capture Compounds with attachment via the benzylic group with free catechol function (5 Tcp-Bz-CC). Entacapone Capture Compounds with attachment via the catechol function (6, Ecp-Ct-CC) and via the amide (free catechol function, 7, Ecp-Am-CC).

Figure 3. Summary of the cellular distribution of the captured proteins (see, also, Figures 5).

Figure 4. Identification of COMT and off-target proteins by capturing in soluble fraction of rat liver. (A) The streptavidin-peroxidase Western-Blot demonstrates covalent crosslink between Capture Compound and protein interaction partners (B) Silver gel showing all captured proteins and (C) Anti-COMT Western Blot: Compounds with free catechol moiety capture COMT. M: Marker; lane 1: Tcp-Ct-CC; lane 2: Tcp-Bz-CC; lane 3: Ecp-Ct-CC; lane 4: Ecp-Am-CC and lane 5: Scaffold. Arrows indicate COMT.

Figure 5. Proteins interacting with Tolcapone in HepG2 cell lysate. A) Capturing in HepG2 lysate shows high number of proteins interacting with Tolcapone (Lanes 2-4) compared to Entacapone Capture Compounds (lanes 5,6) and even less for the Capture compound Scaffold (Lane 1). B) Mapping of gene ontologies revealed the localization to interacting proteins in the cellular compartments. C) A large proportion of Tolcapone interacting proteins is located in the mitochondria and include members of the respiratory chain

Figure 6. Capturing in rat liver mitochondrial fraction enables the identification of Tolcapone off-targets in fatty acid ß-oxidation. L: Mitochondrial lysate M: marker 1: Tcp-Ct-CC1 2: Tcp-Ct-CC2 3: scaffold control 4: Ecp-Ct-CC1, 5: Ecp-Am-CC1.

Table 1. Proteins captured by Tolcapone and Entacapone in the soluble protein fraction of rat liver. The corresponding silver stained SDS-PAGE is shown in Figure 4. Processes are given as retrieved from SwissProt annotation via http://www.expasy.org.

Table 2. Proteins captured by Tolcapone and Entacapone in solubilized mitochondrial and microsomal fraction of rat liver. Corresponding protein bands are depicted in Figure 6. Processes are given as retrieved from SwissProt annotation via www.expasy.org.

Figure 1

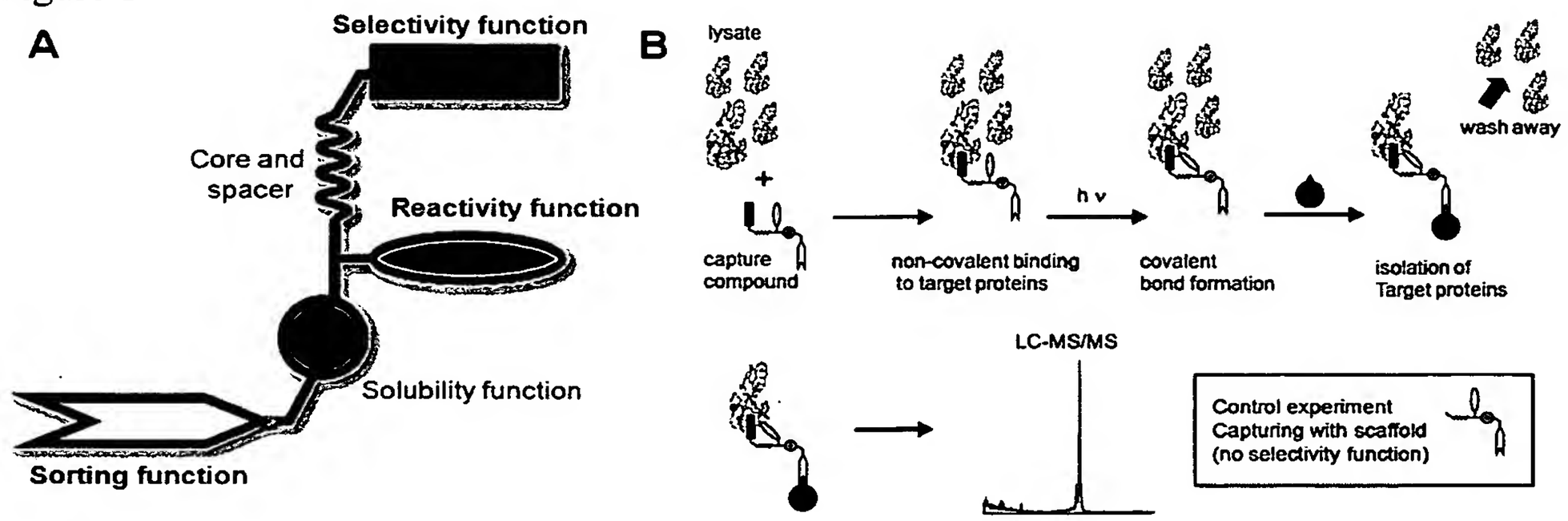

Figure 2

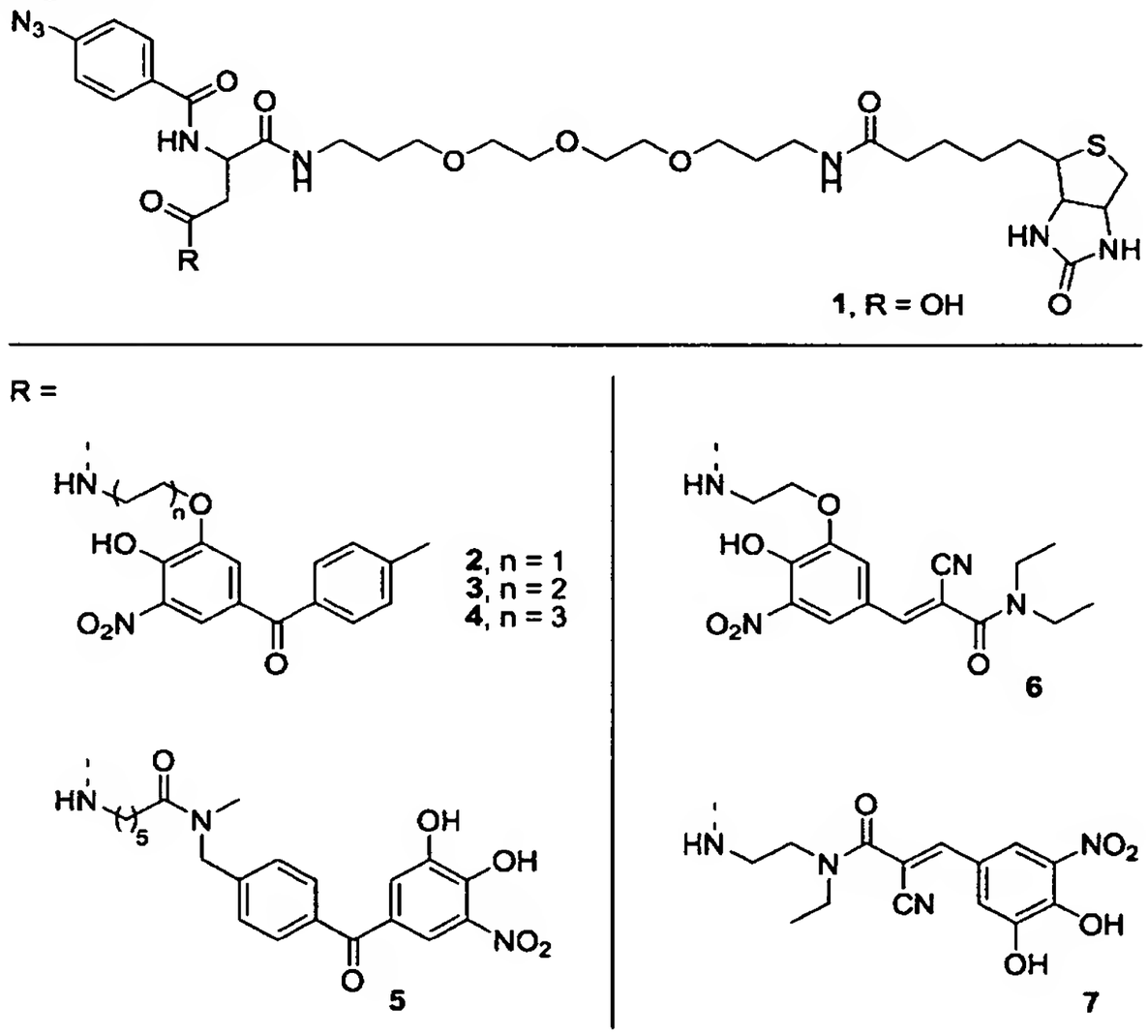

Figure 3A

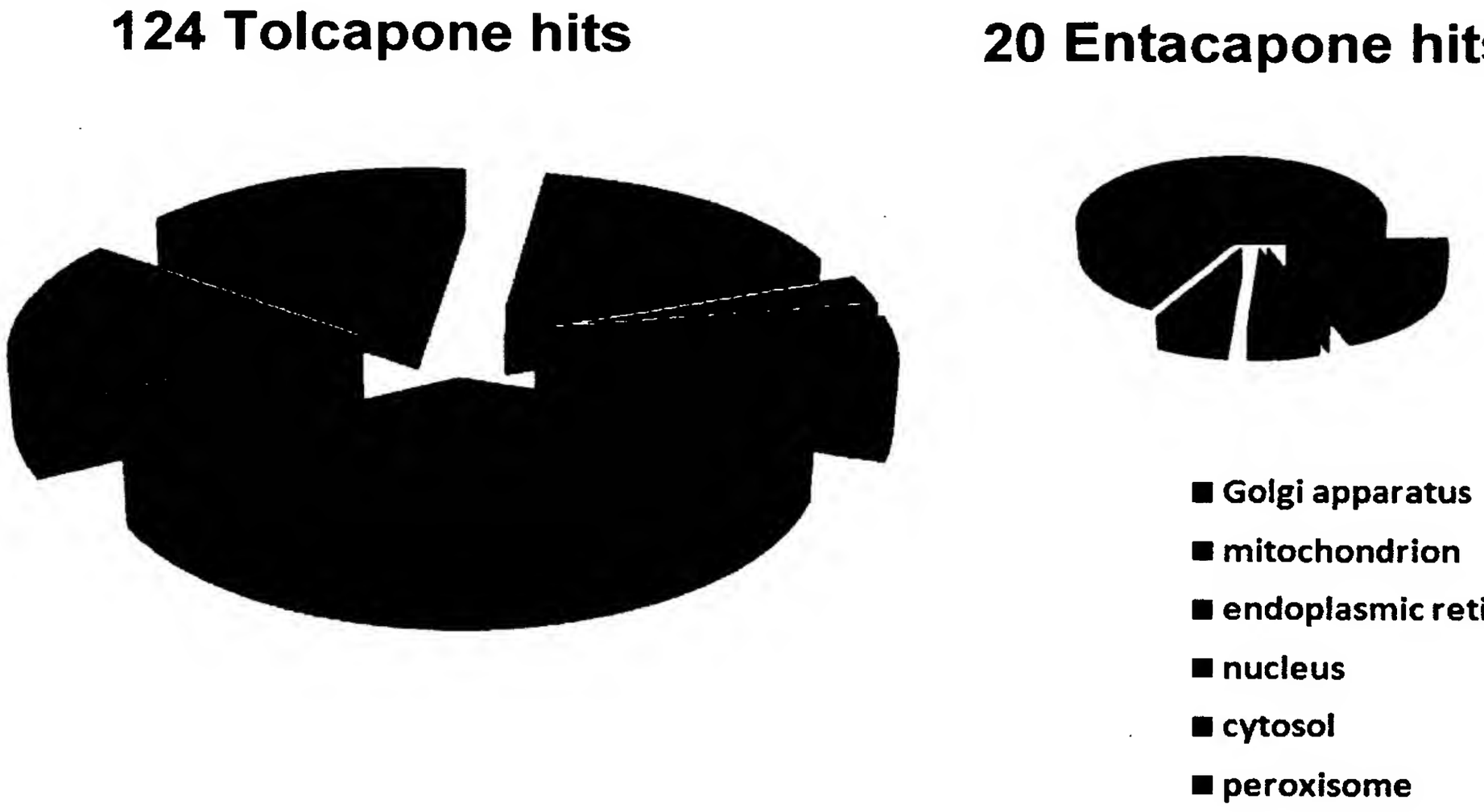

Figure 3B

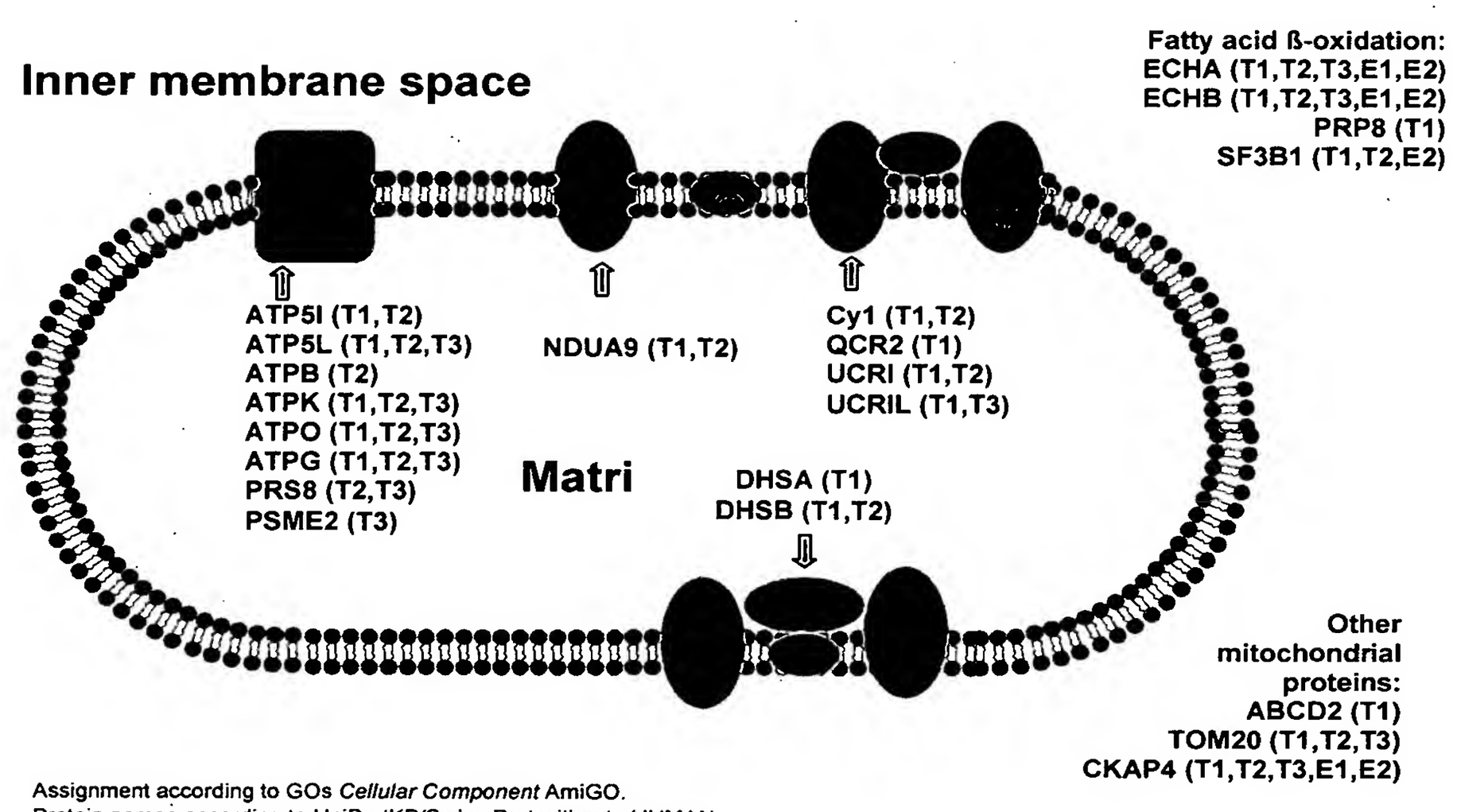

Assignment according to GOs *Cellular Component* AmiGO.
Protein names according to UniProtKB/Swiss-Prot without _HUMAN

Figure 4

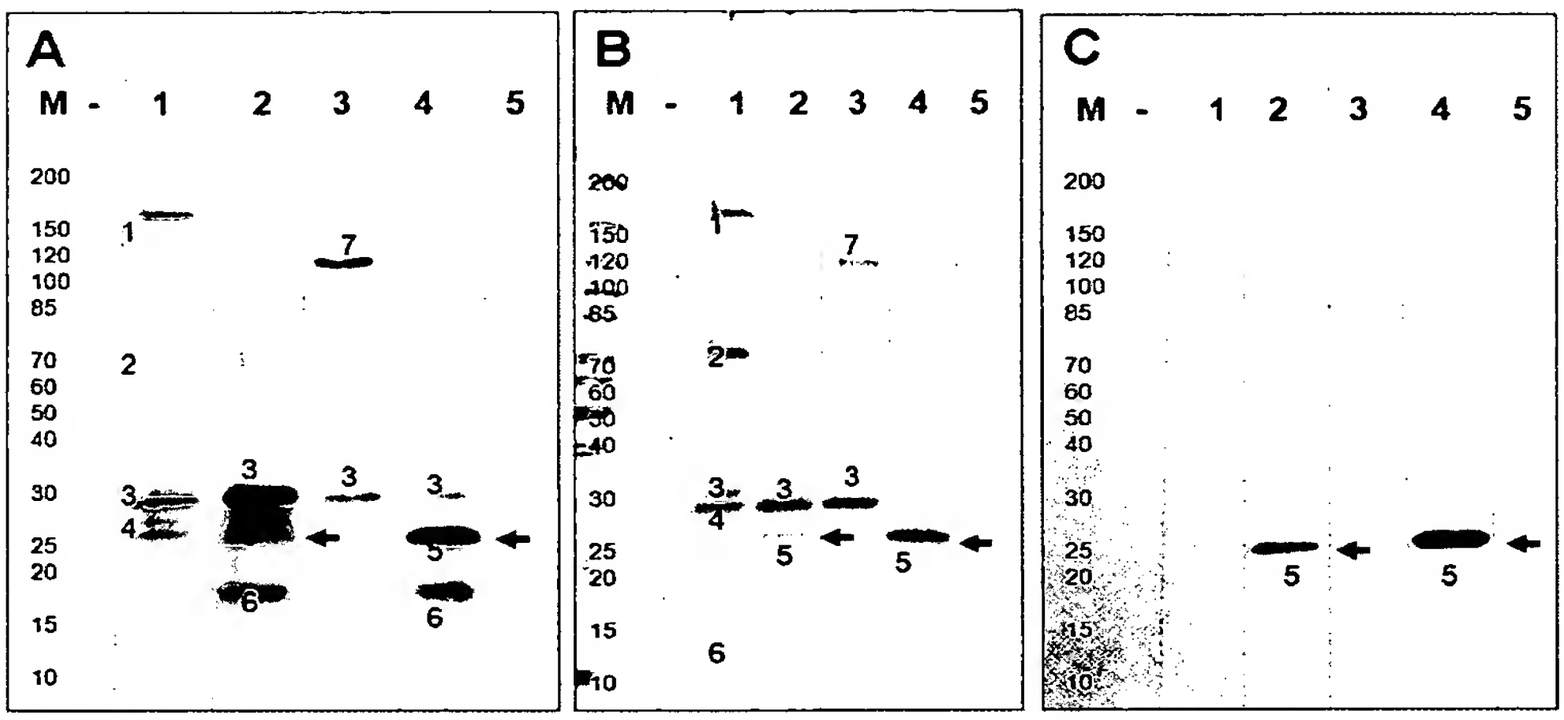
A
M - 1 2 3 4 5
200
150
120
100
85
70
60
50
40
30
25
20
15
10
B
M - 1 2 3 4 5
C
M - 1 2 3 4 5

Figure 5

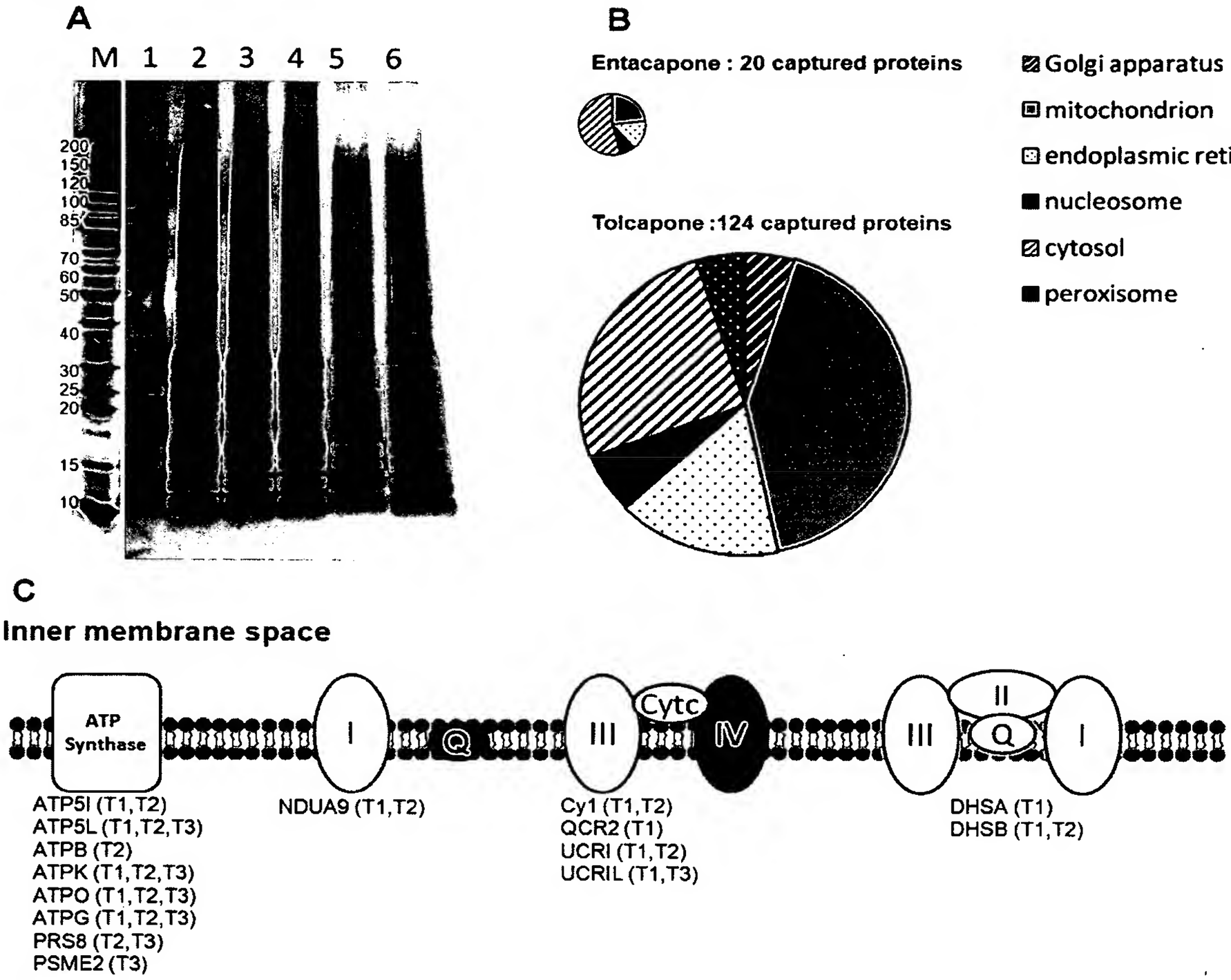
A
M 1 2 3 4 5 6
200
150
120
100
85
70
60
50
40
30
25
20
15
10
B
Entacapone : 20 captured proteins
Tolcapone :124 captured proteins
Golgi apparatus
mitochondrion
endoplasmic reticulum
nucleosome
cytosol
peroxisome
C
Inner membrane space
ATP Synthase
I
Q
III
Cytc
IV
III
II
Q
I
ATP5I (T1,T2)
ATP5L (T1,T2,T3)
ATPB (T2)
ATPK (T1,T2,T3)
ATPO (T1,T2,T3)
ATPG (T1,T2,T3)
PRS8 (T2,T3)
PSME2 (T3)
NDUA9 (T1,T2)
Cy1 (T1,T2)
QCR2 (T1)
UCRI (T1,T2)
UCRIL (T1,T3)
DHSA (T1)
DHSB (T1,T2)
Matrix

Figure 6

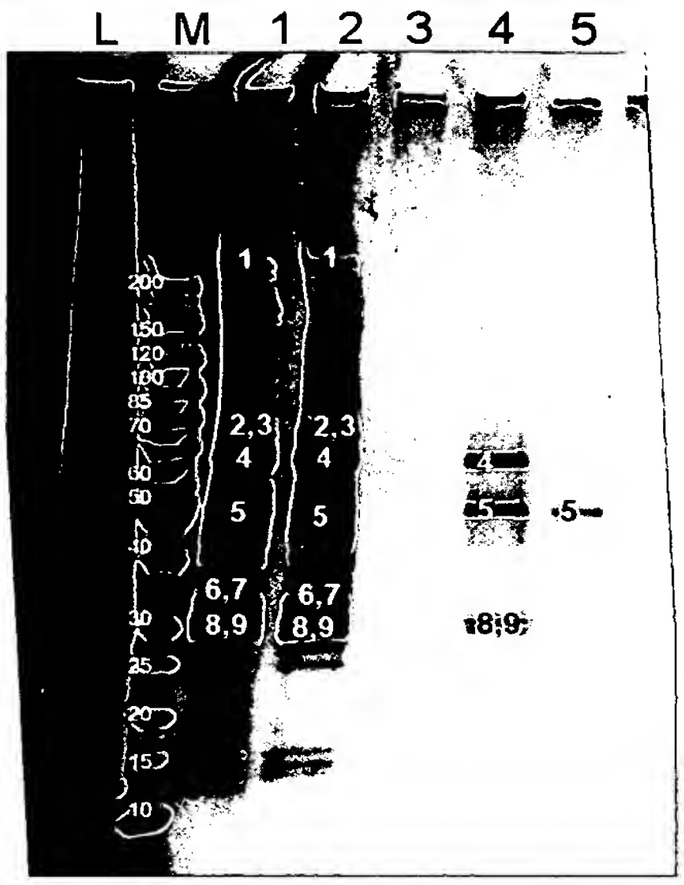

Table 1

Gelband	Abbreviation	Name	MW [kDa]	Accession	Cellular Process
1	CLH	Clathrin heavy chain 1	191	P11442	Endocytosis
2	DHB4	Peroxisomal multifunctional enzyme type 2	79	P97852	Fatty acid ß-Oxidation
2	ACOX3	Peroxisomal acyl-coenzyme A oxidase 3	78	Q63448	Fatty acid ß-Oxidation
3	ST2A2	Alcohol sulfotransferase A	33	P22789	Detoxification
4	ST2A1	Bile salt sulfotransferase	33	P15709	Detoxification
5	COMT	Catechol O-methyltransferase	30	P22734	Dopamin degradation
6	HBB1	Hemoglobin subunit beta-1	16	P02091	Oxygen transport
6	HBA	Hemoglobin subunit alpha-1/2	15	P01946	Oxygen transport
7	PYC	Pyruvate carboxylase	130	P52873	Krebs cycle

Table 2

Gelband	Abbreviation	Name	MW [kDa]	Accession	Cellular Process
1	**CLH**	Clathrin heavy chain 1	193	P49951	Endocytosis
2	DHB4	Peroxisomal multifunctional enzyme type 2	80	P97852	Fatty acid ß-Oxidation
3	ACSL1	Long-chain-fatty-acid-CoA ligase 1	79	P18163	Fatty acid metabolism
4	ACOX3	Peroxisomal acyl-coenzyme A oxidase 3	79	Q63448	Fatty acid ß-Oxidation
5	DHE3	Glutamate dehydrogenase 1, mitochondrial	62	P10860	Glutamate catabolism

Gelband	Abbreviation	Name	MW [kDa]	Accession	Cellular Process
6	ARHL1	Protein ADP-ribosylarginine hydrolase-like protein 1	40	Q5XIB3	Protein-amino acid de-ribolysation
7	DHB13	17-beta hydroxysteroid dehydrogenase 13	34	Q5M875	Oxidation/Reduction
8	AUHM	Methylglutaconyl-CoA hydratase, mitochondrial	34	Q9JLZ3	Branched amino acid catabolism
9	ECHM	Enoyl-CoA hydratase, mitochondrial	32	P14604	Fatty acid ß-oxidation

Synthetic Schemes

Scheme a. Synthesis of catechol-linked Tolcapone Capture Compounds

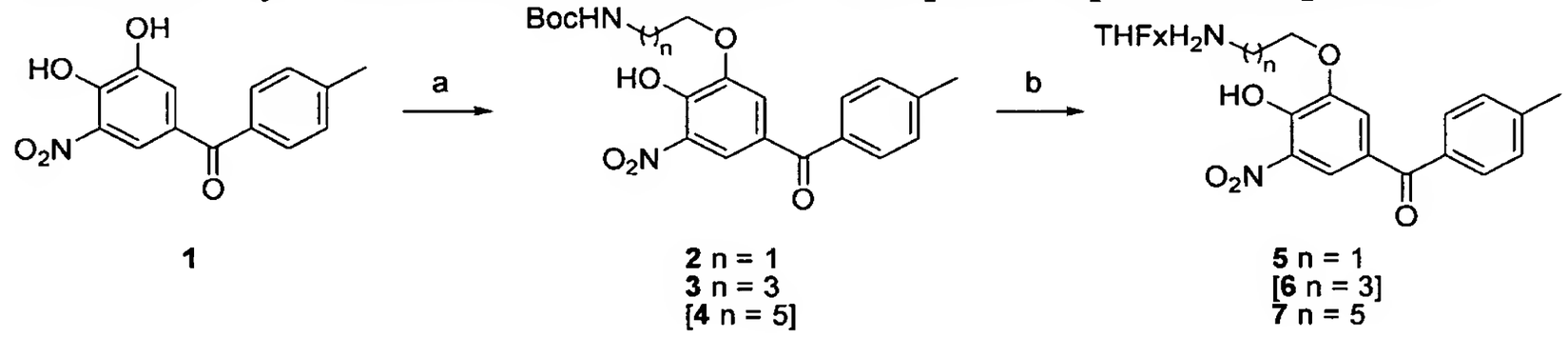

1

2 n = 1
3 n = 3
[**4** n = 5]

5 n = 1
[**6** n = 3]
7 n = 5

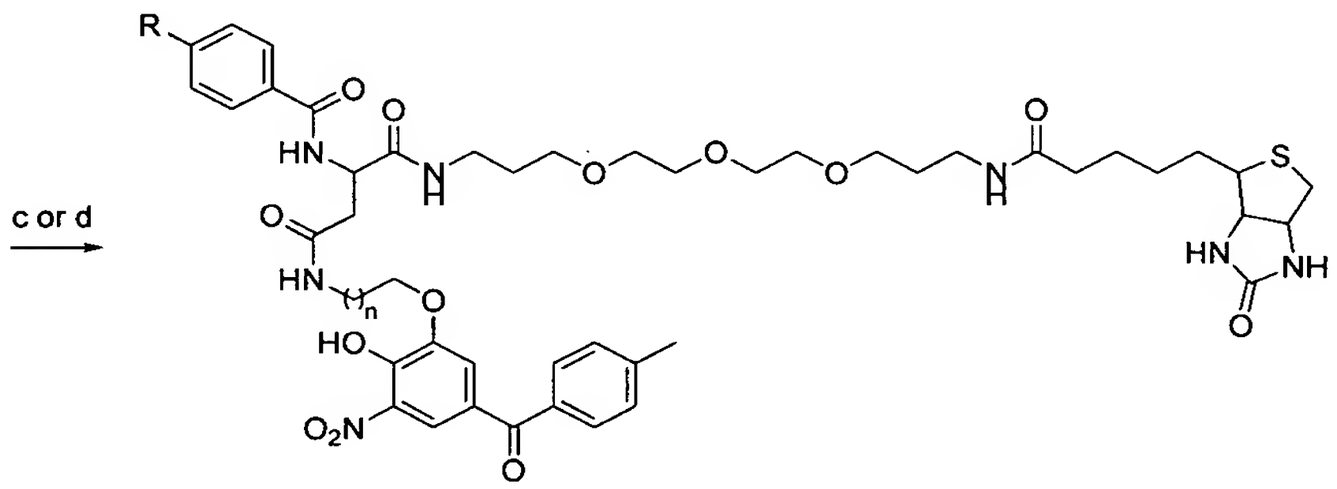

8 R = N_3, n = 1
9 R = N_3, n = 3
10 R = $CF_3CH(N_2)$, n = 3
11 R = N_3, n = 5

[a]Reagents and conditions: (a) NaH, $BocHN(CH_2)_nCH_2Br$, DMF, 23 °C, 17 h, 52% for **2**, 85% for **3**; (b) TFA, DCM, 23 °C, 30 min, 88% for **5**, 44% (over 2 steps) for **7**; (c) B1COOH, TEA, DMAP; HOBt, DIC, DMA, 23 °C, 2-3 d, 40% for **8**, 30% for **9**, 36% for **11**; (d) B2COOH, DIPEA, HATU, DMF, 23 °C, 17 h, 29% for **10**.

Scheme b. Synthesis of catechol-linked Entacapone Capture Compounds

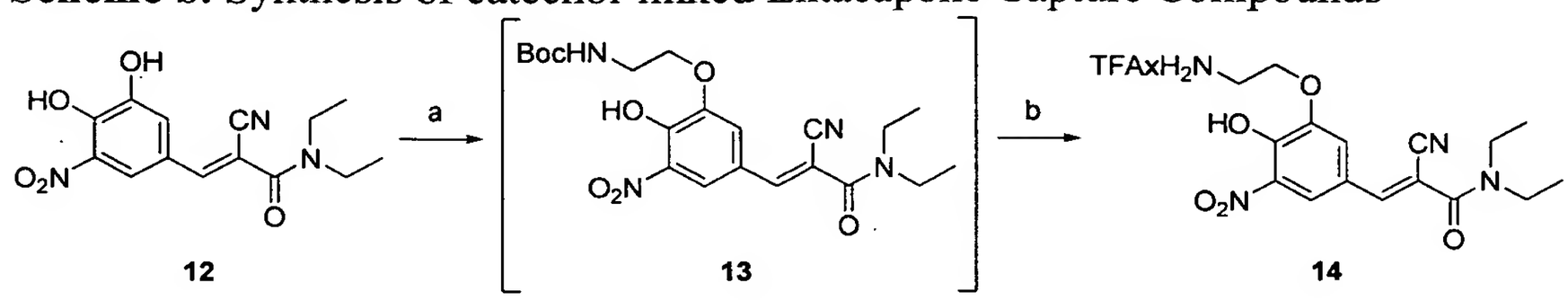

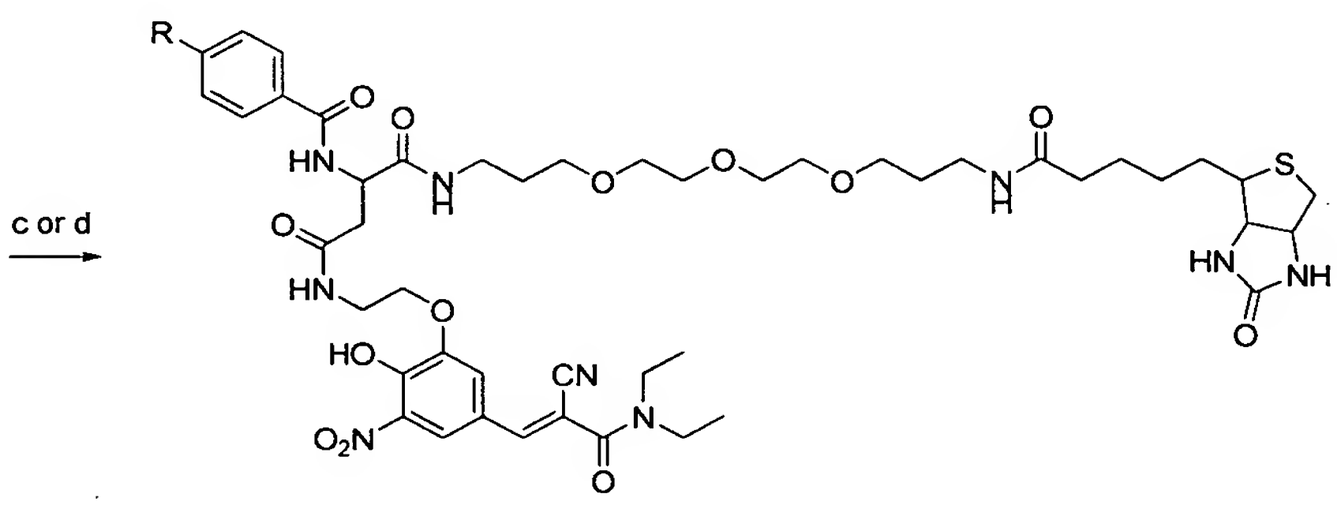

15 R = N_3
16 R = $CF_3CH(N_2)$

[a]Reagents and conditions: (a) NaH, $BocHNCH_2CH_2Br$, DMF, 23 °C, 17 h, used as crude; (b) TFA, DCM, 23 °C, 30 min, 15% (over 2 steps); (c) B1COOH, TEA, DMAP, HOBt, DIC, DMA, 23 °C, 2 d, 25% for **15**; (d) B2COOH, DIPEA, HATU, DMF, 23 °C, 17 h, 27% for **16**.

Scheme c. Synthesis of benzyl-linked Tolcapone Capture Compounds

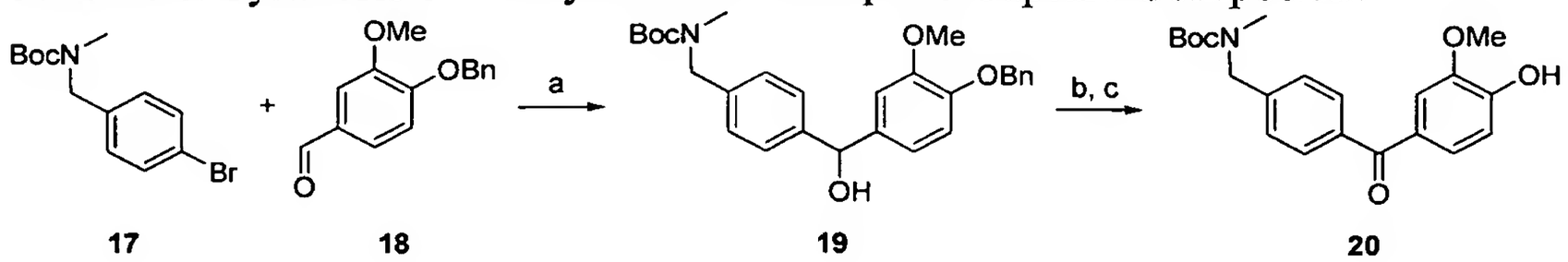

[a]Reagents and conditions: (a) *n*-BuLi, THF, -78 °C to 23 °C, 1 h, 30%; (b) NaO(*t*-Bu), *c*-hexanone, Toluene, 120 °C, 1.5 h, used as crude; (c) Ammonium formate, Pd/C, MeOH, 65 °C, 2 h, 64% (over 2 steps); (d) HNO_3, AcOH, 23 °C, 2 h, 67%; (e) BBr_3, DCM, -78 °C to 23 °C, 17 h, used as crude; (f) Boc-Gly, DCC, DMAP, TEA, DCM, 23 °C, 17 h, then HATU, DMA, 23 °C, 3 h, 37% (over 2 steps) for **22**; (g) Boc-6-Ahx-OH, DIPEA, HATU, DMF, 23 °C, 17 h, 43% (over 2 steps) for **23**; (h) TFA, DCM, 23 °C, 30 min, used as crude, (i) B1COOH, DIPEA, HATU, DMF, 23 °C, 17 h, 32% (over 2 steps) for **24**, 43% (over 2 steps) for **25**.

Scheme d. Synthesis of amide-linked Entacapone Capture Compounds

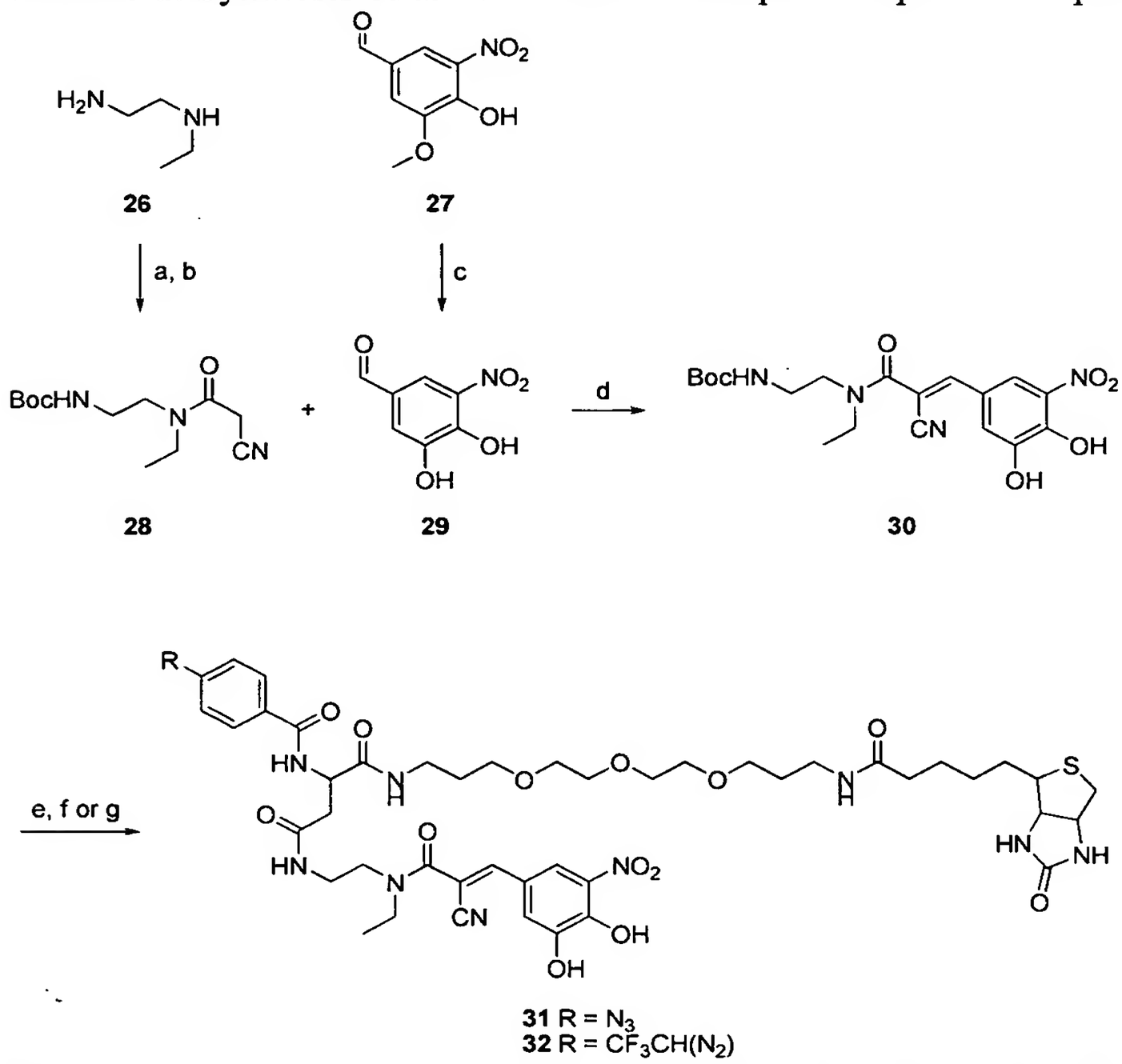

[a]Reagents and conditions: (a) HCl, Boc_2O, MeOH, 23 °C, 1 h, 93%; (b) Cyanoacetic acid, EDC, DMAP, DCM, 23 °C, 17 h, 78%; (c) $AlCl_3$, pyridine, 50 °C, 3 h, 62%; (d) piperidine, Toluene, *c*-Hex, 90 °C, 3 h, 68%; (e) TFA, DCM, 23 °C, 30 min, used as crude, (f) B1COOH, TEA, DMAP, HOBt, DIC, DMA, 23 °C, 3 d, 18% (over 2 steps) for **31**; (g) B2COOH, DIPEA, HATU, DMF, 23 °C, 17 h, 51% (over 2 steps) for **32**.

IN THE UNITED STATES PATENT AND TRADEMARK OFFICE

Applicant	: Hubert Köster, Ph.D. *et al.*	Art Unit	: 1639
Serial No.	: 10/760,085	Examiner	: Sue Xu Liu
Filed	: January 16, 2004	Conf. No.	: 8019
Cust. No.	: 77202		

Title : CAPTURE COMPOUNDS, COLLECTIONS THEREOF AND METHODS FOR ANALYZING THE PROTEOME AND COMPLEX COMPOSITIONS

Commissioner for Patents
P.O. Box 1450
Alexandria, VA 22313-1450

DECLARATION PURSUANT TO 37 C.F.R. §1.132

Sir:

I, HUBERT KÖSTER, declare as follows:

1. Qualifications

a. I obtained my Vordiplom (equivalent to a Bachelors) in Chemistry in 1963 and my Diplomchemiker (equivalent to a Masters) in Chemistry in 1966, both from the University of Hamburg, in Hamburg, Germany. In 1968, I obtained my Doctorate from the Technical University in Braunschweig, Germany based on work performed at the Max-Planck-Institute in Göttingen, Germany. I later became an Assistant Professor at the University of Hamburg in 1969, and became a tenured Professor in 1982 for Organic Chemistry and Biochemistry. I initiated the formation of Germany's first biotech company in 1981, Biosyntech, and have founded or co-founded a total of four biotech companies, primarily around my own inventions: Biosyntech in Hamburg, Germany, Milligen/Biosearch, Bedford/Burlington, MA, Sequenom, San Diego, CA/Hamburg and HK Pharmaceuticals, Inc. in San Diego, CA. At Biosyntech I was Chairman of the Scientific Advisory Board and Chief Technical Officer, at Milligen/Biosearch Vice President Science & Technology; at Sequenom I held the position first of Chief Scientific Officer and Chairman of the Scientific Advisory Board and later President and Chief Executive Officer and director of the Board. At HK Pharmaceuticals I was Chairman, president and CEO and director of the Board. I am currently the Managing Director of caprotec GmbH in Berlin, Germany, which succeeded HK Pharmaceuticals, Inc..

b. At Biosyntech I developed DNA Synthesizers and invented what today is state-of-the-art in DNA synthesis chemistry (inorganic polymeric supports and beta-cyanoethylphosphoamidites), at Milligen/Biosearch I was responsible for the development of systems for chemical synthesis of DNA and peptides as well as protein sequencing and DNA sequencing. At Sequenom we developed high throughput and highly accurate systems for

genotyping (SNP analysis) and allelotyping based on my inventions using mass spectrometry and at HK Pharmaceuticals/caprotec technologies for the analysis of complex protein mixtures (proteome analysis). I have about 120 scientific publications and I am author/inventor in more than 60 issued patents.

2. I am a joint inventor of the technology on which the above-captioned application is based, and I have reviewed the Office Action, mailed on July 28, 2009. The application describes and the claims are directed to methods, which are among those that caprotec has commercialized under the name Capture Compound Mass Spectrometry (CCMS), for identifying and studying small molecule-protein interactions.

3. As described in the response to the Office Action provided herewith, the claims are directed to methods for identifying targeted and non-targeted protein molecules with which small molecules, such as drugs, interact. This is achieved by providing a capture compound that contains a capture function, particularly an activatable group that forms covalent bonds with amino acid side chains (designated X), and that presents the small molecule (designated Y), such as the drug, a function for immobilization or sorting (designated Q). X, Y and Q are presented on a core, designated Z. As described in the application, the capture compounds can include additional components, such as a solubility function to increase or alter solubility as desired.

Capture compounds, including capture compounds whose capture function is activatable, for covalently capturing biomolecules are known (see, *e.g.*, the response with which this Declaration is provided). They, however, have not heretofore been used to present a small molecule whose interactions are to be assess in methods as claimed in this application. This application employs the capture compounds to present the small molecule (Y), such as a drug) in order to assess its interactions. Known capture compounds (with X, Z and Q groups) can be modified to present a drug, as described in the application, for use in this method. In addition, capture compounds for use in the method can be prepared as described in detail in the application.

4. To help appreciate the methods claimed in this application, a study, done under my direction at my company caprotec, is described below. This study has been published as (Fischer *et al.* Toxicol Sci. 2010 Jan;113(1):243-53. Epub 2009 Sep 26). This study provides a practical application of the claimed methods, which should aid in appreciating the methods and their power and elegance. As described in the application, drugs interact with their intended target protein, but also interact with other protein molecules (non-targets). For

drugs, non-targets can be involved with or responsible for undesirable side-effects. The claimed methods provide a way to identify, not only targets of small molecules, such as drugs, if not known, but also, non-targets.

In the study described herein, technology described in the application (referred to as CCMS herein) was used to elucidate the molecular basis for the difference in the toxicological profiles between the drugs Tolcapone and Entacapone. The results show that the claimed methods can unravel the set of proteins that interact with the drugs Tolcapone and Entacapone, respectively. Capture Compounds containing these two drugs capture the target protein COMT. Tolcapone, however, additionally binds to essential proteins in relevant pathways such as fatty acid ß-oxidation and oxidative phosphorylation. The results demonstrate that CCMS is a powerful tool for the generic identification of a drugs mode of action as well as non-target protein interactions.

The drugs Tolcapone and Entacapone are potent inhibitors of catechol-O-methyl transferase (COMT) for the treatment of Parkinson's disease (see, *e.g.*, Schapira et al., Neurology 55, S65-68; discussion S69-71 (2000)). Although these two drugs are similar, and even structurally identical with respect to the COMT binding moiety, they show a number of pharmacological differences and thus different clinical effectiveness (Deane *et al.*, Cochrane Database Syst Rev, CD004554 (2004)). A recent Cochrane meta-analysis of 14 studies in 2566 patients found both drugs to be statistically superior to placebo in increasing "on" time and decreasing „off" time and an approximately twice as long therapeutic effect of Tolcapone. This difference is reflected by the pharmacological profile, where Tolcapone is characterized by greater bioavailability and higher COMT affinity. Tolcapone increases the half-life of the dopamine precursor levodopa by 80 % vs. 40 % for Entacapone (Factor, Neurotherapeutics 5, 164-180 (2008)). A significant number of patients treated with Tolcapone show disturbed levels of liver enzymes and in 1998 three patient fatalities attributed to Tolcapone induced hepatotoxicity were reported (Deane et al. Cochrane Database Syst Rev, CD004554 (2004)).

Hence for these drugs, the target is COMT; any other molecules to with which these molecules interact are non-targets. Differences in non-targets with which these drugs interact elucidate the toxicity of Tolcapone compared to Entacapone. As described below, capture compounds that present each of these drugs (and each of these drugs in different orientations) were prepared. We incubated the capture compounds with protein fractions obtained from rat liver as well as lysates of the human hepatocyte cell line HepG2 to assess

isolate and identify protein molecules with which Tolcapone and Entacapone interact. Application of the CCMS technology reproducibly and unambiguously demonstrated that, in addition binding to COMT (the target protein), Tolcapone interacts with a large number of proteins carrying out essential functions in the respiratory chain, fatty acid ß-oxidation and bile acid synthesis. In the liver, fatty acids are metabolized by ß-oxidation in mitochondria and peroxisomes and by omega-oxidation in microsomes (drug non-targets) with which Entacapone does not interact. Peroxisomal beta-oxidation is responsible for the metabolism of very-long-chain-fatty acids. Impairment of correct peroxisomal function may lead to the accumulation of long-fatty acids or of hydrogen peroxide through the peroxisomal oxidative reactions. Both mechanisms contribute to hepatotoxicity and thus can explain the phenotype of Tolcapone side-effects.

5. The study, results and discussion

Materials and Methods

Chemical synthesis of Entacapone and Tolcapone Capture Compounds

Structures of final compounds are shown in Figure 2, below. The schema for synthesis also are set forth below. Referring to the schemes below, the compounds were synthesized using standard chemical synthetic methods as follows.

General. Unless otherwise noted, all reactions were performed in dried glassware under argon. Commercially available reagents and solvents were used as received without further purification. Column chromatography was carried out by using Geduran® Si 60 silica gel from Merck. MPLC purification was performed on a Buechi system (Buechi control unit C-620; 2 Buechi pump modules C-605; column - omnifit (230 x 15 mm); stationary phase - LiChroprep RP-select B 25-40 µm; Buechi UV photometer C-635; Buechi fraction collector C-660; mobile phase A: 0,1% AcOH Millipore grade; mobile phase B: acetonitrile prepsolv grade). LCT was carried out on a Waters system (HPLC pump Waters 1525; autosampler CTC HTS PAL; column oven Techlab K7 (40°C); diode array detector Waters 2998 (200 – 600 nm); MS detector Waters LCT time of flight mass spectrometer equipped with an electrospray ion source). LCT method A: column - Phenomenex Mercury MS (20 x 2 mm); stationary phase - Phenomenex Synergi Fusion RP, 2,5 µm; guard column Phenomenex Security Guard - Synergi Fusion RP; flow 0,4 mL/min; mobile phase A: 0,1% HCOOH Millipore grade; mobile phase B: acetonitrile LCMS grade; 10% B to 40% B in 9 min; 40% B to 100% B in 2 min; 100% B for 4 min. Accurate mass spectrometric analysis was performed on an LTQ Orbitrap XL mass spectrometer (Thermo Electron, Bremen, Germany)

utilizing a nanoelectrospray ion source (Proxeon Biosystems A/S, Denmark). For the analysis a 5 µM solution of the corresponding sample in water/acetonitrile (50/50, 0.1 % formic acid) was directly injected via the syringe pump with a flow rate of 1 µl/min. The singly-charged polydimethylcyclosiloxane background ion (Si(CH3)2O)6H+ (m/z 445.120025) generated during the electrospray process from ambient air was used as lock mass for real time internal recalibration. Further mass spectrometric settings were as follows: spray voltage was set to 1.7 kV, temperature of the heated transfer capillary was set to 200 °C. MS spectra (from m/z 400–2000) were acquired in the orbitrap with a resolution of r= 60,000 at m/z 400 (after accumulation to a target value of 500,000 charges in the linear ion trap). Proton nuclear magnetic resonance (1H NMR) spectra and carbon nuclear magnetic resonance (13C NMR) spectra were recorded on an Avance 400 (400 MHz) from Bruker. Chemical shifts are reported in ppm relative to CHCl3 (δ 7.27) for 1H NMR and the central resonance of CDCl3 (δ 77.0) for 13C NMR. The synthesis of the scaffolds is published elsewhere (ChemBioChem accepted). DCC = N,N'-Dicyclohexylcarbodiimide; DIC = N,N'-Diisopropylcarbodiimide; DIPEA = N,N-Diisopropylethylamine; DMA = N,N-Dimethylacetamide; DMF = N,N-Dimethylformamide; EDC = N-(3-Dimethylaminopropyl)-N'-ethylcarbodiimide; HATU = O-(7-Azabenzotriazol-1-yl)-N,N,N'-tetramethyluronium hexafluoro-phosphate; HOBt = 1-Hydroxybenzotriazole; DMAP = 4-Dimethylaminopyridine; TEA = Triethylamine; TFA = Trifluoroacetic acid; cHex = Cyclohexane.

General procedure "phenol-substitution." Under an atmosphere of argon, a solution of the mentioned phenol in dry DMF (0.1 M) was treated with NaH (2.2 eq) and stirred for 10 min. A highly concentrated solution of the corresponding bromide (1.2 eq) in dry DMF was added dropwise and the reaction mixture was stirred for 17 h at 23 °C. If LCT analysis showed incomplete conversion, additionally NaH (1.1 eq) was added and the reaction mixture was stirred for 10 min before additionally bromide (0.6 eq) was added. Stirring was continued for additionally 17 h at 23 °C, then the reaction was quenched with water and HCl solution (2 M) and extracted with DCM. The solvents were removed under reduced pressure and the crude product was purified by column chromatography.

General procedure "Boc deprotection." A suspension of the mentioned Boc-protected amine in DCM (0.2 M) was treated with TFA (DCM/TFA, 3/1 v/v) at 0 °C. The reaction mixture was allowed to warm gradually to 23 °C and was stirred for 30 min. The solvent and TFA was intensively removed under reduced pressure. The crude product generally was used without further purification or was purified by MPLC in special cases.

General procedure "HATU mediated amide coupling". Under an atmosphere of argon, a solution of the mentioned amine (mostly as TFA-salt) in dry DMF (0.05 M) was treated with a highly concentrated solution of B1- or B2-Scaffold respectively (1.0 eq) in dry DMF and DIPEA (5 eq). After being stirred for 10 min, HATU (1.2 eq) was added and the reaction mixture was stirred for 17 h at 23 °C with exclusion of light. The solvent was removed under reduced pressure and the crude product was purified by MPLC.

General procedure "DIC/DMAP mediated amide coupling." Under an atmosphere of argon, a solution of the mentioned amine (mostly as TFA-salt) in dry DMA (0.02 M) was treated with B1- or B2-Scaffold respectively (1 eq), Triethylamine (2 eq), DMAP (2 eq), HOBt (2 eq) and 1,3-Diisopropylcarbodiimide (5 eq). The reaction mixture was stirred for 2-3 d at 23 °C with exclusion of light. The solvent was removed under reduced pressure and the crude product was purified by MPLC.

Compound 2. Starting from commercial available Tolcapone 1 (compound 1) and according to general procedure "phenol-substitution", title compound 2 (39.4 mg, 52%) could be observed after column chromatography (cHex/EtOAc, 2:1 to 1:2) as a yellow solid. 1H NMR (CDCl3): δ 11.03 (br s, 1H), 8.14 (d, J = 1.7 Hz, 1H), 7.69 (d, J = 1.7 Hz, 1H), 7.67 (d, J = 8.0 Hz, 2H), 7.32 (d, J = 8.0 Hz, 2H), 5.09 (br s, 1H), 4.19 (t, J = 5.0 Hz, 2H), 3.63 (m, 1H), 2.46 (s, 3H), 1.45 (s, 9H). LCT method A.

Compound 3. Starting from commercial available Tolcapone 1 and according to general procedure "phenol-substitution", title compound 3 (69.2 mg, 85%) could be observed after column chromatography (cHex/EtOAc, 2:1) as a yellow solid.

Compound 4. Starting from commercial available Tolcapone 1 and according to general procedure "phenol-substitution", crude compound 4 was observed after filtration over silica as a yellow solid and was used for the next step without further purification.

Compound 5. Starting from compound 2 and according to general procedure "Boc deprotection", title compound 5 (31.9 mg, 88%) could be observed after column chromatography (DCM/MeOH, 100:1 to 5:1) as a yellow solid.

Compound 6. Starting from compound 3 and according to general procedure "Boc deprotection", crude compound 5 could be observed as a yellow, solid product and was used without further purification.

Compound 7. Starting from crude compound 4 and according to general procedure "Boc deprotection", title compound 7 (57.9 mg, 44% over 2 steps) could be observed as an orange solid after MPLC.

Compound 8. Starting from compound 5 and according to general procedure "DIC/DMAP mediated amide coupling", title compound 8 (5 mg, 40%) could be observed as a yellow solid after MPLC.

Compound 9. Starting from crude 6 and according to general procedure "DIC/DMAP mediated amide coupling", title compound 9 (8.3 mg, 30%) could be observed as a yellow solid after MPLC.

Compound 10. Starting from crude 6 and according to general procedure "HATU mediated amide coupling", title compound 10 (8 mg, 29%) could be observed as a yellow solid after MPLC.

Compound 11. Starting from compound 7 and according to general procedure "DIC/DMAP mediated amide coupling", title compound 11 (10.0 mg, 36%) could be observed as a yellow solid after MPLC.

Compound 12. Entacapone 12 was prepared according to literature. Analytical data was consistent to those reported.

Compound 14. Under an atmosphere of argon, a solution of Entacapone 12 (76 mg, 0.25 mmol) in dry DMF (0.6 mL) was treated with NaH (13.1 mg, 0.55 mmol) and stirred for 10 min. A solution of tert-butyl 2-bromoethylcarbamate (100 mg, 0.45 mmol) in dry DMF (0.1 mL) was added dropwise and the reaction mixture was stirred for 17 h at 23 °C. As LCT analysis showed incomplete conversion, additionally NaH (6.6 mg, 0.28 mmol) was added, the mixture was stirred for 10 min, and tert-butyl 2-bromoethylcarbamate (50 mg, 0.23 mmol) was added. The reaction mixture was stirred for additionally 5 h at 23 °C, quenched with water (60 µL) and the crude product was filtered over silica. The solvents were removed under reduced pressure to complete dryness and the crude product was dissolved in DCM (2.5 mL). TFA (1 mL) was added at 0 °C, the reaction mixture was stirred for 10 min, was then allowed to warm gradually to 23 °C and was stirred for additionally 30 min. The solvent and TFA was removed under reduced pressure and the crude product was purified by MPLC to yield title compound 14 (17.7 mg, 15%) as an orange solid.

Compound 15. Starting from compound 14 and according to general procedure "DIC/DMAP mediated amide coupling", title compound 15 (3.4 mg, 25%) could be observed as a yellow oil after MPLC.

Compound 16. Starting from compound 14 and according to general procedure "HATU mediated amide coupling", title compound 16 (3.7 mg, 27%) could be observed as an orange oil after MPLC.

Compound 17. Under an atmosphere of argon, a solution of commercial available 4-Bromo-N-methylbenzylamine (500 mg, 2.5 mmol) in dry DCM (12.5 mL) was treated with TEA (0.42 mL, 3 mmol) and Boc2O (654 mg, 3.0 mmol) at 0 °C. The reaction mixture was stirred for 1 h at 0 °C, was allowed to warm gradually to 23 °C and stirred additionally 2 h. The crude product was portioned between water and DCM. The organic solvent was removed under reduced pressure and the crude product was purified by column chromatography (cHex/EtOAc, 20:1 to 2:1) to give title compound 17 (716 mg, 95%) as a clear, colorless oil.

Compound 19. Under an atmosphere of Argon, a solution of n-BuLi (1.55 ml, 1.6 M in hexanes, 2.48 mmol) was added dropwise to a solution of compound 17 (679 mg, 2,26 mmol) in dry THF (7 mL) at -78 °C. The solution was stirred for 30 min at -78 °C. Then, a solution of aldehyde 18 (522 mg, 2.15 mmol) in dry THF (3 mL) was added dropwise that the temperature did not rise over -70 °C. The reaction mixture was stirred for 30 min at -78 °C, gradually warmed to 23 °C and stirred additionally 30 min. The reaction was quenched with water (20 mL), extracted with DCM and the solvents were removed under reduced pressure. The crude product was purified by column chromatography (cHex/EtOAc, 20:1 to 3:1) to give the title compound (296 mg, 30%) as a colorless oil.

Compound 20. Sodium tert-butoxide (83 mg, 0.86 mmol) was added to a solution of alcohol 19 (266 mg, 0.57 mmol) in Toluene (2.9 mL) under argon. Cyclohexanone (364 µL, 3.51 mmol) was added dropwise under stirring and the reaction mixture was stirred for 1.5 h at 120 °C. Then, 20 mL water were added, the layers were separated, and the water layer was extracted with EtOAc. The combined organic layers were washed with brine, dried over MgSO4 and the solvents were removed under reduced pressure. The crude product was dissolved in dry MeOH under argon and treated with Ammonium formate (181 mg, 2.87 mmol) and Palladium (7.1 mg, 10% on carbon, 0.067 mmol). The reaction mixture was stirred for 2.5 h under reflux. After cooling to 23 °C, the crude product was filtered over a pad of Celite®, the filter cake was washed with MeOH and the solvent was removed under reduced pressure. The crude product was purified by column chromatography (cHex/EtOAc, 20:1 to 2:1) to give title compound 20 (137 mg, 64%) as a colorless oil.

Compound 21. At 18 °C, a solution of compound 20 (73 mg, 0.2 mmol) in AcOH (0.4 mL) was treated with nitric acid (15 µl, 0.22 mmol) and stirred for 2 h at 23 °C. Then, DCM (5 mL) and water (5 mL) were added, the layers were separated and the water layer was extracted with DCM. The organic layers were combined; the solvent was removed under

reduced pressure and the crude product was purified by column chromatography (DCM/MeOH, 100:1) to give title compound 21 (54.9 mg, 67%) as a yellow solid.

Compound 22. At -78 °C a solution of Boron tribromide (84 µl, 1.0 M in DCM, 0.084 mmol) was added dropwise to a solution of compound 21 (10 mg, 0.024 mmol) in dry DCM (0.25 mL) under argon. The reaction mixture was stirred for 10 min at -78 °C and additionally 17 h at 23 °C. The solvent was removed under reduced pressure to complete dryness, MeOH was added carefully and the solution was stirred for 5 min. The solvent was removed under reduced pressure and the crude product was suspended in dry DCM (0.2 mL). At 0 °C BocGly (4.2 mg, 0.024 mmol), DCC (5.94 mg, 0.029 mmol), DMAP (0.3 mg, 2.4 µmol) and TEA (17 µl, 0.12 mmol) were added. The reaction mixture was stirred for 2 h at 0 °C and additionally 17 h at 23 °C. As LCT analysis showed incomplete conversion, BocGly (2.1 mg, 0.012 mmol), HATU (5.48 mg, 0.014 mmol) and dry DMA (0.2 mL) were added. The reaction mixture was stirred for 3 h at 23 °C. The solvents were removed under reduced pressure and the crude product was purified by MPLC ~~(~~to give title compound 22 (4.1 mg, 37%) as a red oil.

Compound 23. At -78 °C a solution of Boron tribromide (84 µl, 1.0 M in DCM, 0.084 mmol) was added dropwise to a solution of compound 21 (10 mg, 0.024 mmol) in dry DCM (0.25 mL) under argon. The reaction mixture was stirred for 10 min at -78 °C and additionally 17 h at 23 °C. The solvent was removed under reduced pressure to complete dryness, MeOH was added carefully and the solution was stirred for 5 min. The solvent was removed under reduced pressure and a portion of crude product (10.6 mg, 0.035 mmol) was suspended in dry DMF (0.5 mL). At 0 °C 6-(Boc-amino)hexanoic acid (8.9 mg, 0.039 mmol), DIPEA (30.5 µL mg, 0.175 mmol) and HATU (16.0 mg, 0.12 mmol) were added. The reaction mixture was stirred for 2 h at 0 °C and additionally 17 h at 23 °C. The solvent was removed under reduced pressure and the crude product was purified by MPLC to give title compound 23 (7.7 mg, 43%) as a red oil.

Compound 24. Starting from compound 22 and according to general procedures "Boc deprotection" and "HATU mediated amide coupling", title compound 24 (3 mg, 32%) could be observed as a red solid after MPLC.

Compound 25. Starting from compound 22 and according to general procedures "Boc deprotection" and "HATU mediated amide coupling", title compound 25 (7 mg, 43%) could be observed as a red solid after MPLC.

Compound 28. At 0 °C, N-Ethylethylenediamine (2.0 g, 22.7 mmol) was added dropwise to a solution of HCl in MeOH (18.2 mL, 1.25 M) under argon. The solution was allowed to warm gradually to 23 °C and was stirred for 15 min. Water was added and stirred for 30 min. A solution of Boc2O (4.95 g, 22.7 mmol) in MeOH (15 mL) was added dropwise and the reaction mixture was stirred for additionally 1 h. The solvent was removed under reduced pressure, NaOH solution (60 mL, 2 N) was added and the crude product was extracted with DCM (3 x 100 mL). The combined organic layers were washed with brine, dried over $MgSO_4$ and the solvent was removed under reduced pressure to yield a crude product (3.98 g, 93 %) as colorless needles. The crude product (2.0 g, 10.6 mmol) was added to a solution of Cyanoacetic acid (0.9 g, 10.6 mmol) in dry DCM (100 mL). At 0 °C the solution was treated with EDC (2.44 g, 12.7 mmol) and DMAP (32 mg, 0.27 mmol) and stirred for 2 h at 0 °C and additionally 17 h at 23 °C. Water was added and the crude product was extracted with DCM (3 x 100 mL). The combined organic layers were washed with HCl solution (1 M) and brine, dried over MgSO4 and the solvent was removed under reduced pressure. The crude product was purified by column chromatography (cHex/EtOAc, 1:1 to 1:2) to give title compound 28 (2.11 g, 78%) as a colorless oil (rotamers or regioisomers).

Compound 29. Under an atmosphere of argon, a solution of Nitrovanillin (5.0 g, 25.36 mmol) in dry pyridine (13 mL) was treated with AlCl3 (4.06 g, 30.43 mmol) at 0 °C. The reaction mixture was stirred for 3 h at 50 °C. After cooling to 0 °C, HClconc (15 mL) was added and the crude product was extracted with EtOAc. The organic layers were combined, washed with brine, dried over MgSO4 and the solvents were removed under reduced pressure. The crude product was purified by recrystallization from cHex/EtOAc (4:1) to give a clean batch of title compound 29 (2.86 g, 62%) and a second batch mainly containing the title compound (1,66 g) as a yellow-orange solid.

Compound 30. A solution of compound 28 (67 mg, 0.26 mmol) in a solvent mixture of Toluene and cHex (0.35 mL, 1:1 (v/v)) was treated with aldehyde 29 (36.6 mg, 0.2 mmol) and piperidine (2.0 µL, 0.02 mmol). The reaction mixture was stirred for 3 h at 90 °C. Then, the solvent was removed with a stream of nitrogen at 90 °C and the crude product was purified by MPLC to yield title compound 30 (57 mg, 68%) as an orange oil.

Compound 31. Starting from compound 30 and according to general procedures "Boc deprotection" and "DIC/DMAP mediated amide coupling" title compound 31 (8.1 mg, 18%) could be observed as a yellow oil after MPLC.

Compound 32. Starting from compound 30 and according to general procedures "Boc deprotection" and "HATU mediated amide coupling" title compound 32 (13.2 mg, 51%) could be observed as a an orange oil after MPLC.

Analysis of the Capture Compounds by mass spectrometry and NMR confirmed the identity and structure of the final reaction products. Purity of the compounds was determined by 1H-NMR and was found to be greater than 95 %.

Computational methods

Preparation of Molecular Structures: Atomic coordinates for the ternary complex between COMT, the cosubstrate S-adenosyl-methionine, and the inhibitor BIA3-335 was obtained from the Protein Data Bank (PDB, www.rcsb.org) file 1H1D. The magnesium ion was considered covalently bound to Asp141 and Asp169. The side chain of Lys144 was modeled in the neutral form. The structure was minimized with the molecular modeling package SYBYL8.1 (Tripos Inc., St. Louis, USA) using the Tripos force field, Gasteiger-Marsili charges and the Powell gradient algorithm. The backbone, the magnesium ion, and its coordination atoms (O1 in Asp141, O2 in Asp169, OD1 in Asn170, the oxygen of HOH53, and both oxygens in the catechol moiety of the ligand) were frozen during minimization. Molecular docking: In order to reduce the rotational degrees of freedom and to focus on the interactions of the selectivity and the reactivity functions with the protein, the Capture Compounds were modelled without the polyethyleneglycol linker and the biotin moiety. Unrestrained flexible docking between COMT and Tcp-Bz-CC was performed with Surflex-Dock5 included in the SYBYL Package using the default settings. The co-crystallized ligand was extracted and the protomol was generated based on the ligand. Twenty poses were sampled.

The results were investigated for the correct binding of the catechol moiety in the binding pocket and the positioning of the crosslinking unit in vicinity of the protein surface, especially close to polar side chains. The polyethyleneglycole linker and the biotin moiety (based on the PDB file with the accession number 1STP) were added manually and minimized using standard procedures.

COMT affinity assay

Bioanalytical services for the determination of KD values were provided by MDS Pharma Services Inc (Peitou Taipei, Taiwan).

Preparation of rat liver subcellular fractions

Fractionation of rat liver was carried out essentially as described in the study of Emig *et al.* (J. Biol. Chem. 270, 13787-13793 (1995)). Briefly, rat liver was homogenized using a motor-driven glass-Teflon homogenizer (Sartorius Stedim Biotech GmbH, Aubagne Cedex, France) in 10 volumes of homogenization buffer per gram of tissue wet weight (0.32 M sucrose, 5 mM HEPES/NaOH pH 7.4, completeTM EDTA-free protease inhibitor cocktail (Roche, Mannheim, Germany), using 12 strokes at 900 rpm at 4 °C. The homogenate was centrifuged at 1000 ×g (Universal 300R centrifuge, Hettich Centrifuges, Beverly, USA) for 10 min. The supernatant was decanted and further centrifuged at 12000 ×g for 20 min. The supernatant (soluble fraction, cytosol) from this procedure was concentrated using iCon Concentrators® (Thermo Fisher Scientific, Schwerte, Germany), aliquoted, and snap frozen. The protein concentration was determined according to Bradford (Anal Biochem 72, 248-254 (1976)). The Pellet was resuspended to 0.32 M sucrose (30 × weight in grams), and further homogenized in a motor-driven glass-teflon homogenizer (Potter S, Sartorius Stedim Biotech, Aubagne Cedex, France) using 6 strokes at 900 rpm at 4 °C. The suspension was centrifuged again at 12000 × g for 20 mins. The pellet was resuspended in 0.25 M sucrose, Tris/HCl pH 8.1 using 6 strokes at 900 rpm, and carefully placed on top of a sucrose solution with 1.5 M sucrose. The sample was centrifuged at 90,000 × g for 1h in an ultracentrifuge (WX-80 Ultra, Rotor TH641, Thermo Fisher Scientific, Schwerte, Germany).

Microsomes were recovered from the interphase between the 0.25 M and 1.5 M sucrose solutions, while mitochondria were pelleted. These fractions were each solubilized for 1 h at room temperature using cell opening buffer (6.7 mM 4-morpholineethanesulfonic acid, 6.7 M sodium acetate, 6.7 mM 4-(2-hydroxyethyl)piperazine-1-ethanesulfonic acid (HEPES), 200 mM NaCl, 10 mM ß mercaptoethanol, pH 7.6), supplemented with completeTM protease inhibitor (Roche, Mannheim, Germany) and 0.5 % dodecylmaltoside (DDM). Subsequently, the suspensions were cleared by centrifugation at 10,000 rpm for 15 min. The protein concentrations of the supernatants were determined according to Bradford (Anal Biochem 72, 248-254 (1976)).

Capturing experiment in HepG2 and rat liver subcellular fractions

Capture experiment: 0.4 mg HepG2 cell lysate was supplemented with 20 µl of 5 x capture buffer (20 mM HEPES, 50 mM potassium acetate, 10 mM magnesium acetate and 50 % glycerol), and the reaction volume was adjusted to 100 µl with ultrapure water. Capture beads were obtained by vigorously mixing 25 µL of the respective Capture Compound or

scaffold (100 µM) with 50 µL of Dynabeads® MyOneTM Streptavidin C1, (Invitrogen, Karlsruhe, Germany) at room temperature for 5 min. After washing twice with wash buffer (WB, containing 50 mM Tris HCl, pH 7.5, 1 mM EDTA, 1 M NaCl, 0.5 µM octyl-ß-D-glucopyranoside) the respective magnetic capture beads were added to the reaction mix and rotated at 4 °C for ca 3 hrs with protection from light. Subsequently, the reaction mixture was irradiated using the device for irradiation from caprotec sold as caproBox^{TM} (wavelength 310 nm, irradiance Ie≥10 mW/cm^2) for 20 min with mixing at intervals of 2.5 min. After UV light exposure, the beads were collected using the caprotec device called caproMagTM, a device for the handling of magnetic beads (caprotec bioanalytics GmbH, Berlin, Germany), and washed first six times with 200 µL WB (caprotec bioanalytics GmbH, Berlin, Germany), and then twice with ultrapure water. Until further analysis beads were stored at 4 °C in ultrapure water.

For capture experiments using fractions of rat liver, the initial protein amounts in the capture reactions were 0.4 mg for mitochondrial or microsomal, and 1.4 mg in case of the cytosolic fraction, respectively. Capture buffer and WB were supplemented with 0.1 % n dodecyl-ß-maltoside (Glycon, Luckenwalde, Germany).

Western Blot

After separation by SDS-PAGE captured proteins were transferred to a nitrocellulose membrane (Whatman, Kent, UK). Proteins were stained with Ponceau red (Sigma, Steinheim, Germany) to control the blotting efficiency (data not shown). The membrane was blocked for 1 h at room temperature with a solution of 5 % (w/v) skimmed milk powder in Tris buffered saline (20 mM Tris HCl, pH 7.5, 150 mM NaCl (TBS), supplemented with 0.1 % (v/v) Tween 20 (TBS T)). Incubation with the primary antibody was performed for 1 h at room temperature or over night at 4 °C followed by three wash steps in TBS T and incubation with the secondary antibody for 1 h at room temperature. Antibodies were diluted in 5 % skimmed milk powder in TBS T as follows: anti-COMT 1:2,500, secondary anti-goat antibody conjugated to horseradish peroxidase 1:2,000. After three washes in TBS-T and one wash in TBS membranes were treated using Pierce ECL Western Blotting Substrate (Thermo Fisher Scientific, Schwerte, Germany) according to the manufacturer's instructions. Hyperfilm ECL films (GE Healthcare, München, Germany) were used to detect the chemoluminescence. In case of blots for the detection of biotinylated proteins streptavidin-horseradish peroxidase was used instead of a first antibody at a dilution of 1:1,000 in 5 % skimmed milk powder in

TBS T and Blots developed directly after washing three times with TBS-T and once with TBS.

In solution digest

For analysis of the complex protein mixture obtained after capture experiments, the washed beads were resuspended in 10 µl 50 mM ammonium bicarbonate and 1 µl trypsin (0.5 µg/µl) (sequencing grade, Roche, Mannheim, Germany) for 16 h at 37 °C on a thermoshaker (Eppendorf, Hamburg, Germany). Subsequently, tryptic peptides were desalted using Stage Tips® (Proxeon Biosystems A/S, Odense, Denmark) and eluted with methanol according to the manufacturer's instructions. The eluate was evaporated to dryness in a miVac DNA vacuum centrifuge (Genevac®, UK) and stored at -20 °C until mass spectrometric analysis.

In-gel digestion

For subsequent analysis by SDS-PAGE, the beads with captured proteins were resuspended in 7 µl Laemmli buffer and heated to 95 °C for 5 min. Gels were stained using the FireSilver® Kit (Proteome Factory, Berlin, Germany) according to the manufacturer's instructions and washed twice for 10 min with LC-MS grade water. Gel bands were excised, cut into small pieces, and washed twice with each 100 µl water and 100 µl 50 % ethanol (v/v). Gel bands were shrunk with 50 µl 100 % ethanol for approximately 5 min. Subsequently, the washing and shrinking steps were repeated. Protein digestion was carried out by rehydration of bands for 20 min on ice with 12.5 ng/µl of trypsin solution in 50 mM NH_4HCO_3 and subsequent incubation for 16 h at 37 °C. The extraction of peptides was carried out in two consecutive steps by incubating the gel pieces with 50 % acetonitril (ACN) with 2.5 % formic acid (FA) for 15 min. The pooled supernatants were then dried in a miVac DNA vacuum centrifuge (Genevac®). Desalting, elution, evaporation and storage of tryptic peptides were performed as described for in-solution digested samples.

Nano LC-MS/MS

The protein digest was redissolved in 5 µl of 5 % FA. Subsequently, peptides were loaded onto a nanoflow Biosphere C18 pre-column (5 µm, 120 Å, 20 x 0.1 mm, nanoseparations, Netherlands) coupled to a nanoflow Biosphere C18 analytical column (5 µm, 120 Å, 105 x 0.075 mm). The experiments were performed on an Easy-nLC™ liquid chromatography system (Proxeon Biosystems A/S, Odense, Denmark) connected to an LTQ Orbitrap XL mass spectrometer (Thermo Electron, Bremen, Germany) using a nano-electrospray ion source (Proxeon Biosystems A/S, Odense, Denmark). For the analysis of in-solution digest samples peptides were eluted during an 80-min linear gradient from 5 %

ACN/0.1 % FA to 40 % ACN/0.1 % FA followed by an additional 2 min to 100 % ACN/0.1 % FA and remaining at 100 % for another 8 min with a controlled flow rate of 300 nl/min. For the analysis of extracted gel bands a linear 40-min gradient increasing from 5 % ACN/0.1 % FA to 40 %ACN/0.1 % FA followed by an additional 2 min to 100 % ACN/0.1 % FA and remaining at 100 % for another 8 min with a controlled flow rate of 300 nl/min.

The mass spectrometric analysis was performed in the data-dependent mode to automatically switch between orbitrap-MS and LTQ-MS/MS (MS2) acquisition. The mass spectrometer duty cycle was controlled by setting the IT automatic gain control. Survey full scan MS spectra (from m/z 400–2000) were acquired in the orbitrap with a resolution of r= 60,000 at m/z 400 (after accumulation to a target value of 500,000 charges in the linear ion trap). The most intense ions (up to five, depending on signal intensity) were sequentially isolated for fragmentation in the linear ion trap using collision- induced dissociation (CID) at a target value of 10,000 charges. The resulting fragment ions were recorded in LTQ.
For accurate mass measurements in the MS mode the singly-charged polydimethylyclo-iloxane background ion (Si(CH3)2O)6H+ (m/z 445.120025) generated during the electrospray process from ambient air was used as lock mass for real time internal recalibration. Target ions already mass selected for CID were dynamically excluded for the duration of 60 s. Charge state screening and rejection of ions for CID with unassigned charge were set. Further mass spectrometric settings were as follows: spray voltage was set to 1.7 kV, temperature of the heated transfer capillary was set to 200 °C, and relative normalized collision energy was 35 % for MS2. The minimal signal required for MS2 was 500 counts. An activation q = 0.25 and an activation time of 30 ms was applied for MS2 acquisitions. After each analysis of an in-solution digest sample the system was washed by performing at least one linear gradient that was used for the respective peptide separation.

Peptide identification via database search

Proteins were identified by automated database searching against the UniProtKB/Swiss-Prot (release 56.5) database using SEQUEST implemented in Bioworks 3.3.1 SP1 (Thermo Fisher Scientific, Schwerte, Germany). Specific search parameters used in the SEQUEST analyses were 5 ppm precursor tolerance, 1 amu fragment ions tolerance, and full trypsin specificity allowing for up to 2 missed cleavages. Phosphorylation at serine, threonine, and tyrosine, oxidation of methionines, deamidation at asparagines and glutamine, acetylation at lysine and serine, formylation at lysine, and methylation at arginine, lysine,

serine, threonine and asparagine were allowed as variable modifications. No fixed modifications were used in the database search.

The SEQUEST peptide identifications were required to satisfy minimum XCorr values of 2, 2.5, and 3 for singly, doubly, and triply charged peptides, a minimum ΔCn of 0.1, and a peptide probability ≥0.001. Peptides with a greater score than this were accepted for analysis without further validation. The estimated percentage of false discovery peptide identifications was determined using the reversed protein database approach and was <1 %.

Results

Capture Compounds

Tolcapone and Entacapone are potent inhibitors of catechol-O-methyl transferase (COMT) for the treatment of Parkinson's disease. The catechol groups of these drugs compete with dopamine for coordination of the catechol moiety with the magnesium ion in the COMT binding pocket (Bonifacio *et al.*, CNS Drug Rev 13, 352-379 (2007)). The drugs have shown significant hepatoxicity limiting their therapeutic utility. In particular, Tolcapone was temporarily withdrawn, due to the drug's implication in fulminant liver failure and the consequent death of 3 patients; now monitoring of liver enzymes is mandatory during drug treatment (Unger *et al.*, Eur Neurol 60, 122-126 (2008). In order to investigate the molecular mechanisms underlying the cause of hepatoxicity we prepared Capture Compounds containing Tolcapone and Entacapone as selectivity functions (Y groups), respectively (Figure 2). Different moieties of a drug may form different interactions with cellular proteins inducing different pharmacogenic responses. Thus, we choose two points of attachment for each drug to the scaffold (Figure 2). In one set we used the catechol responsible for the interaction with COMT as the attachment point (Figure 2. 2, 3, 4: Tcp-Ct-CC and 6: Ecp-Ct-CC), and in addition we linked the drugs at the opposite end via the benzylic or the amino group, respectively (Figure 2. 5: Tcp-Bz-CC and 7: Ecp-Am-CC). As a result, different pharmacophoric elements of Entacapone and Tolcapone were presented to the complex protein mixtures tested. As a control the Capture Compound without selectivity group (scaffold) was used. "...each drug to the scaffold (Figure 2). The design of the Capture Compounds was carried out with the aim that for one attachment position the Capture Compound functionalities should not interfere with the interaction between the drug and it's target COMT. For Entacapone, the Capture Compound with attachment via the amino group should be able to bind COMT as does the original drug. To verify the quality of our molecular design we commissioned standard affinity measurements between one of the

Capture Compounds and the purified target protein COMT. Published K_D values for the affinity of the drug Entacapone to COMT vary by one order of magnitude between 0.3 nM and 10nM). The KD of the Entacapone Capture Compound Ecp-Am-CC was determined to be 430 nM. These results demonstrate that although the attachment of the Capture Compound scaffold may lead to a slight reduction of affinity Entacapone still effectively binds COMT, demonstrating that the pharmacophoric potential of the drug is retained within the Capture Compound.

Validation of the CCMS approach with soluble rat liver proteins

We first tested our Capture Compounds in the cytosolic fraction of rat liver, which shows a reduced protein complexity compared to whole cell lysates. UV irradiation induces a covalent bond between the reactivity function of the Capture Compound and the protein interacting with the drug. As the Capture Compound contains a biotin moiety (sorting function), interacting proteins become biotinylated during the capture process and can not only be isolated by streptavidin beads but also detected in an anti-biotin (e.g. streptavidin) Western Blot (Figure 4A), demonstrating the covalent bond to the Capture Compound. By SDS-PAGE (Figure 4B) all isolated proteins were visualized. The comparison of silver stained SDS-PAGE and anti-biotin Western Blot clearly demonstrated that the isolated proteins were covalently bound. Western Blots directed against the COMT protein (Figure 4C) demonstrated that the target is indeed captured and – comparing Figure 4 A and C – covalently bound. Analysis of the respective samples by mass spectrometry in addition to Western Blots demonstrated the unambiguous and reproducible isolation and identification of the known drug target COMT with the Capture Compounds containing the free catechol moiety (Tcp-Bz-CC and Ecp-Am-CC) Table 1), while, as expected, compounds with attachment at the opposite end (Tcp-Ct-CC and Ecp-Ct-CC) did not bind COMT. These, however, presented different pharmacophoric elements of the drugs to the protein mixture, and allowed capturing of proteins that interacted with these elements of the drugs.

Notably, the Capture Compounds interacted with bile salt sulfotransferase (ST2A1) and alcohol sulfotransferase A (ST2A2), independently of the attachment point. ST2A1 and ST2A2 belong to the group of cytosolic sulfotransferases, phase II detoxification enzymes involved in the biotransformation of a wide variety of structurally diverse endo- and xenobiotics, including many therapeutic agents and endogenous steroids. Binding of all four Capture Compounds to these enzymes is in accord with the rather unspecific role of the sulfotranferases in detoxification processes (Nowell *et al.*,. Oncogene 25; 1673-1678 (2006)).

As the scaffold control did not show this interaction, this indicates that the binding of sulfotranfarases is specific and might be triggered by toxicologically relevant events.

The Capture Compounds with free catechol moieties exposed to the cytosol showed, apart from the sulfotransferases, strong and specific interaction only with the target protein COMT. Those Capture Compounds with attachment via the catechol group (Tcp-Ct-CC1 and Ecp-Ct-CC1) revealed additional interacting proteins in the cell lysate. Notably, for the Tolcapone Capture Compound Tcp-Ct-CC1, additional peroxisomal proteins were captured. Peroxisomal acyl-coenzyme A oxidase 3 (ACOX3) and peroxisomal multifunctional enzyme type 2 (DBH4 also MFP-2 or MFE-2) play essential roles in fatty acid β-oxidation. The phenotypical data (Yu *et al.*. Curr Mol Med 3, 561-572 (2003); Huyghe, S. *et al.* Am J Pathol 168, 1321-1334 (2006); and Baes, M., *et al.*, J Biol Chem 275, 16329-16336 (2000)) associated with the two captured peroxisomal enzymes, indicate that Tolcapone related side-effects may be due, in part, to the interaction of these enzymes with Tolcapone. Moreover, these results show that CCMS can identify the molecular basis of drug side-effects.

Tolcapone as decoupling reagent of the respiratory chain

In order to reveal the mode of hepatotoxic action of Tolcapone and Entacapone in the human liver, we performed capture experiments in whole cell lysates of the human hepatocyte cell line HepG2. As the chemical structure of Entacapone and Tolcapone at the catecholic site is identical and the experiments using cytosolic rat liver fractions indicated that Tolcapone attached via the catecholic group captures relevant drug non-targets, we employed compounds with this attachment point. To generate a comprehensive coverage of drug-protein interactions we designed two additional Capture Compounds differing in the linker length between the drug molecule and the reactivity group (Tcp-Ct-CC2 and –CC3 Figure2A).

Capture experiments in HepG2 whole cell lysates revealed that Tolcapone Capture compounds, independent of linker length, interacted with a large number of different proteins in the cell, while Entacapone Capture Compounds showed relatively few interactions independent of attachment point. Even fewer proteins were found when capturing was performed with the scaffold control (Figure 5A). LC-MS/MS analysis of the respective complex protein mixtures led to the identification of the Tolcapone and Entacapone interaction partners. Proteins identified in the control experiment with scaffold were excluded from further analysis. We established the overlap between the captured proteins to classify the interaction partners of the respective drugs. The Tolcapone compounds captured a total of

124 proteins; with the Entacapone Capture Compounds, however, only **20** proteins were captured (Figure 3). While some proteins were captured exclusively by one Capture Compound, the majority of proteins was captured independent of the linker length, and, thus, considered as interaction partners with highest confidence. For an overall functional classification of the proteins we performed Gene Ontology annotation via BioMart of the ENSEMBL Genome Browser (www.ensembl.org, build 52 NCBI63) according to Cellular Component Terms.

For Entacapone Capture Compounds, twenty proteins were specifically captured and their cellular distribution showed no distinctive features regarding toxic side effects. For Tolcapone, a considerably large proportion of the 124 captured proteins were assigned to the mitochondria (Figures 3 and 5B) and, in particular, within the mitochondrial membrane. To gain deeper insight into the role of the captured proteins in metabolism, we performed out a KEGG Pathway (Aoki *et al.* Curr Protoc Bioinformatics Chapter 1, Unit 1 12 (2005)) analysis via the Database for Annotation, Visualization and Integrated Discovery (DAVID, V6, 2008 david.abcc.ncifcrf.gov/; Dennis *et al.* DAVID: Database for Annotation, Visualization, and Integrated Discovery. Genome Biol 4, P3 (2003)). We found that the captured proteins are essential components of the respiratory chain, the bile acid synthesis, and peroxisomal fatty acid ß-oxidation (summarized in Figure 3). Enzymes functioning in bile acid synthesis and peroxisomal fatty acid ß-oxidation are in accord with the results obtained from the soluble fraction of rat liver. In particular, the human homolog of ACOX3 was again reproducibly captured, confirming a possible disturbance of fatty acid ß-oxidation by Tolcapone in humans. Notably, the captured mitochondrial proteins contained subunits from each of the complex in the respiratory chain (Figure 5C), for example, eight subunits of ATP synthase. While nearly all subunits were captured by two or three of the Tolcapone capture compounds none were isolated by Entacapone Capture Compounds. The comparison to the structurally similar but far less toxic drug Entacapone indicates that the observed Tolcapone-protein interactions likely are the cause of toxicity.

Detailed analysis of proteins interacting with Tolcapone in rat liver mitochondria and microsomal fractions

To investigate the interaction partners of Tolcapone in mitochondria and peroxisomes in detail, we carried out capture experiments in the mitochondria and microsomal fractions of rat liver. In both preparations, we again found that Tolcapone Capture Compounds capture significantly more proteins than the respective Entacapone compounds. Consistent with the

results described above, we identified key-enzymes of fatty acid ß-oxidation, such as peroxisomal multifunctional enzyme type2, peroxisomal acyl-coenzyme A oxidase 3, and the long-chain-fatty-acid-CoA ligase 1 which is found both in the mitochondrial and peroxisomal membrane as specific interaction partners of Tolcapone with the potential to induce side-effects (see, Table 2, below).

Discussion

Application of CCMS technology reproducibly and unambiguously demonstrated that besides binding COMT, Tolcapone interacts with a large number of proteins carrying out essential functions in the respiratory chain, fatty acid ß-oxidation and bile acid synthesis. In the liver, fatty acids are metabolized by ß-oxidation in mitochondria and peroxisomes and by omega-oxidation in microsomes. Peroxisomal beta-oxidation is responsible for the metabolism of very-long-chain-fatty acids. Impairment of correct peroxisomal function may lead to the accumulation of long-fatty acids or of hydrogen peroxide through the peroxisomal oxidative reactions. Both mechanisms contribute to hepatotoxicity and thus can explain the phenotype of Tolcapone side-effects.

Peroxisomal acyl-coenzyme A oxidase 3 (ACOX3) belongs to the family of fatty acyl-CoA oxidases. Recently, it has been shown that mice lacking fatty acyl-CoA oxidases developed steatohepatitis, demonstrating the importance of this class of enzymes for proper liver function (Yu *et al.* Curr Mol Med 3, 561-572 (2003). Peroxisomal multifunctional enzyme type 2 (MFP-2, also D-bifunctional protein, DHB4) plays a central role in peroxisomal ß-oxidation as it handles most, if not all, peroxisomal ß-oxidation substrates (Huyghe *et al.* Biochim Biophys Acta 1761, 973-994 (2006)).. In humans, deficiency of this enzyme causes a severe developmental syndrome with abnormalities in several organs leading to death within the first year of life (Huyghe et al. Biochim Biophys Acta 1761, 973-994 (2006)). Accumulation of branched-long-chain fatty acids and very-long-chain fatty acids as well as a disturbed synthesis of bile acids were documented for these patients. Moreover, lack or mutations of DHB4 are a cause of D-bifunctional protein deficiency (DBPD). The clinical manifestations of this deficiency is similar to those of disorders of peroxisomal assembly, including X-linked adrenoleukodystrophy, Zellweger cerebrohepatorenal syndrome, and neonatal adrenoleukodystrophy (Watkins *et al.* J Clin Invest 83, 771-777 (1989); Wanders *et al.*, J Inherit Metab Dis 13, 375-379 (1990)). Premature death is observed in one third of MFP-2 knockout mice accompanied by more severe aberrations in bile acid metabolism and excessive accumulation of very-long-chain

fatty acids in brain and liver (Huyghe, S. et al. Am J Pathol 168, 1321-1334 (2006); and Baes, M., et al., J Biol Chem 275, 16329-16336 (2000)).

Besides interference with fatty acid ß-oxidation, our results show that Tolcapone inserts into the inner mitochondrial membranes and interacts with components of the respiratory chain. A molecular mechanism in which Tolcapone compromises the function of the respiratory chain is in accordance with cell physiological data reporting a decrease of membrane potential in the presence of Tolcapone (Haasio *et al.*, Eur J Pharmacol 453, 21-26 (2002) similar to the *bona fide* decoupling agent 2,4-dinitrophenol. A toxicological study (Haasio *et al.* J Neural Transm 109, 1391-1401 (2002)) in which rats were treated either with Entacapone or Tolcapone reported that no treatment related findings were observed in Entacapone-treated rats. Animals treated with Tolcapone showed increased respiration, decreased activity and drowsiness, and elevation of the rectal body temperature.

The results presented herein provide a molecular basis for the reported clinical and cell physiological observations. Mitochondria and peroxisomes in the liver were identified as the cellular compartments mainly affected during Tolcapone treatment. Indeed, the malfunction of the respiratory chain, fatty acid ß-oxidation or bile acid synthesis alone would likely lead to hepatotoxicity (Pessayre *et al.*. Cell Biol Toxicol 15, 367-373 (1999); Jaeschke *et al.*, Toxicol Sci 65, 166-176 (2002)).

* * *

I further declare that all statements made herein of my own knowledge are true and that all statements made on information and belief are believed to be true; and further, that these statements were made with knowledge that willful false statements and the like so made are punishable by fine or imprisonment, or both, under section 1001 of Title 18 of the United States Code, and that such willful false statements may jeopardize the validity of the application or any patent resulting therefrom.

Signature _____

Hubert Köster

Berlin, February 3, 2010
Date:

Figure and Table Legends

Figure 1. Schematic depiction of Capture Compounds (A) and the capture process (B). Capture Compounds are trifunctional probes: based on affinity a selectivity function (the drug, red) interacts with the proteins in a biological sample in equilibrium, a reactivity function (orange) irreversibly forms a covalent bond, and a sorting function (yellow) allows the captured protein(s) to be isolated for mass spectrometric analysis.

Figure 2. Chemical structures of Tolcapone (Tcp) and Entacapone (Ecp) Capture Compounds. 1) The scaffold without selectivity function was used as a control. Tolcapone Capture Compounds with attachment via the catechol group and with free benzylic function (2 to 4, Tcp-Ct-CC). Tolcapone Capture Compounds with attachment via the benzylic group with free catechol function (5 Tcp-Bz-CC). Entacapone Capture Compounds with attachment via the catechol function (6, Ecp-Ct-CC) and via the amide (free catechol function, 7, Ecp-Am-CC).

Figure 3. Summary of the cellular distribution of the captured proteins (see, also, Figures 5).

Figure 4. Identification of COMT and off-target proteins by capturing in soluble fraction of rat liver. (A) The streptavidin-peroxidase Western-Blot demonstrates covalent crosslink between Capture Compound and protein interaction partners (B) Silver gel showing all captured proteins and (C) Anti-COMT Western Blot: Compounds with free catechol moiety capture COMT. M: Marker; lane 1: Tcp-Ct-CC; lane 2: Tcp-Bz-CC; lane 3: Ecp-Ct-CC; lane 4: Ecp-Am-CC and lane 5: Scaffold. Arrows indicate COMT.

Figure 5. Proteins interacting with Tolcapone in HepG2 cell lysate. A) Capturing in HepG2 lysate shows high number of proteins interacting with Tolcapone (Lanes 2-4) compared to Entacapone Capture Compounds (lanes 5,6) and even less for the Capture compound Scaffold (Lane 1). B) Mapping of gene ontologies revealed the localization to interacting proteins in the cellular compartments. C) A large proportion of Tolcapone interacting proteins is located in the mitochondria and include members of the respiratory chain

Figure 6. Capturing in rat liver mitochondrial fraction enables the identification of Tolcapone off-targets in fatty acid ß-oxidation. L: Mitochondrial lysate M: marker 1: Tcp-Ct-CC1 2: Tcp-Ct-CC2 3: scaffold control 4: Ecp-Ct-CC1, 5: Ecp-Am-CC1.

Table 1. Proteins captured by Tolcapone and Entacapone in the soluble protein fraction of rat liver. The corresponding silver stained SDS-PAGE is shown in Figure 4. Processes are given as retrieved from SwissProt annotation via http://www.expasy.org.

Table 2. Proteins captured by Tolcapone and Entacapone in solubilized mitochondrial and microsomal fraction of rat liver. Corresponding protein bands are depicted in Figure 6. Processes are given as retrieved from SwissProt annotation via www.expasy.org.

Figure 1

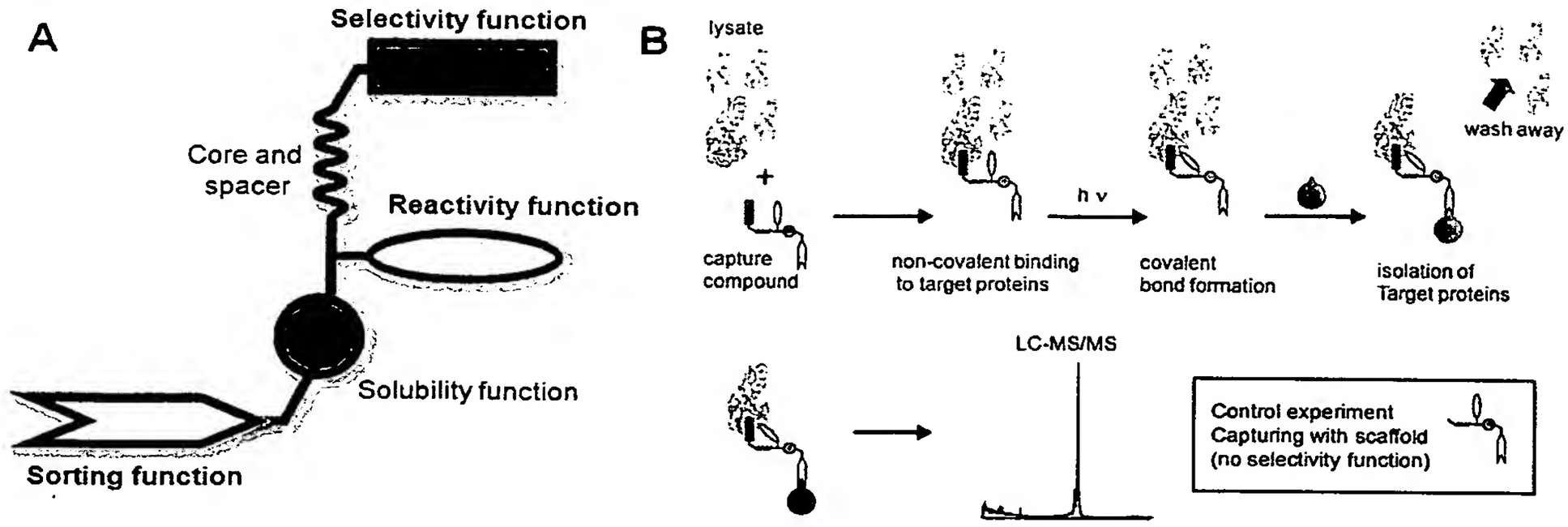

Figure 2

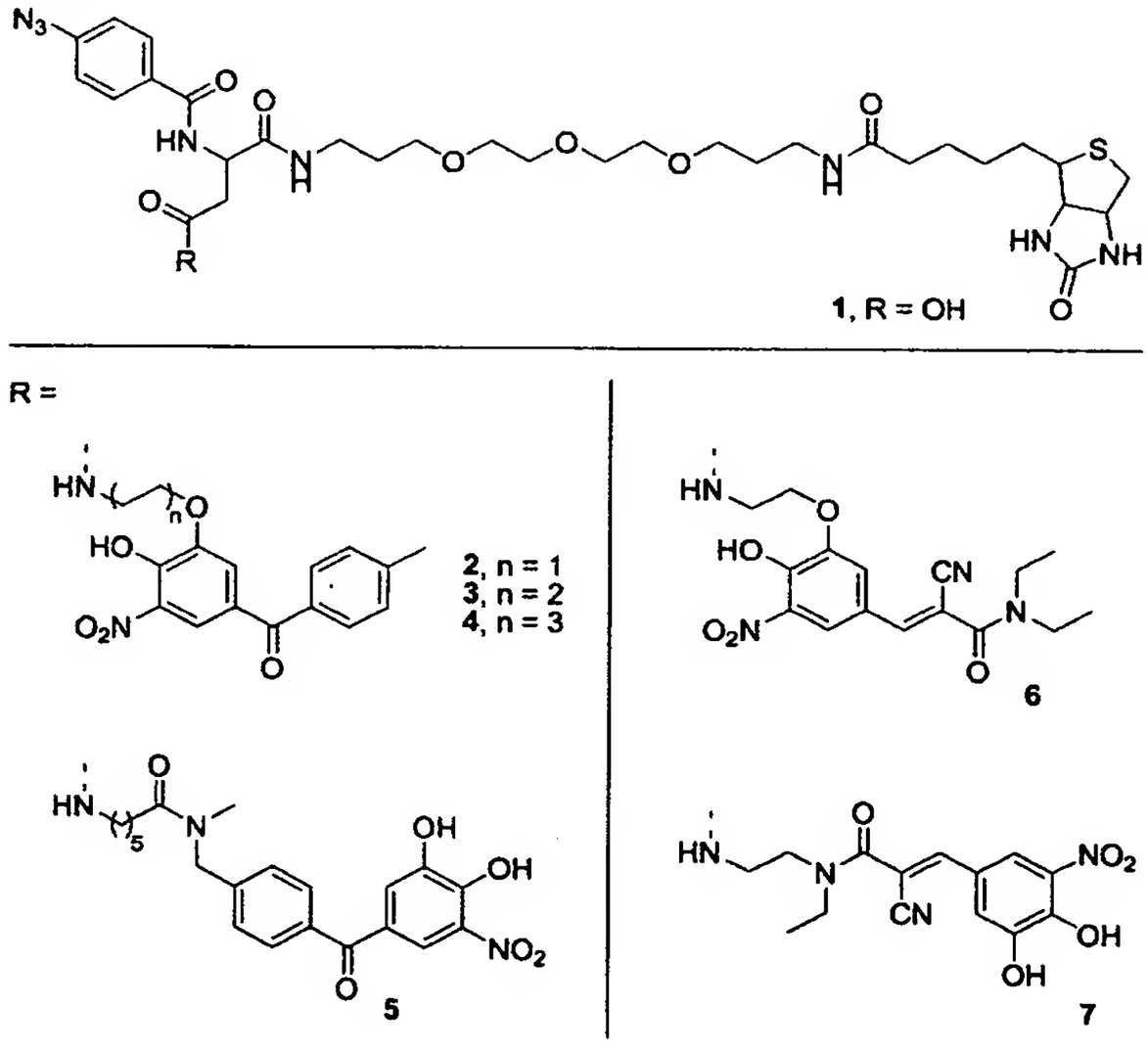

Figure 3A

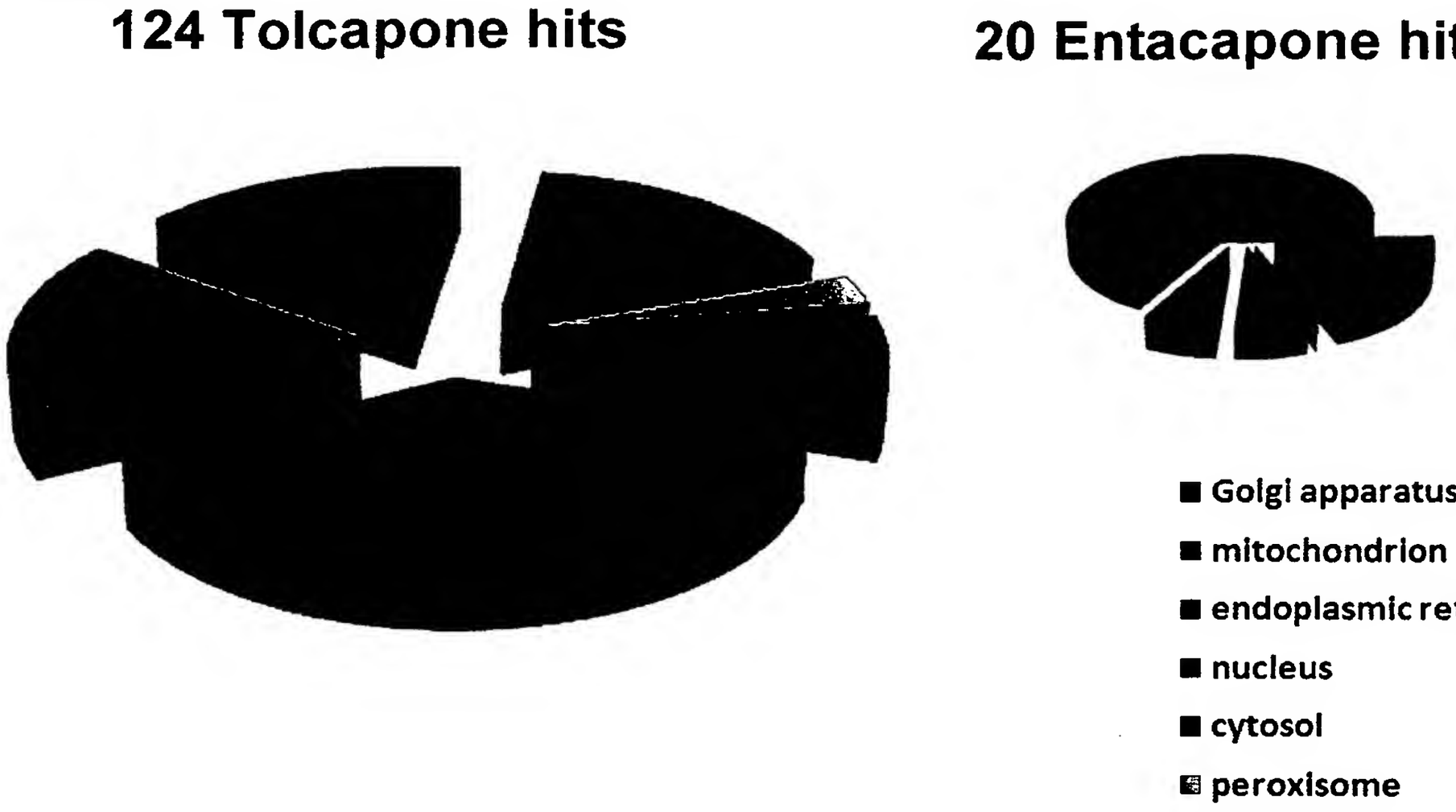

Figure 3B

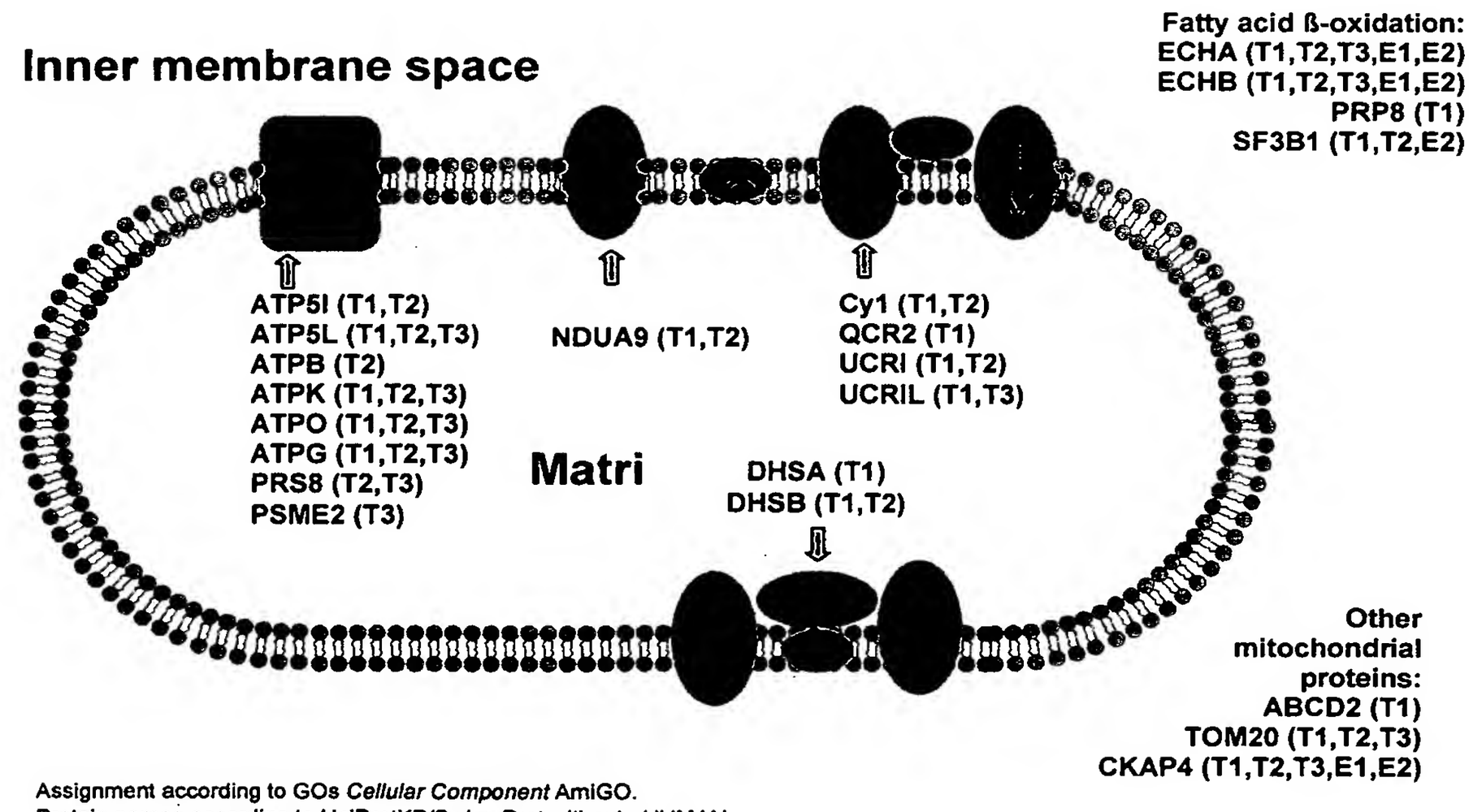

Assignment according to GOs *Cellular Component* AmiGO.
Protein names according to UniProtKB/Swiss-Prot without _HUMAN

Figure 4

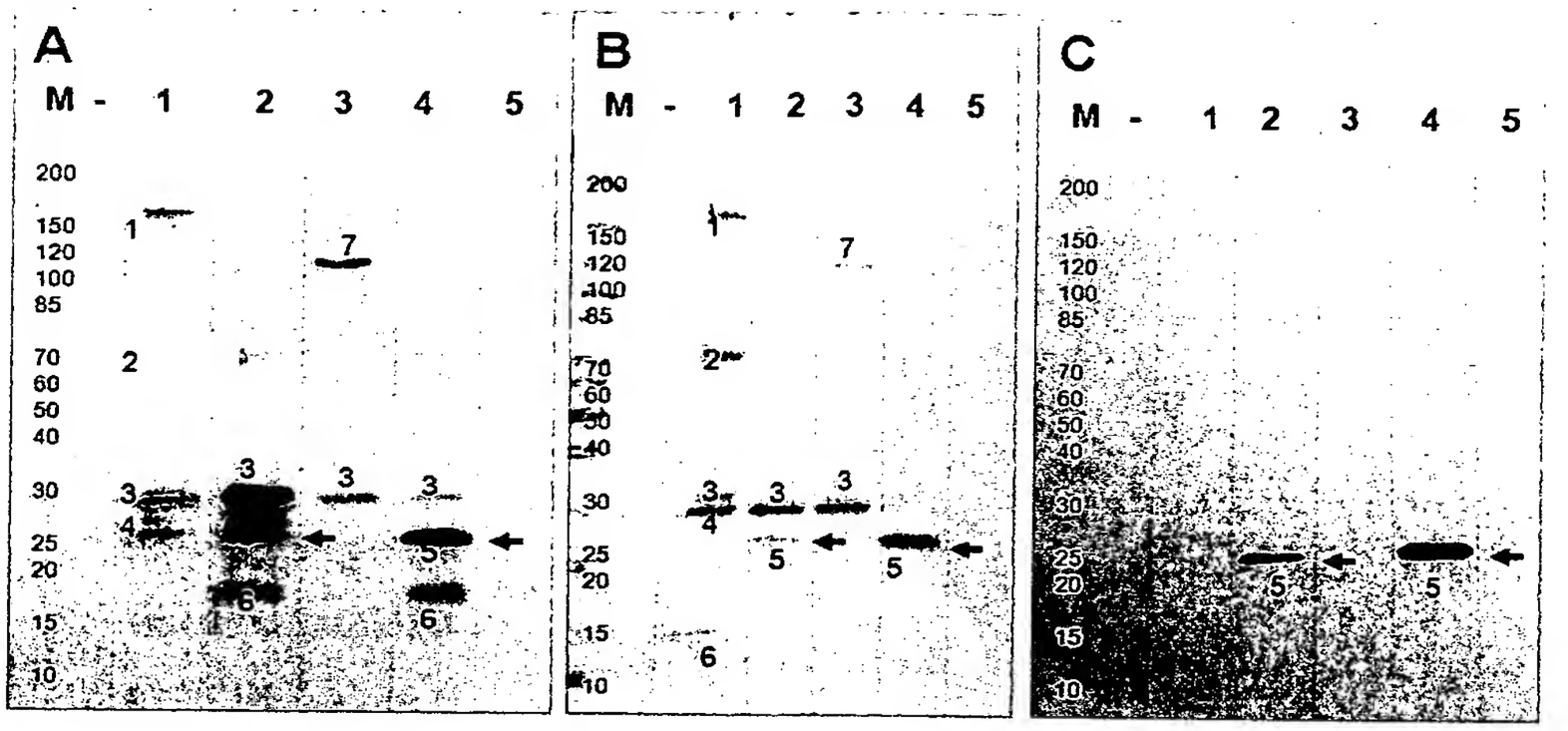
A
M - 1 2 3 4 5
200
150
120
100
85
70
60
50
40
30
25
20
15
10
1
2
3
4
5
6
7
B
M - 1 2 3 4 5
C
M - 1 2 3 4 5

Figure 5

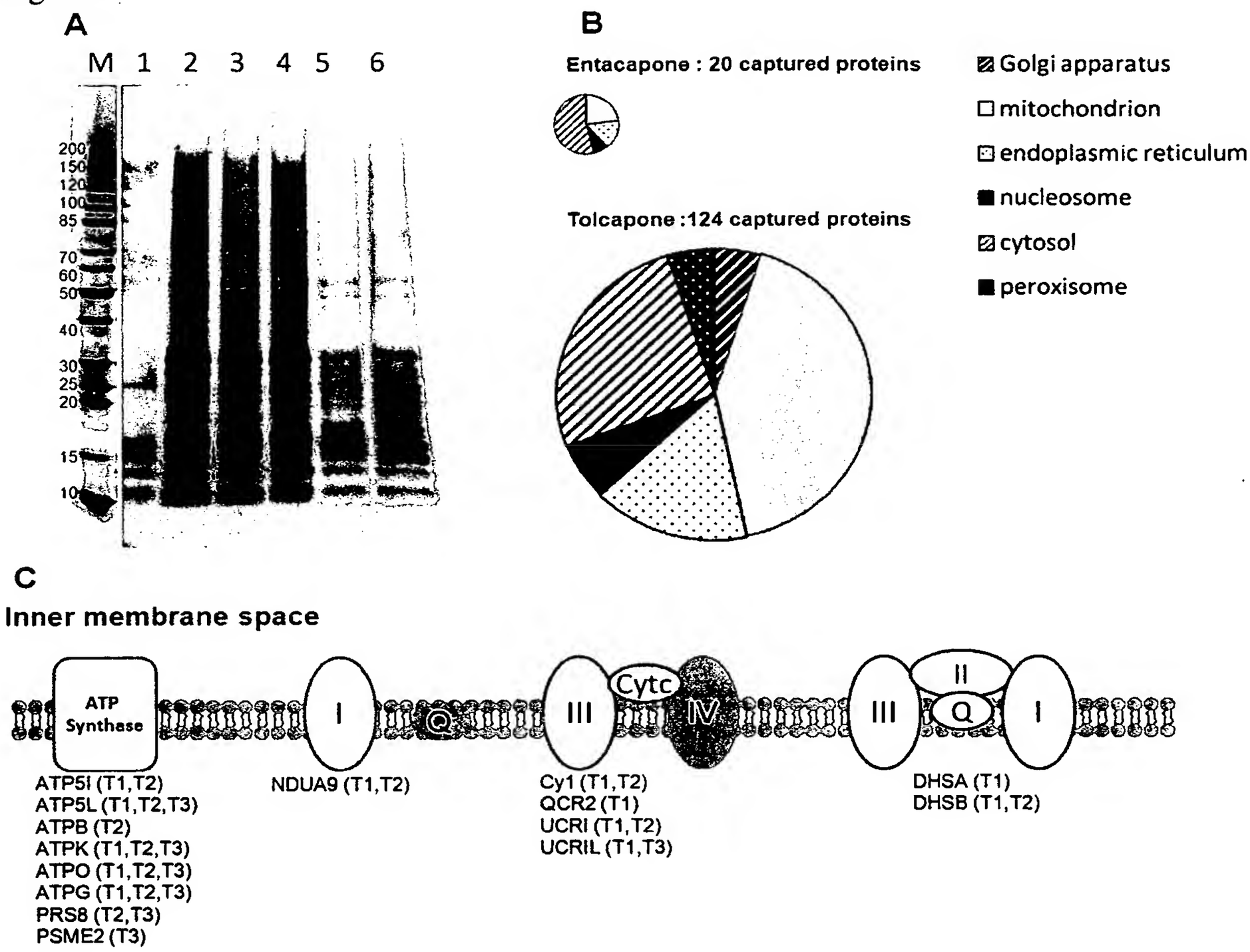
A
M 1 2 3 4 5 6
200
150
120
100
85
70
60
50
40
30
25
20
15
10
B
Entacapone : 20 captured proteins
Tolcapone :124 captured proteins
Golgi apparatus
mitochondrion
endoplasmic reticulum
nucleosome
cytosol
peroxisome
C
Inner membrane space
ATP Synthase
I
Q
III
Cytc
IV
III
II
Q
I
ATP5I (T1,T2)
ATP5L (T1,T2,T3)
ATPB (T2)
ATPK (T1,T2,T3)
ATPO (T1,T2,T3)
ATPG (T1,T2,T3)
PRS8 (T2,T3)
PSME2 (T3)
NDUA9 (T1,T2)
Cy1 (T1,T2)
QCR2 (T1)
UCRI (T1,T2)
UCRIL (T1,T3)
DHSA (T1)
DHSB (T1,T2)
Matrix

Figure 6

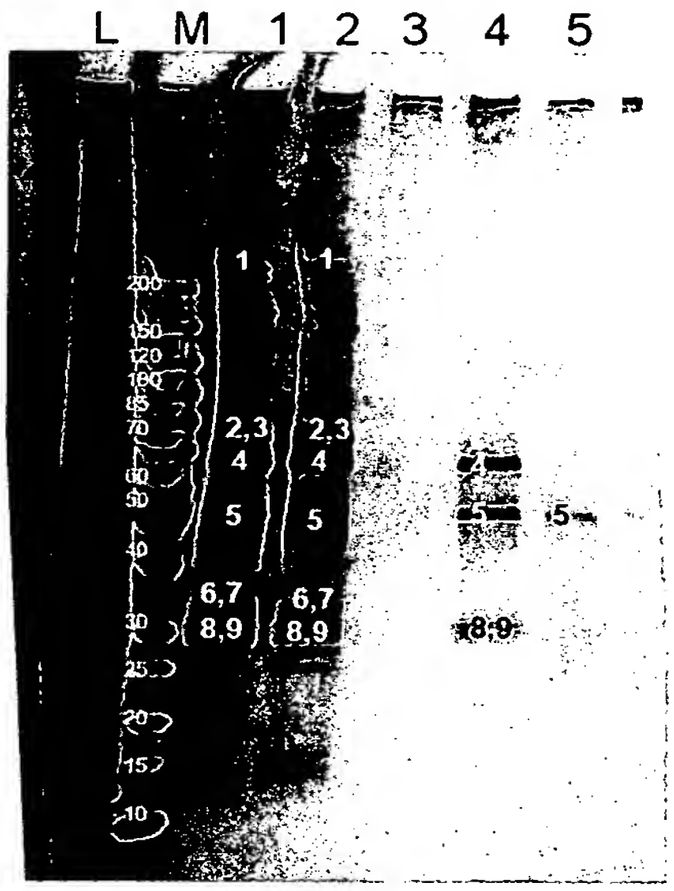

Table 1

Gelband	Abbreviation	Name	MW [kDa]	Accession	Cellular Process
1	CLH	Clathrin heavy chain 1	191	P11442	Endocytosis
2	DHB4	Peroxisomal multifunctional enzyme type 2	79	P97852	Fatty acid ß-Oxidation
2	ACOX3	Peroxisomal acyl-coenzyme A oxidase 3	78	Q63448	Fatty acid ß-Oxidation
3	ST2A2	Alcohol sulfotransferase A	33	P22789	Detoxification
4	ST2A1	Bile salt sulfotransferase	33	P15709	Detoxification
5	COMT	Catechol O-methyltransferase	30	P22734	Dopamin degradation
6	HBB1	Hemoglobin subunit beta-1	16	P02091	Oxygen transport
6	HBA	Hemoglobin subunit alpha-1/2	15	P01946	Oxygen transport
7	PYC	Pyruvate carboxylase	130	P52873	Krebs cycle

Table 2

Gelband	Abbreviation	Name	MW [kDa]	Accession	Cellular Process
1	CLH	Clathrin heavy chain 1	193	P49951	Endocytosis
2	DHB4	Peroxisomal multifunctional enzyme type 2	80	P97852	Fatty acid ß-Oxidation
3	ACSL1	Long-chain-fatty-acid-CoA ligase 1	79	P18163	Fatty acid metabolism
4	ACOX3	Peroxisomal acyl-coenzyme A oxidase 3	79	Q63448	Fatty acid ß-Oxidation
5	DHE3	Glutamate dehydrogenase 1, mitochondrial	62	P10860	Glutamate catabolism

Gelband	Abbreviation	Name	MW [kDa]	Accession	Cellular Process
6	ARHL1	Protein ADP-ribosylarginine hydrolase-like protein 1	40	Q5XIB3	Protein-amino acid de-ribolysation
7	DHB13	17-beta hydroxysteroid dehydrogenase 13	34	Q5M875	Oxidation/Reduction
8	AUHM	Methylglutaconyl-CoA hydratase, mitochondrial	34	Q9JLZ3	Branched amino acid catabolism
9	ECHM	Enoyl-CoA hydratase, mitochondrial	32	P14604	Fatty acid ß-oxidation

Synthetic Schemes

Scheme a. Synthesis of catechol-linked Tolcapone Capture Compounds

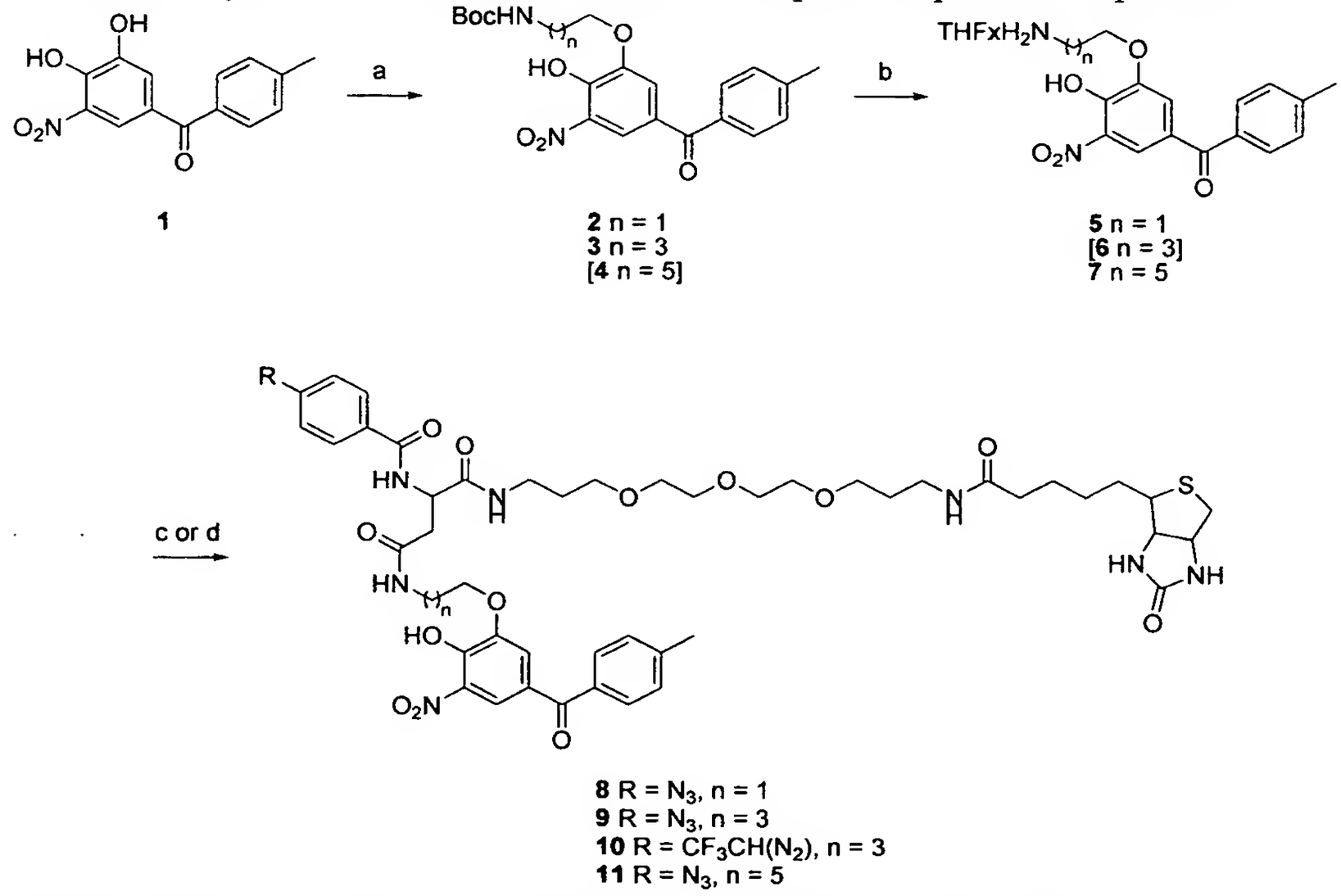

1

2 n = 1
3 n = 3
[**4** n = 5]

5 n = 1
[**6** n = 3]
7 n = 5

8 R = N_3, n = 1
9 R = N_3, n = 3
10 R = $CF_3CH(N_2)$, n = 3
11 R = N_3, n = 5

[a]Reagents and conditions: (a) NaH, $BocHN(CH_2)_nCH_2Br$, DMF, 23 °C, 17 h, 52% for **2**, 85% for **3**; (b) TFA, DCM, 23 °C, 30 min, 88% for **5**, 44% (over 2 steps) for **7**; (c) B1COOH, TEA, DMAP; HOBt, DIC, DMA, 23 °C, 2-3 d, 40% for **8**, 30% for **9**, 36% for **11**; (d) B2COOH, DIPEA, HATU, DMF, 23 °C, 17 h, 29% for **10**.

Scheme b. Synthesis of catechol-linked Entacapone Capture Compounds

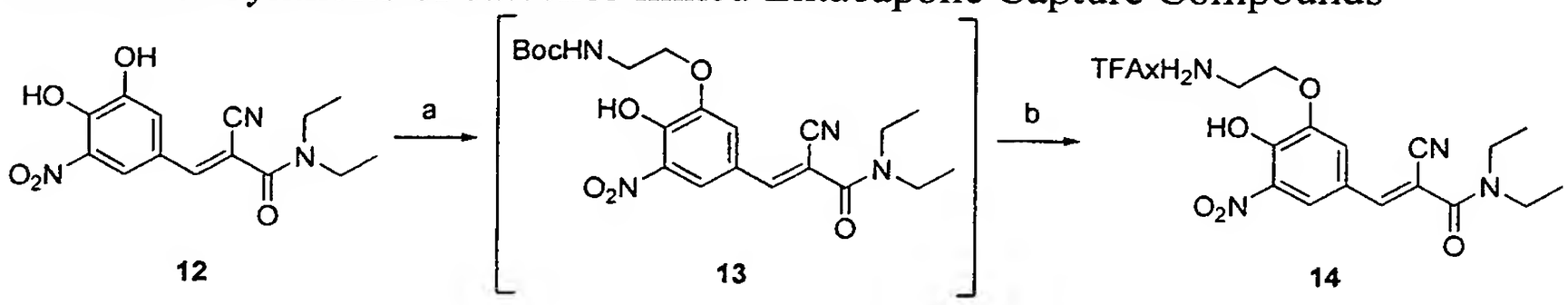

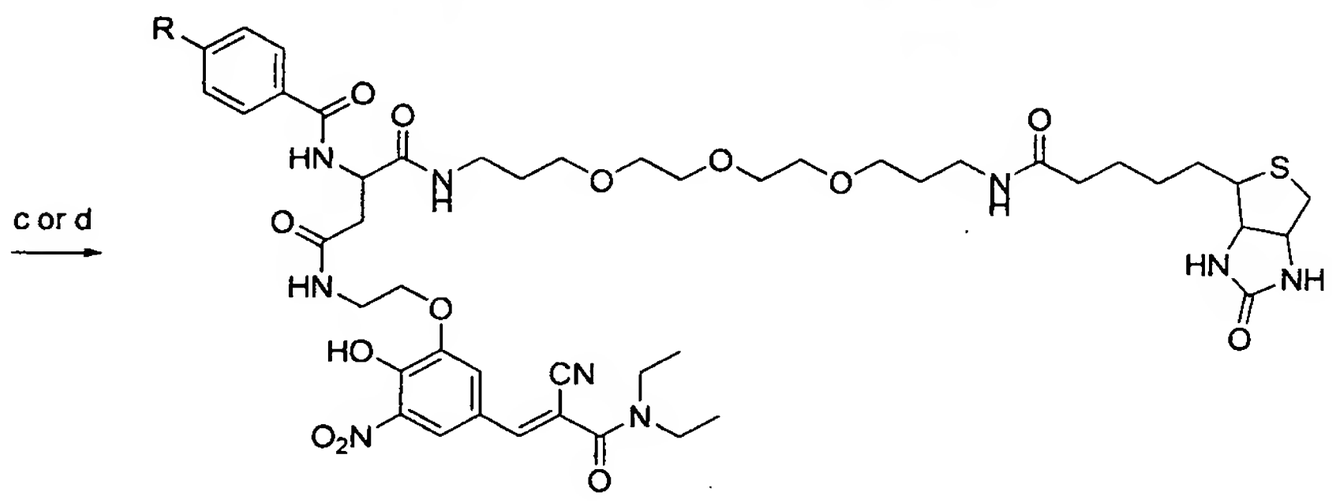

15 R = N_3
16 R = $CF_3CH(N_2)$

[a]Reagents and conditions: (a) NaH, $BocHNCH_2CH_2Br$, DMF, 23 °C, 17 h, used as crude; (b) TFA, DCM, 23 °C, 30 min, 15% (over 2 steps); (c) B1COOH, TEA, DMAP, HOBt, DIC, DMA, 23 °C, 2 d, 25% for **15**; (d) B2COOH, DIPEA, HATU, DMF, 23 °C, 17 h, 27% for **16**.

Scheme c. Synthesis of benzyl-linked Tolcapone Capture Compounds

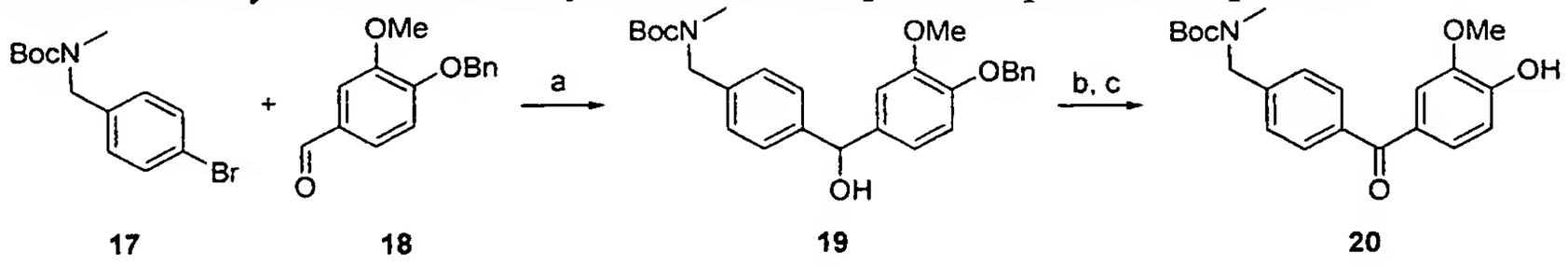

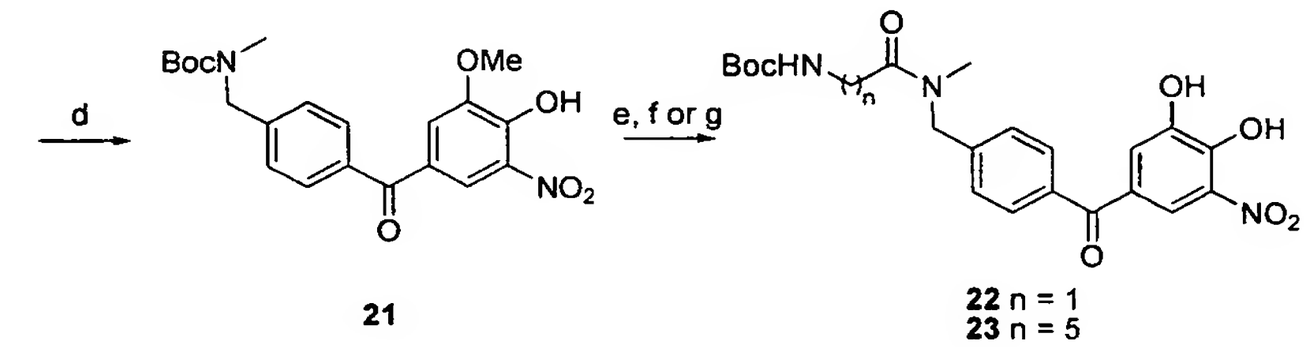

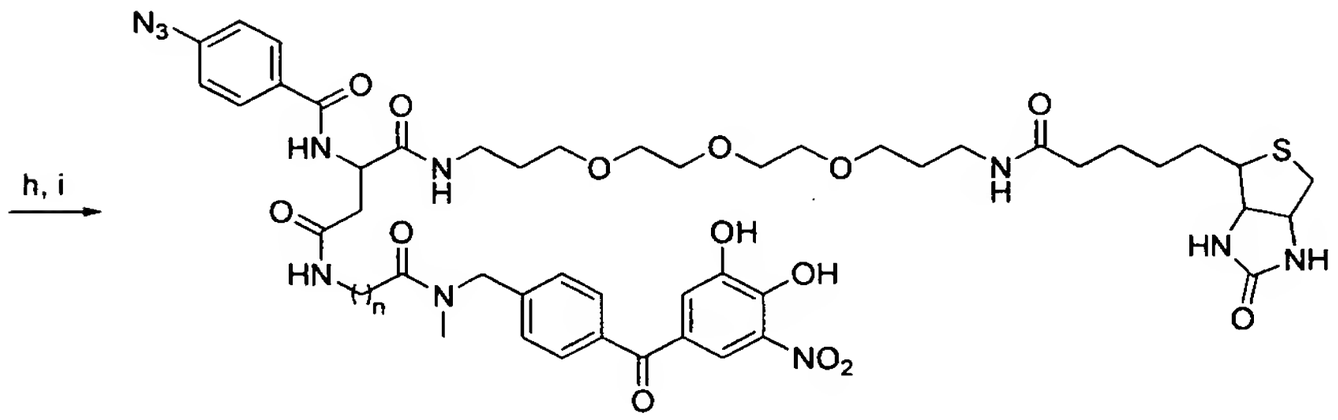

[a]Reagents and conditions: (a) *n*-BuLi, THF, -78 °C to 23 °C, 1 h, 30%; (b) NaO(*t*-Bu), *c*-hexanone, Toluene, 120 °C, 1.5 h, used as crude; (c) Ammonium formate, Pd/C, MeOH, 65 °C, 2 h, 64% (over 2 steps); (d) HNO_3, AcOH, 23 °C, 2 h, 67%; (e) BBr_3, DCM, -78 °C to 23 °C, 17 h, used as crude; (f) Boc-Gly, DCC, DMAP, TEA, DCM, 23 °C, 17 h, then HATU, DMA, 23 °C, 3 h, 37% (over 2 steps) for **22**; (g) Boc-6-Ahx-OH, DIPEA, HATU, DMF, 23 °C, 17 h, 43% (over 2 steps) for **23**; (h) TFA, DCM, 23 °C, 30 min, used as crude, (i) B1COOH, DIPEA, HATU, DMF, 23 °C, 17 h, 32% (over 2 steps) for **24**, 43% (over 2 steps) for **25**.

Scheme d. Synthesis of amide-linked Entacapone Capture Compounds

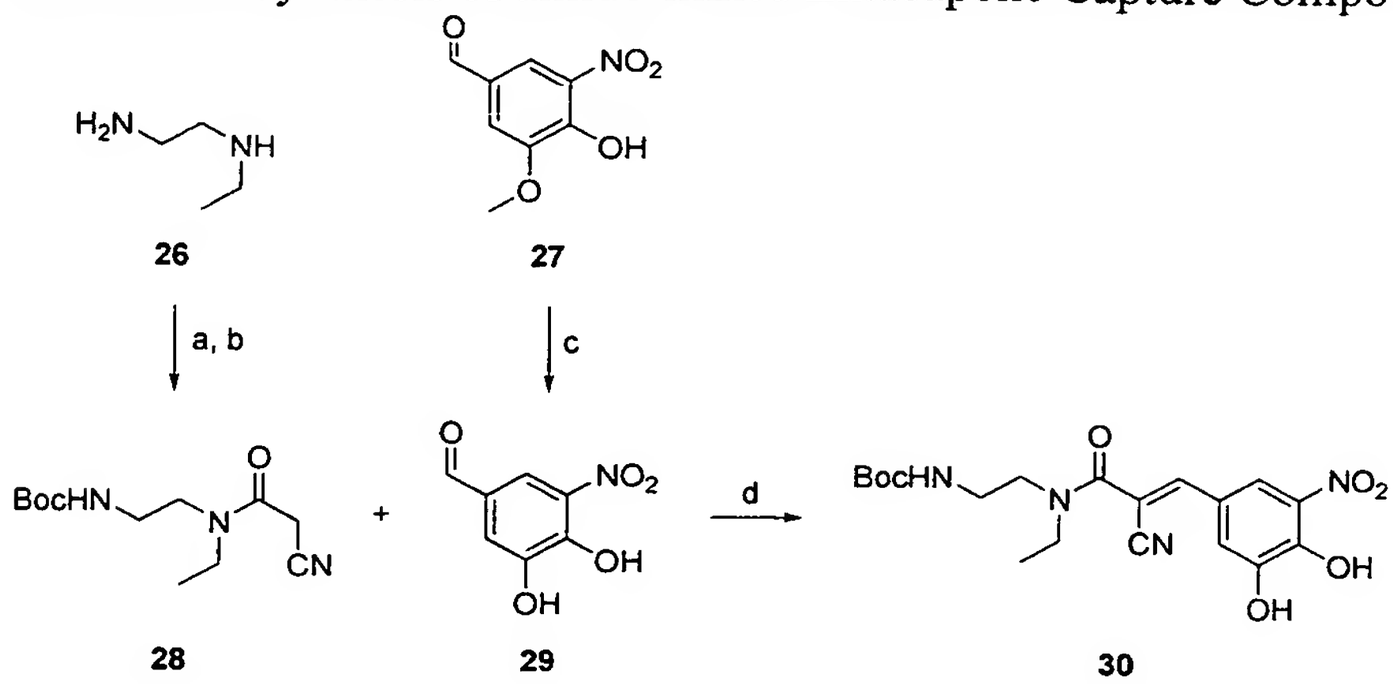

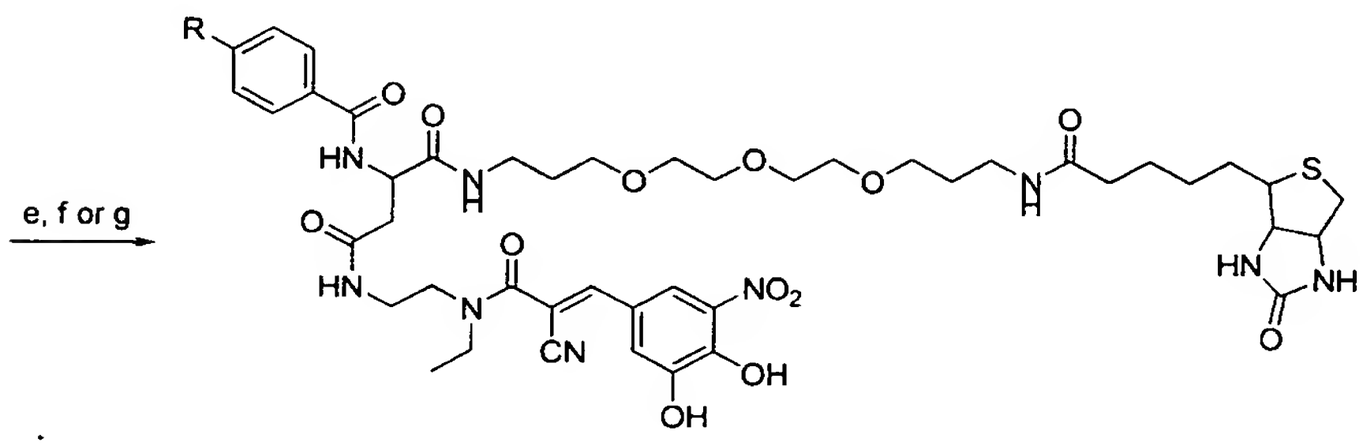

31 R = N_3
32 R = $CF_3CH(N_2)$

[a]Reagents and conditions: (a) HCl, Boc_2O, MeOH, 23 °C, 1 h, 93%; (b) Cyanoacetic acid, EDC, DMAP, DCM, 23 °C, 17 h, 78%; (c) $AlCl_3$, pyridine, 50 °C, 3 h, 62%; (d) piperidine, Toluene, *c*-Hex, 90 °C, 3 h, 68%; (e) TFA, DCM, 23 °C, 30 min, used as crude, (f) B1COOH, TEA, DMAP, HOBt, DIC, DMA, 23 °C, 3 d, 18% (over 2 steps) for **31**; (g) B2COOH, DIPEA, HATU, DMF, 23 °C, 17 h, 51% (over 2 steps) for **32**.

TOXICOLOGICAL SCIENCES 113(1), 243–253 (2010)
doi:10.1093/toxsci/kfp236
Advance Access publication September 26, 2009

Capture Compound Mass Spectrometry Sheds Light on the Molecular Mechanisms of Liver Toxicity of Two Parkinson Drugs

Jenny J. Fischer,* Simon Michaelis,* Anna K. Schrey,† Olivia Graebner nee Baessler,* Mirko Glinski,* Mathias Dreger,* Friedrich Kroll,*,[1] and Hubert Koester*

*Caprotec Bioanalytics GmbH, 12489 Berlin, Germany; and †Leibniz-Institut fuer Molekulare Pharmakologie, Molecular Modeling and Drug Design, 13125 Berlin, Germany

[1] To whom correspondence should be addressed. Fax: +49 (0) 30 6392 3985. E-mail: friedrich.kroll@caprotec.com.

Received April 9, 2009; accepted September 21, 2009

Capture compound mass spectrometry (CCMS) is a novel technology that helps understand the molecular mechanism of the mode of action of small molecules. The Capture Compounds are trifunctional probes: A selectivity function (the drug) interacts with the proteins in a biological sample, a reactivity function (phenyl-azide) irreversibly forms a covalent bond, and a sorting function (biotin) allows the captured protein(s) to be isolated for mass spectrometric analysis. Tolcapone and entacapone are potent inhibitors of catechol-*O*-methyltransferase (COMT) for the treatment of Parkinson's disease. We aimed to understand the molecular basis of the difference of both drugs with respect to side effects. Using Capture Compounds with these drugs as selectivity functions, we were able to unambiguously and reproducibly isolate and identify their known target COMT. Tolcapone Capture Compounds captured five times more proteins than entacapone Capture Compounds. Moreover, tolcapone Capture Compounds isolated mitochondrial and peroxisomal proteins. The major tolcapone-protein interactions occurred with components of the respiratory chain and of the fatty acid β-oxidation. Previously reported symptoms in tolcapone-treated rats suggested that tolcapone might act as decoupling reagent of the respiratory chain (Haasio *et al.*, 2002b). Our results demonstrate that CCMS is an effective tool for the identification of a drug's potential off targets. It fills a gap in currently used *in vitro* screens for drug profiling that do not contain all the toxicologically relevant proteins. Thereby, CCMS has the potential to fill a technological need in drug safety assessment and helps reengineer or to reject drugs at an early preclinical stage.

Key Words: **Capture compound mass spectrometry; tolcapone; entacapone; hepatotoxicity; drug safety; Parkinson's disease.**

The main challenge for the pharmaceutical industry is the selection of drug candidates that possess not only high efficacy but also low toxicity. Even in the past decade, hepatotoxicity and cardiovascular toxicity were the most prominent reasons accounting for two-thirds of market withdrawals (Schuster *et al.*, 2005). More than 70% of toxic reactions were identified during the compulsory regulatory animal toxicity tests (Olson *et al.*, 2000). Only half of the new pharmaceuticals that produced hepatotoxicity in the clinical stage had already shown concordant reactions in the obligatory animal toxicity studies. Therefore, the development of additional new tools for the investigation of potential human hepatotoxicity is a necessity for the pharmaceutical industry (Schuster *et al.*, 2005).

Traditional drug safety assessment is based either on selectivity screens against a panel of target-related recombinant proteins or on phenotypical cell-based assays. However, there is a shortage of technologies that can detect unforeseen drug off-target interactions to native endogenous proteins. We show here that capture compound mass spectrometry (CCMS) (Koster *et al.*, 2007) can be used to identify the sets of proteins that interact with two drugs for Parkinson's disease, tolcapone and entacapone. Tolcapone and entacapone are potent inhibitors of catechol-*O*-methyltransferase (COMT), a key enzyme in the metabolism of dopamine (Axelrod and Tomchick, 1958). Inhibition of COMT gives rise to elevated levodopa levels and thereby exerts a therapeutic effect on patients suffering from Parkinson's disease. Tolcapone has a much higher efficacy; however, it showed hepatotoxic effects in humans and rats (Assal *et al.*, 1998), while this has not been reported for entacapone. With respect to animal toxicity, the literature appears contradictory: While preclinical trials on tolcapone in animal species, among them rats, appear to have not shown toxic effects (Schläppi *et al.*, 1996, cited in Haasio, 2003), severe toxic effects were reproducibly observed in more recent studies in rats (Haasio *et al.*, 2002a,b). This effect must be attributed to the structural features of the drug molecules different from the moiety required for COMT binding because the latter is identical in tolcapone and entacapone.

CCMS can identify the set of proteins that interact with the drug directly from biological samples containing native endogenous proteins. From this set of interactions, conclusions can be drawn with respect to which molecular pathways may be affected by the drug. This information can be used to guide follow-up experiments to assess drug safety. This makes CCMS a platform technology that helps foresee adverse events

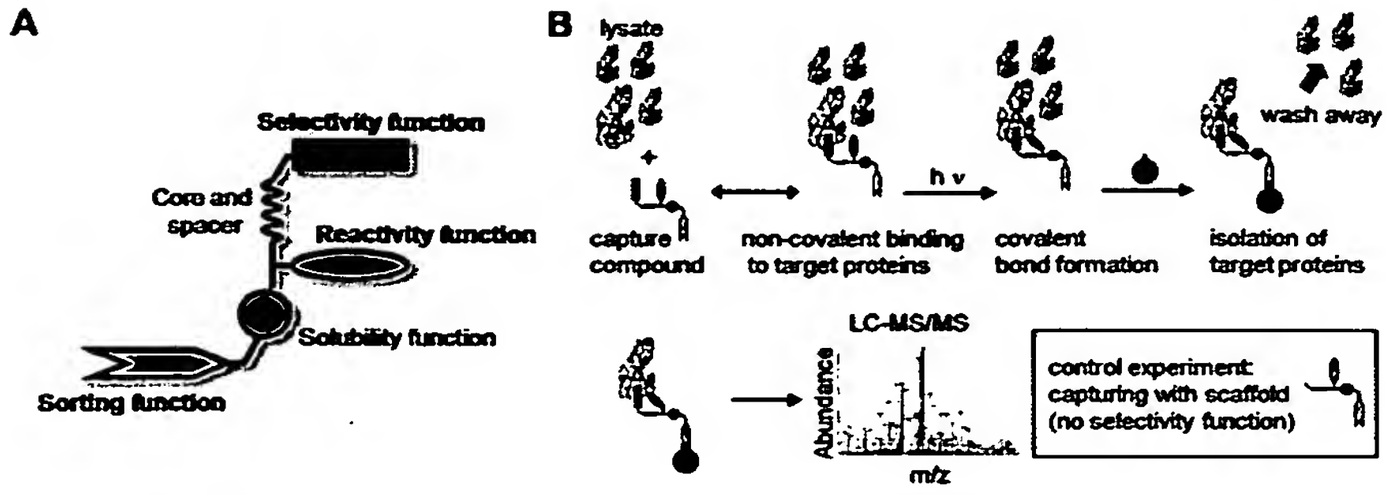

FIG. 1. Schematic depiction of Capture Compounds (A) and the capture process (B). Capture Compounds are trifunctional probes: Based on affinity, a selectivity function (the drug, red) interacts with the proteins in a biological sample in equilibrium, a reactivity function (orange) irreversibly forms a covalent bond, and a sorting function (yellow) allows the captured protein(s) to be isolated for mass spectrometric analysis. A polyethylene glycol moiety (green) in the backbone increases the hydrophilicity of the Capture Compounds and consequently their solubility in biological samples.

in humans. The mechanism by which a drug is potentially hepatotoxic can be better understood and compared to a related drug exhibiting lower hepatotoxicity, e.g., entacapone.

A Capture Compound consists of three main functionalities: (1) the drug molecule to be investigated, (2) an adjacent photoreactive functionality for photo cross-linking, and (3) the more distant sorting function, e.g., biotin for the isolation of captured proteins (Fig. 1). A sorting function permits the isolation of the proteins that are covalently linked to the Capture Compounds. In our case study, streptavidin magnetic beads were used to isolate all biotinylated proteins. The technology exclusively probes those proteins that interact with the drug molecule that is part of the Capture Compound. The complexity of a biological sample is reduced to the interaction partners of the drug. The identification of the captured proteins is accomplished by high-resolution mass spectrometry.

The capture process is simple and easy to perform. After incubation of the Capture Compound with a cell lysate, photolysis leads to the generation of a nitrene within the reactivity group. The nitrene then forms a covalent cross-link between the Capture Compound and the proteins that show an affinity-based interaction with the drug molecule in the Capture Compound. Non–cross-linked proteins can be washed away employing the sorting function biotin, streptavidin magnetic beads, and stringent washing conditions. The captured biotinylated proteins are then digested by trypsin, and the resulting peptides are analyzed by high-resolution mass spectrometric analysis.

We show that CCMS discriminates between tolcapone and entacapone. Both are of the same type and have the same mode of action but distinguish themselves by their therapeutic efficacy and the strength of the hepatotoxic effects. Capture Compounds containing these two drugs allow the capturing of the target protein COMT; however, tolcapone additionally binds to essential proteins in critical pathways such as fatty acid β-oxidation and oxidative phosphorylation. Our results demonstrate that CCMS is an effective tool for the generic and swift identification of both a drug's mode of action and its potential off targets responsible for adverse side effects.

MATERIALS AND METHODS

Chemical Synthesis of Entacapone and Tolcapone Capture Compounds

The detailed description of the Capture Compound synthesis will be published elsewhere. Structures of final compounds are shown in Figure 2. Analysis of the Capture Compounds by mass spectrometry and nuclear magnetic resonance (NMR) confirmed the identity and structure of the final reaction products. Purity of the compounds was determined by ^{1}H-NMR and was found to be greater than 95%.

Computational Methods

Preparation of molecular structures. Atomic coordinates for the ternary complex between COMT, the cosubstrate *S*-adenosyl-methionine, and the

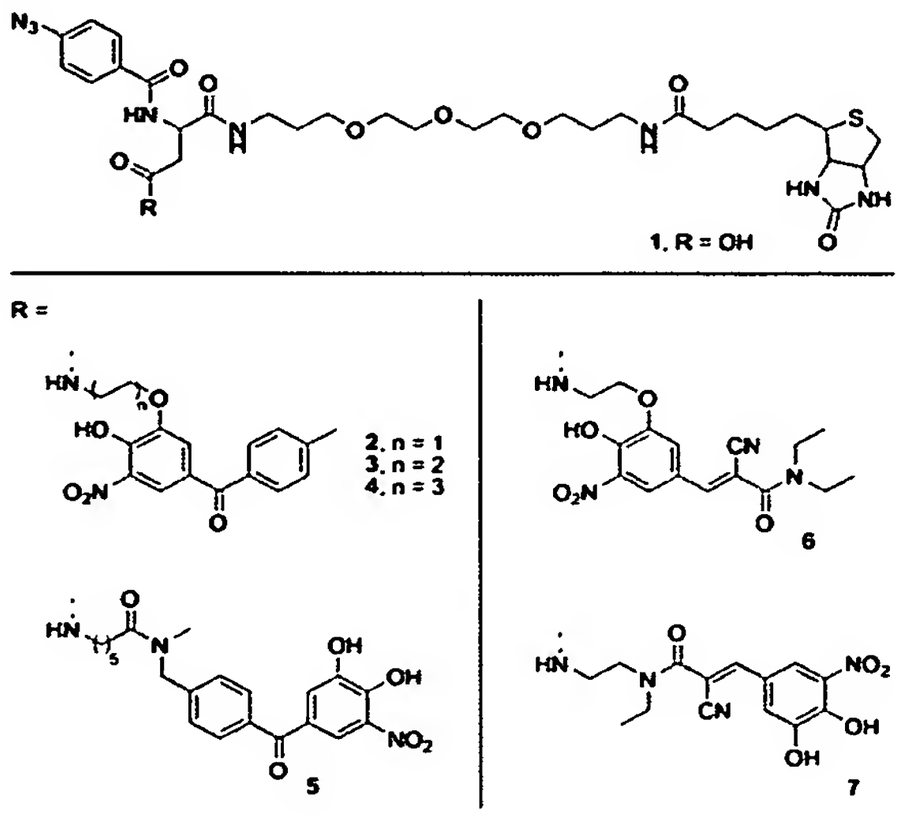

FIG. 2. Chemical structures of tolcapone (Tcp) and entacapone (Ecp) Capture Compounds. (**1**) The scaffold without selectivity function was used as a control. Tolcapone Capture Compounds with attachment via the catechol group and with free benzylic function (**2–4**, Tcp-Ct-CC). Tolcapone Capture Compounds with attachment via the benzylic group with free catechol function (**5**, Tcp-Bz-CC). Entacapone Capture Compounds with attachment via the catechol function (**6**, Ecp-Ct-CC) and via the amide (free catechol function, **7**, Ecp-Am-CC).

inhibitor BIA3-335 were obtained from the Protein Data Bank (PDB; http://www.rcsb.org) file 1H1D. The magnesium ion was considered covalently bound to Asp141 and Asp169. The side chain of Lys144 was modeled in the neutral form (Learmonth *et al.*, 2004). The structure was minimized with the molecular modeling package SYBYL 8.1 (Tripos Inc., St Louis, MO) using the Tripos force field, Gasteiger-Marsili charges, and the Powell gradient algorithm. The backbone, the magnesium ion, and its coordination atoms (O1 in Asp141, O2 in Asp169, OD1 in Asn170, the oxygen of HOH53, and both oxygens in the catechol moiety of the ligand) were frozen during minimization.

Molecular docking. In order to reduce the rotational degrees of freedom and to focus on the interactions of the selectivity and the reactivity functions with the protein, the Capture Compounds were modeled without the polyethylene glycole linker and the biotin moiety. Unrestrained flexible docking between COMT and Tcp-Bz-CC was performed with Surflex-Dock (Jain, 2003) included in the SYBYL package using the default settings. The cocrystallized ligand was extracted, and the protomol was generated based on the ligand. Twenty poses were sampled. The results were investigated for the correct binding of the catechol moiety in the binding pocket and the positioning of the cross-linking unit in vicinity of the protein surface, especially close to polar side chains. The polyethylene glycole linker and the biotin moiety (based on the PDB file with the accession number 1STP) were added manually and minimized using standard procedures.

COMT Affinity Assay

Bioanalytical services for the determination of 50% inhibitory concentration (IC_{50}) values were provided by MDS Pharma Services Inc. (Peitou, Taipei, Taiwan). IC_{50} equals the molar concentration of an antagonist, which produces 50% of the maximum possible inhibitory response for that antagonist.

Preparation of Cell Lysates and Rat Liver Subcellular Fractions

HepG2 cell lysate was purchased from InVivo Biotech (Berlin, Germany), and frozen rat livers were purchased from BLS Preclinical Services (Berlin, Germany). Fractionation of rat liver was carried out essentially as described (Emig *et al.*, 1995). Briefly, rat liver was homogenized using a motor-driven glass-Teflon homogenizer (Sartorius Stedim Biotech GmbH, Aubagne Cedex, France) in 10 volumes of homogenization buffer per gram of tissue wet weight (0.32M sucrose, 5mM 4-(2-hydroxyethyl)piperazine-1-ethanesulfonic acid [HEPES]/NaOH, pH 7.4, complete EDTA-free protease inhibitor cocktail [Roche, Mannheim, Germany]) using 12 strokes at 900 rpm at 4°C. The homogenate was centrifuged at 1000 × g (Universal 300R centrifuge; Hettich Centrifuges, Beverly, MA) for 10 min. The supernatant was decanted and further centrifuged at 12,000 × g for 20 min. The supernatant (soluble fraction, cytosol) from this procedure was concentrated using iCon Concentrators (Thermo Fisher Scientific, Schwerte, Germany), aliquoted, and snap frozen. The protein concentration was determined according to Bradford (1976). The pellet was resuspended in 0.32M sucrose (30 × weight in grams) and further homogenized in a motor-driven glass-Teflon homogenizer (Potter S; Sartorius Stedim Biotech GmbH) using six strokes at 900 rpm at 4°C. The suspension was centrifuged again at 12,000 × g for 20 min. The pellet was resuspended in 0.25M sucrose and Tris-HCl, pH 8.1, using six strokes at 900 rpm and carefully placed on top of a sucrose solution with 1.5M sucrose. The sample was centrifuged at 90,000 × g for 1 h in an ultracentrifuge (WX-80 Ultra, Rotor TH641; Thermo Fisher Scientific).

Microsomes were recovered from the interphase between the 0.25M and 1.5M sucrose solutions, while mitochondria were pelleted. These fractions were each solubilized for 1 h at room temperature using cell-opening buffer (6.7mM 4-morpholineethanesulfonic acid, 6.7M sodium acetate, 6.7mM HEPES, 200mM NaCl, 10mM β-mercaptoethanol, pH 7.6) and supplemented with complete protease inhibitor (Roche) and 0.5% dodecylmatoside. Subsequently, the suspensions were cleared by centrifugation at 10,000 rpm for 15 min. The protein concentrations of the supernatants were determined according to Bradford (1976).

Capturing Experiment in HepG2 and Rat Liver Subcellular Fractions

Capture experiment. HepG2 cell lysate (0.4 mg) was supplemented with 20 µl of 5× capture buffer (Caprotec Bioanalytics GmbH, Berlin, Germany) (100mM HEPES, 250mM potassium acetate, 50mM magnesium acetate, and 50% glycerol), and the reaction volume was adjusted to 100 µl with ultrapure water. Capture beads were obtained by vigorously mixing 25 µl of the respective Capture Compound or scaffold (100µM) with 50 µl of Dynabeads MyOne Streptavidin C1 (Invitrogen, Karlsruhe, Germany) at room temperature for 5 min. After washing twice with wash buffer (Caprotec Bioanalytics GmbH) (WB, containing 50mM Tris-HCl, pH 7.5, 1mM EDTA, 1M NaCl, 0.5µM octyl-β-D-glucopyranoside), the respective magnetic capture beads were added to the reaction mix and rotated at 4°C for 3 h with protection from light. Subsequently, the reaction mixture was irradiated using the caproBox (Caprotec Bioanalytics GmbH). The characteristics of the caproBox are as follows: capture temperature 0.5°C–4°C, λ = 275–375 nm with λ_{max} = 312 nm, irradiance I_e 10–12 mW/cm^2, and irradiation energy for each sample (15 mm^2 irradiation area of the closed tube and 10 mm height of the reaction mixture) ~1.4 J. Irradiation with the caproBox was carried out for 20 min, with mixing at intervals of 2.5 min. After ultraviolet (UV) light exposure, the beads were collected using the caproMag, a device for handling of magnetic beads (Caprotec Bioanalytics GmbH), and washed first six times with 200 µl WB and then twice with ultrapure water. Until further analysis, beads were stored at 4°C in ultrapure water.

For capture experiments using fractions of rat liver, the initial protein amounts in the capture reactions were 0.4 mg for mitochondrial or microsomal fraction and 1.4 mg in case of the cytosolic fraction, respectively. Capture buffer and WB were supplemented with 0.1% n-dodecyl-β-maltoside (Glycon, Luckenwalde, Germany).

SDS-Polyacrylamide Gel Electrophoresis

Subsequent to the capture experiments, the captured proteins with the covalently attached Capture Compounds are bound to the streptavidin beads via biotin-streptavidin interactions. To analyze the captured proteins by SDS-polyacrylamide gel electrophoresis (PAGE), the beads were resuspended in 7 µl Laemmli buffer (Laemmli, 1970) and heated to 95°C for 5 min. Subsequently, the beads were separated from the released proteins using a magnet. For comparability, sets of different Capture Compounds must be used in parallel with the same amount of protein starting material. The entire amount from one capture experiment was loaded in one lane (if not indicated otherwise). Consequently, Capture Compounds interacting with few proteins will show fewer bands on a gel than those interacting with many proteins. Gels were stained using the FireSilver Kit (Proteome Factory, Berlin, Germany) according to the manufacturer's instructions.

Western Blot

After separation by SDS-PAGE, captured proteins were transferred to a nitrocellulose membrane (Whatman, Kent, UK). Proteins were stained with Ponceau red (Sigma, Steinheim, Germany) to control the blotting efficiency (data not shown). The membrane was blocked for 1 h at room temperature with a solution of 5% (wt/vol) skimmed milk powder in Tris-buffered saline (20mM Tris-HCl, pH 7.5, 150mM NaCl [TBS], supplemented with 0.1% [vol/vol] Tween 20 [TBS-T]). Incubation with the primary antibody was performed for 1 h at room temperature or overnight at 4°C, followed by three wash steps in TBS-T and incubation with the secondary antibody for 1 h at room temperature. Antibodies were diluted in 5% skimmed milk powder in TBS-T as follows: anti-COMT 1:2500, secondary anti-goat antibody conjugated to horseradish peroxidase 1:2000. After three washes in TBS-T and one wash in TBS, membranes were treated with Pierce ECL Western Blotting Substrate (Thermo Fisher Scientific) according to the manufacturer's instructions. Hyperfilm ECL films (GE Healthcare, Muenchen, Germany) were used to detect the chemiluminescence. In case of blots for the detection of biotinylated proteins, streptavidin-horseradish peroxidase was used instead of a first antibody at a dilution of 1:1000 in 5% skimmed milk powder in TBS-T and blots were developed directly after washing three times with TBS-T and once with TBS.

In-Solution Digest

For analysis of the complex protein mixture obtained after capture experiments, the washed beads were resuspended in 10 µl 50mM ammonium bicarbonate and 1 µl trypsin (0.5 µg/µl) (sequencing grade; Roche) for 16 h at 37°C on a thermoshaker (Eppendorf, Hamburg, Germany). Subsequently, tryptic peptides were desalted using Stage Tips (Proxeon Biosystems A/S, Odense, Denmark) and eluted according to the manufacturer's instructions. The eluate was evaporated to dryness in a miVac DNA vacuum centrifuge (Genevac, Ipswich, UK) and stored at −20°C until mass spectrometric analysis.

In-Gel Digestion

Silver-stained gels were washed twice for 10 min with LC-MS grade water. Gel bands were excised, cut into small pieces, and washed twice with each 100 µl water and 100 µl 50% ethanol (vol/vol). Gel bands were shrunk with 50 µl 100% ethanol for ~5 min. Subsequently, the washing and shrinking steps were repeated. Protein digestion was carried out by rehydration of bands for 20 min on ice with 12.5 ng/µl of trypsin solution in 50mM NH_4HCO_3 and subsequent incubation for 16 h at 37°C. The extraction of peptides was carried out in two consecutive steps by incubating the gel pieces with 50% acetonitrile (ACN) with 2.5% formic acid (FA) for 15 min. The pooled supernatants were then dried in a miVac DNA vacuum centrifuge (Genevac). Desalting, elution, evaporation, and storage of tryptic peptides were performed as described for in-solution digested samples.

Nano LC-MS/MS

The protein digest was redissolved in 5 µl of 5% FA. Subsequently, peptides were loaded onto a nanoflow Biosphere C_{18} precolumn (5 µm, 120 Å, 20 × 0.1 mm; Nanoseparation, Nieuwkoop, the Netherlands) coupled to a nanoflow Biosphere C_{18} analytical column (5 µm, 120 Å, 105 × 0.075 mm). The experiments were performed on an Easy-nLC liquid chromatography system (Proxeon Biosystems A/S) connected to an LTQ Orbitrap XL Mass Spectrometer (Thermo Electron, Bremen, Germany) utilizing a nanoelectrospray ion source (Proxeon Biosystems A/S). For the analysis of in-solution digest samples, peptides were eluted during an 80-min linear gradient from 5% ACN/0.1% FA to 40% ACN/0.1% FA, followed by an additional 2-min increase to 100% ACN/0.1% FA and remaining at 100% for another 8 min with a controlled flow rate of 300 nl/min.

For the analysis of extracted gel bands, a linear 40-min gradient increasing from 5% ACN/0.1% FA to 40% ACN/0.1% FA, followed by an additional 2-min increase to 100% ACN/0.1% FA and remaining at 100% for another 8 min with a controlled flow rate of 300 nl/min was used.

The mass spectrometric analysis was performed in the data-dependent mode to automatically switch between orbitrap-MS and LTQ-MS/MS (MS^2) acquisition. The mass spectrometer duty cycle was controlled by setting the injection time automatic gain control. Survey full-scan MS spectra (from m/z 400–2000) were acquired in the orbitrap with a resolution of $r = 60{,}000$ at m/z 400 (after accumulation to a target value of 500,000 charges in the linear ion trap). The most intense ions (up to five. depending on signal intensity) were sequentially isolated for fragmentation in the linear ion trap using collision-induced dissociation (CID) at a target value of 10,000 charges. The resulting fragment ions were recorded in the LTQ.

For accurate mass measurements in the MS mode, the singly charged polydimethylcyclosiloxane background ion $(Si(CH_3)_2O)_6H^+$ (m/z 445.120025) generated during the electrospray process from ambient air was used as lock mass for real-time internal recalibration. Target ions already mass selected for CID were dynamically excluded for the duration of 60 s. Charge-state screening and rejection of ions for CID with unassigned charge state were set. Further mass spectrometric settings were as follows: Spray voltage was set to 1.7 kV, temperature of the heated transfer capillary was set to 200°C, and relative normalized collision energy was 35% for MS^2. The minimal signal required for MS^2 was 500 counts. An activation $q = 0.25$ and an activation time of 30 ms were applied for MS^2 acquisitions. After each analysis of an in-solution digest sample, the system was washed by performing at least one linear gradient that was used for the respective peptide separation.

Peptide Identification via Database Search

Proteins were identified by automated database searching against the UniProtKB/Swiss-Prot (release 56.5) database using SEQUEST implemented in Bioworks 3.3.1 SP1 (Thermo Fisher Scientific). Specific search parameters used in the SEQUEST analyses were 5-ppm precursor tolerance, 1-amu fragment ions tolerance, and full trypsin specificity allowing for up to two missed cleavages. Phosphorylation at serine, threonine, and tyrosine; oxidation of methionines; deamidation of asparagines and glutamine; acetylation at lysine and serine; formylation at lysine; and methylation at arginine, lysine, serine, threonine, and asparagine were allowed as variable modifications. No fixed modifications were used in the database search.

The SEQUEST peptide identifications were required to satisfy minimum XCorr values of 2, 2.5, and 3 for singly, doubly, and triply charged peptides, respectively; a minimum ΔCn of 0.1; and a peptide probability ≥ 0.001. Peptides fulfilling these criteria were accepted for analysis without further validation. The estimated percentage of false discovery peptide identifications was determined using the reversed protein database approach and was < 1%.

RESULTS

Design of Capture Compounds

Tolcapone and entacapone are potent inhibitors of COMT for the treatment of Parkinson's disease. The catechol groups of these drugs compete with dopamine for coordination of the catechol moiety with the magnesium ion in the COMT-binding pocket (Bonifacio *et al.*, 2007). While tolcapone is much more efficacious than entacapone in raising dopamine levels in the brain, tolcapone is well known for serious side effects, limiting its therapeutic utility. In particular, tolcapone was temporarily withdrawn due to the drug's implication in fulminant liver failure and the consequent death of three patients; now monitoring of liver enzymes is mandatory during drug treatment (Unger *et al.*, 2008).

In order to investigate the molecular mechanisms underlying the cause of tolcapone's hepatotoxicity, we designed Capture Compounds containing tolcapone and entacapone as selectivity functions, respectively (Fig. 2). With these Capture Compounds, we aimed to identify the proteins interacting with tolcapone and entacapone, respectively, thereby identifying interactions that are potentially related to tolcapone's underlying hepatotoxicity. To ensure optimal interaction of the selectivity and the photoreactivity groups with the target protein, molecular docking studies were carried out and the molecular design was adjusted accordingly. Figure 3 shows a molecular model visualizing the interaction between COMT and the tolcapone Capture Compound with accessible catechol moiety (Tcp-Bz-CC). The model showed that the catechol moieties were expected to target the binding pocket, whereas the amide residue of entacapone and the benzylic side of tolcapone protruded outside the protein and pointed in opposite direction of the catechol group. Due to the preferred mechanisms of the cross-linking reaction, the linker between the selectivity and the reactivity groups had to ensure a position of the photoreactivity group close to polar side chains on the protein surface. We observed a 100-fold reduction of the affinity of the entacapone Capture Compound Ecp-Am-CC

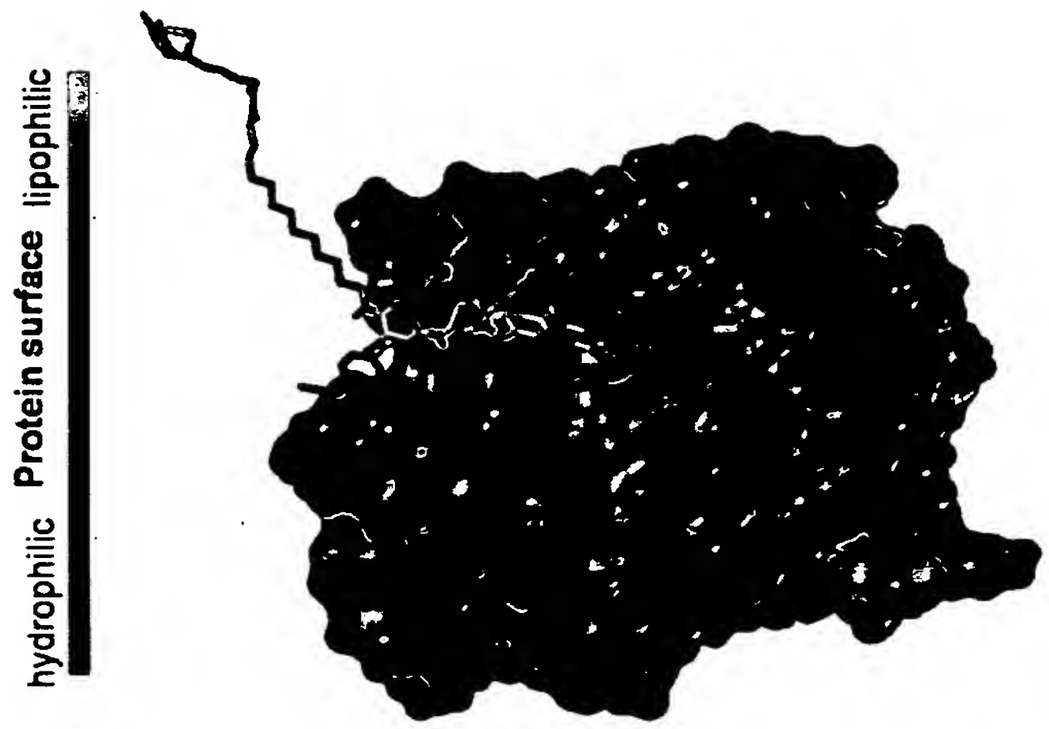

FIG. 3. Docking of the tolcapone Capture Compound with free catechol moiety (Tcp-Bz-CC) into the dopamine-binding pocket of COMT. The surface of COMT is colored according to the lipophilic potential. The catechol group of tolcapone is nestled into the lipophilic COMT crevice, while the photoreactivity group (magenta) is positioned close to polar side chains on the protein surface and the biotin-sorting function with linker (orange) protrudes from the protein.

compared to entacapone and concluded that the model may not show the entire picture. It is possible that the linker might play an important role and due to its flexibility cannot be modeled perfectly.

Different parts of a drug may produce different interactions with cellular proteins inducing different responses. Thus, we chose two points of attachment for each drug to the scaffold (Fig. 2, **1**). In one set, we used the catechol moiety responsible for the interaction with COMT as attachment point (**2**, Tcp-Ct-CC, and **6**, Ecp-Ct-CC, Fig. 2). In addition, we linked the drugs at the opposite end via the benzylic or the amino group, respectively (**5**, Tcp-Bz-CC, and 7, Ecp-Am-CC, Fig. 2). As a result, different pharmacophoric elements of entacapone and tolcapone were presented to the complex protein mixtures tested. As a control, the Capture Compound without selectivity group (scaffold) was used.

The design of the Capture Compounds was carried out with the aim that for one attachment position, the Capture Compound functionalities should not interfere with the interaction between the drug and its known target COMT. In case of entacapone, the Capture Compound with attachment via the amino group should be able to bind COMT as the original drug. To verify the quality of our molecular design, we commissioned standard affinity measurements between three of the Capture Compounds and the purified target protein COMT. Published K_D values for the affinity of the drug entacapone to COMT vary by one order of magnitude between 0.3nM (Bonifacio *et al.*, 2007) and 10nM (Tervo *et al.*, 2003). We determined the IC_{50} of the entacapone drug to be 430nM for the entacapone Capture Compound Ecp-Am-CC (Supplementary data). As outlined above, the reduction of affinity is probably due to the linker properties and its lack of affinity to the proteins. As expected, Capture Compounds with the reversed architecture in which the drugs were linked by the catechol had no affinity to COMT. Their IC_{50} were larger than 10,000nM. We performed the experiments at concentrations that were about 10-fold to 20-fold higher than the IC_{50}. This is a C_{max} aimed for in drug development. Our results demonstrate that although the attachment of the Capture Compound scaffold may lead to a reduction of affinity, entacapone is still able to effectively bind COMT—the pharmacophoric properties of the drug are retained.

Validation of the CCMS Approach with Soluble Rat Liver Proteins

In order to demonstrate the validity of the CCMS approach, we first tested our Capture Compounds in the cytosolic fraction of rat liver, which shows a reduced protein complexity compared to whole-cell lysates. We used rat liver lysates due to the availability of healthy rat organs and used the cytosolic fraction to demonstrate the effectiveness of our methodology. Other fractions of the lysates were used as well to explore which proteins interact with the drug. UV irradiation induces a covalent bond between the reactivity function of the Capture Compound and the protein interacting with the drug. As the Capture Compound contains a biotin moiety (sorting function), interacting proteins become biotinylated by irreversible cross-link to the Capture Compound during the capture process and can be not only isolated by streptavidin beads but also detected in an anti-biotin (i.e., streptavidin) Western blot (Fig. 4A), demonstrating the covalent bond to the Capture Compound. By SDS-PAGE and silver staining (Fig. 4B), all isolated proteins were visualized. In classic pull-down experiments, frequently background proteins are isolated that do not interact with the selectivity group, but stick to the beads, or are only interaction partners of proteins that directly bind the selectivity group. In capture experiments, direct binders of the selectivity group will form covalent bonds with the Capture Compounds and can be visualized in the anti-biotin Western blot. Unspecific background proteins should be visible in the silver-stained gel however; they should not be visible in the anti-biotin Western blot. Comparison of Figures 4A and 4B shows that all protein bands visualized in the silver-stained SDS-PAGE are also visible in the anti-biotin Western blot. Consequently, the comparison of silver-stained SDS-PAGE and anti-biotin Western blot clearly shows that the isolated proteins were indeed covalently bound to the biotin-containing Capture Compounds. Western blots directed against the COMT protein (Fig. 4C) demonstrated that the target is indeed captured and—comparing Figures 4A and 4C—covalently bound. Analysis of the respective samples by mass spectrometry in addition to Western blots revealed the unambiguous and reproducible isolation and identification of the known drug target COMT with the Capture Compounds containing the free

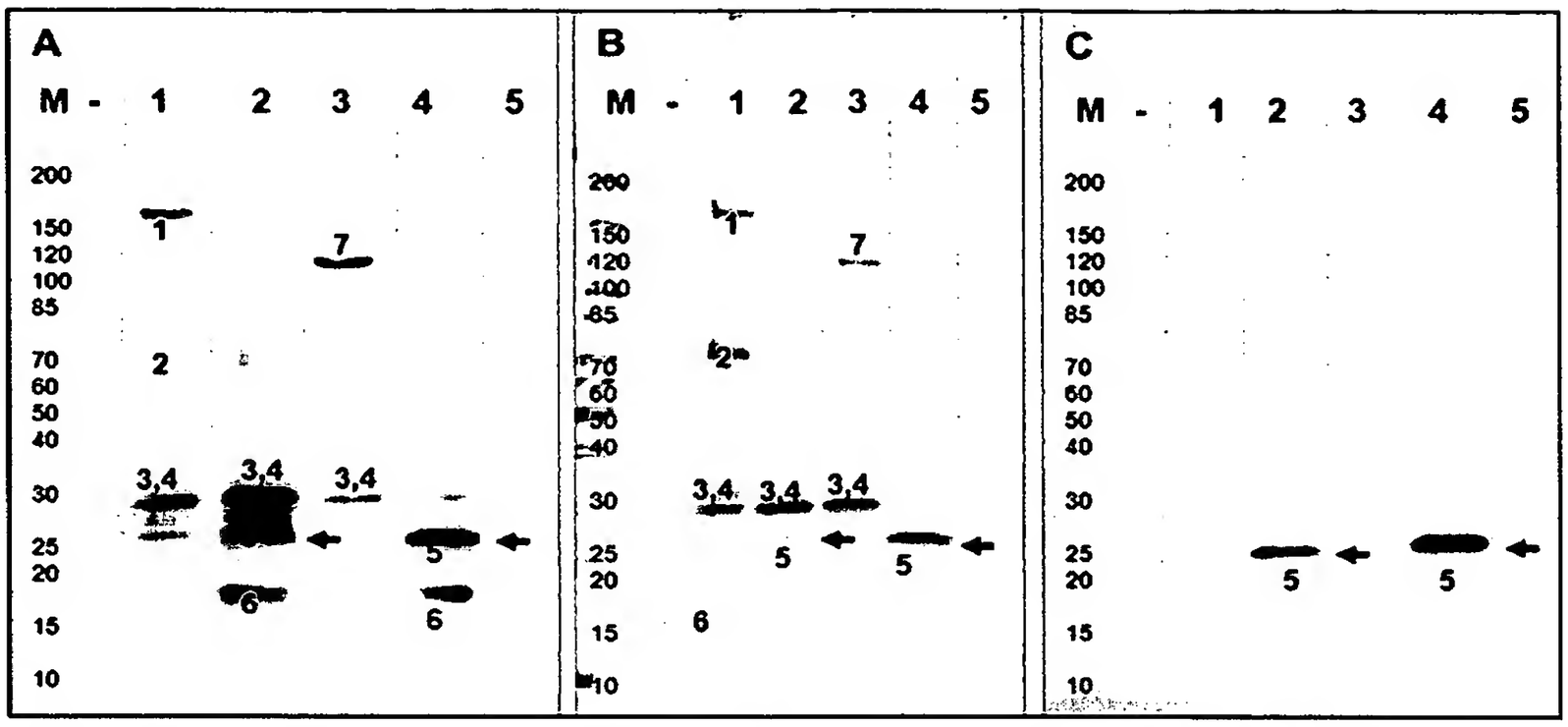

FIG. 4. Identification of COMT and off-target proteins by capturing in the soluble fraction of rat liver. One capture experiment per capture compound was carried out in parallel, starting with 1.4 mg protein each. For each Capture Compound, the captured proteins were released from the beads by boiling in gel loading buffer and then split into three equal aliquots. With one aliquot, a streptavidin-peroxidase Western blot (A) was carried out, demonstrating covalent cross-link between Capture Compound and protein interaction partners. With the second aliquot, an SDS-PAGE was carried out and silver stained (B), showing all released proteins. With the third aliquot, an anti-COMT Western blot (C) was carried out, demonstrating that Capture Compounds with free catechol moiety capture COMT. The protein bands are indicated by numbers and are identified by the same numbers in Table 1. M, marker. Description of the gel lanes: The name of the Capture Compound and the number referring to the compound's structure in Figure 2 are given in brackets. 1, Tolcapone with free benzylic group (Tcp-Ct-CC1, 2); 2, tolcapone with free catechol group (Tcp-Bz-CC2, 5); 3, entacapone with free amide group (Ecp-Ct-CC1, 6); 4, entacapone with free catechol group (Ecp-Am-CC1, 7); 5, no selectivity function (scaffold, 1). Arrows indicate COMT.

catechol moiety (Tcp-Bz-CC and Ecp-Am-CC) (Table 1), while compounds with attachment at the opposite end (Tcp-Ct-CC and Ecp-Ct-CC) did not bind COMT, as expected. These, however, presented different pharmacophoric elements of the drugs to the protein mixture and allowed capturing of proteins that interacted with these elements of the drugs.

Notably, the tolcapone Capture Compounds interacted with bile salt sulfotransferase (ST2A1) and alcohol sulfotransferase A (ST2A2), independently of the attachment point (Tcp-Bz-CC and Tcp-Ct-CC, Figs. 4A and 4B, lanes 1 and 2). Due to the very similar molecular weight, the two sulfotransferases comigrated in SDS-PAGE but were unambiguously identified by mass spectrometry. An interaction with these proteins was also observed with the entacapone Capture Compound linked via the catechol moiety (Ecp-Ct-CC, Figs. 4A and 4B, lane 3) but not or to a much lower extent with the amide-linked entacapone Capture Compound (Ecp-Am-CC, Figs. 4A and 4B, lane 4). ST2A1 and ST2A2 belong to the group of cytosolic sulfotransferases, phase II detoxification enzymes involved in the biotransformation of a wide variety of structurally diverse endo- and xenobiotics, including many therapeutic agents and endogenous steroids (Nowell and Falany, 2006). Binding of both drugs by these enzymes is in accordance with the rather unspecific role of the sulfotranferases in detoxification processes (Nowell and Falany, 2006). As the scaffold control did not show this interaction, we suggest that the binding of sulfotranferases with both Capture Compounds is likely to reflect the physiological detoxification

TABLE 1

Proteins Captured by Tolcapone and Entacapone in the Soluble Protein Fraction of Rat Liver. The Corresponding Silver-Stained SDS-PAGE is Shown in Figure 4. Processes are Given as Retrieved from SwissProt Annotation via http://www.expasy.org

Gel band	Abbreviation	Name	Molecular weight (kDa)	Accession	Cellular process
1	CLH	Clathrin heavy chain 1	191	P11442	Endocytosis
2	DHB4	Peroxisomal multifunctional enzyme type 2	79	P97852	Fatty acid β-oxidation
2	ACOX3	Peroxisomal acyl-coenzyme A oxidase 3	78	Q63448	Fatty acid β-oxidation
3	ST2A2	Alcohol sulfotransferase A	33	P22789	Detoxification
4	ST2A1	Bile salt sulfotransferase	33	P15709	Detoxification
5	COMT	Catechol *O*-methyltransferase	30	P22734	Dopamine degradation
6	HBB1	Hemoglobin subunit beta-1	16	P02091	Oxygen transport
6	HBA	Hemoglobin subunit alpha-1/2	15	P01946	Oxygen transport
7	PYC	Pyruvate carboxylase	130	P52873	Krebs cycle

pathway of these two compounds. Indeed, it has been shown previously that tolcapone is metabolized by sulfation (Jorga *et al.*, 1999).

The Capture Compounds with free catechol moiety exposed to the cytosol showed, apart from the sulfotransferases, strong and specific interaction only with the target protein COMT. Similarly, the entacapone Capture Compound Ecp-Am-CC1 revealed no interaction except for the sulfotransferases. However, the tolcapone Capture Compounds with attachment via the catechol group (Tcp-Ct-CC1) revealed additional interacting proteins in the cell lysate. Notably, additional peroxisomal proteins were captured. Peroxisomal acyl-coenzyme A oxidase 3 (ACOX3) and peroxisomal multifunctional enzyme type 2 (DBH4, also MFP-2 or MFE-2) play essential roles in fatty acid β-oxidation. The phenotypical data (Baes *et al.*, 2000; Huyghe *et al.*, 2006b; Yu *et al.*, 2003) associated with the two captured peroxisomal enzymes suggest that tolcapone-related side effects may be partly due to the interaction of these enzymes with tolcapone (see "Discussion" section). These off-target proteins could only be identified using the tolcapone Capture Compounds attached via the phenolic group, confirming the importance of several different attachment points. Moreover, these results gave an initial indication that CCMS can indeed identify the molecular basis of drug side effects in general and tolcapone in particular.

Tolcapone Interacts with Components of the Respiratory Chain

In order to reveal the mode of hepatotoxic action of both tolcapone and entacapone in the human liver, we performed capture experiments in whole-cell lysates of the human hepatocyte cell line HepG2. As the chemical structure of entacapone and tolcapone at the catechol end is identical and the pilot experiments using cytosolic rat liver fractions suggested that primarily tolcapone attached via the catechol group captures relevant off targets, we decided to focus on compounds with this attachment point. To generate a comprehensive coverage of drug-protein interactions, we designed two additional Capture Compounds differing in the linker length between the drug molecule and the reactivity group (**3** and **4**, Tcp-Ct-CC, Fig. 2).

Capture experiments in HepG2 whole-cell lysates revealed that tolcapone Capture Compounds, independent of linker length, interacted with a large number of different proteins in the cell, while entacapone Capture Compounds showed relatively few interactions, independent of the attachment point. As expected, even fewer proteins were found when capturing was performed with the scaffold control (Fig. 5A). LC-MS/MS analysis of the respective complex protein mixtures led to the identification of the tolcapone and entacapone interaction partners. Proteins identified in the control experiment with scaffold were excluded from further analysis. We established the overlap between the captured proteins to classify the interaction partners of the respective drugs. The tolcapone compounds captured a total of 124 proteins; with the entacapone Capture Compounds, however, only 20 proteins were identified (full protein lists are given in the Supplementary data: table of LC-MS/MS results). While some proteins were captured exclusively by one Capture Compound, the majority of proteins were captured independent of the linker length and thus considered as interaction partners with highest confidence. For an overall functional classification of the proteins, we performed Gene Ontology (Ashburner *et al.*, 2000) annotation via BioMart (Smedley *et al.*, 2009) of the ENSEMBL Genome Browser (http://www.ensembl.org, build 52 NCBI63) according to cellular component terms.

For the 20 proteins specifically captured with the entacapone Capture Compounds, the cellular distribution could not be linked in a straightforward way to mitochondrial function and toxicity based on literature. However, in case of tolcapone, a considerably large proportion of the 124 captured proteins were assigned to the mitochondria (Fig. 5B) and, in particular, within the mitochondrial membrane. To gain deeper insight into the role of the captured proteins in metabolism, we then carried out a Kyoto Encyclopedia of Genes and Genomes pathway (Aoki and Kanehisa, 2005) analysis via the Database for Annotation, Visualization and Integrated Discovery (DAVID, V6, 2008, http://david.abcc.ncifcrf.gov/) (Dennis *et al.*, 2003). We found that the captured proteins are essential components of the respiratory chain, the bile acid synthesis, and peroxisomal fatty acid β-oxidation. Enzymes functioning in bile acid synthesis and peroxisomal fatty acid β-oxidation are in accordance with the results obtained from the soluble fraction of rat liver. In particular, the human homolog of ACOX3 was again reproducibly captured, implicating a possible impact on fatty acid β-oxidation by tolcapone in humans. In a previous study, focally mild microvesicular steatosis was observed (Assal *et al.*, 1998). Our finding may hint at the mechanism that could underlie steatosis induction. Notably, the captured mitochondrial proteins contained subunits from each of the complex in the respiratory chain (Fig. 5C), e.g., eight subunits of ATP synthase. While nearly all subunits were captured by two or three of the tolcapone Capture Compounds, none were isolated by entacapone Capture Compounds. The comparison to the structurally similar but far less toxic drug entacapone suggests that the observed tolcapone-protein interactions are a possible cause of its toxicity. Further experiments should clarify to what extent this contributes to the overall toxicity of the compound. Publications by Haasio *et al.* (2002a,b) showed unambiguously that tolcapone in contrast to entacapone produces symptoms in rats that are typical for decoupling agents of the respiratory chain. Our results are in very good agreement with these *in vivo* observations.

Detailed Analysis of Proteins Interacting with Tolcapone in Rat Liver Mitochondria and Microsomal Fractions

To investigate the interaction partners of tolcapone in mitochondria and peroxisomes in detail, we carried out capture experiments in the mitochondria and microsomal fractions of

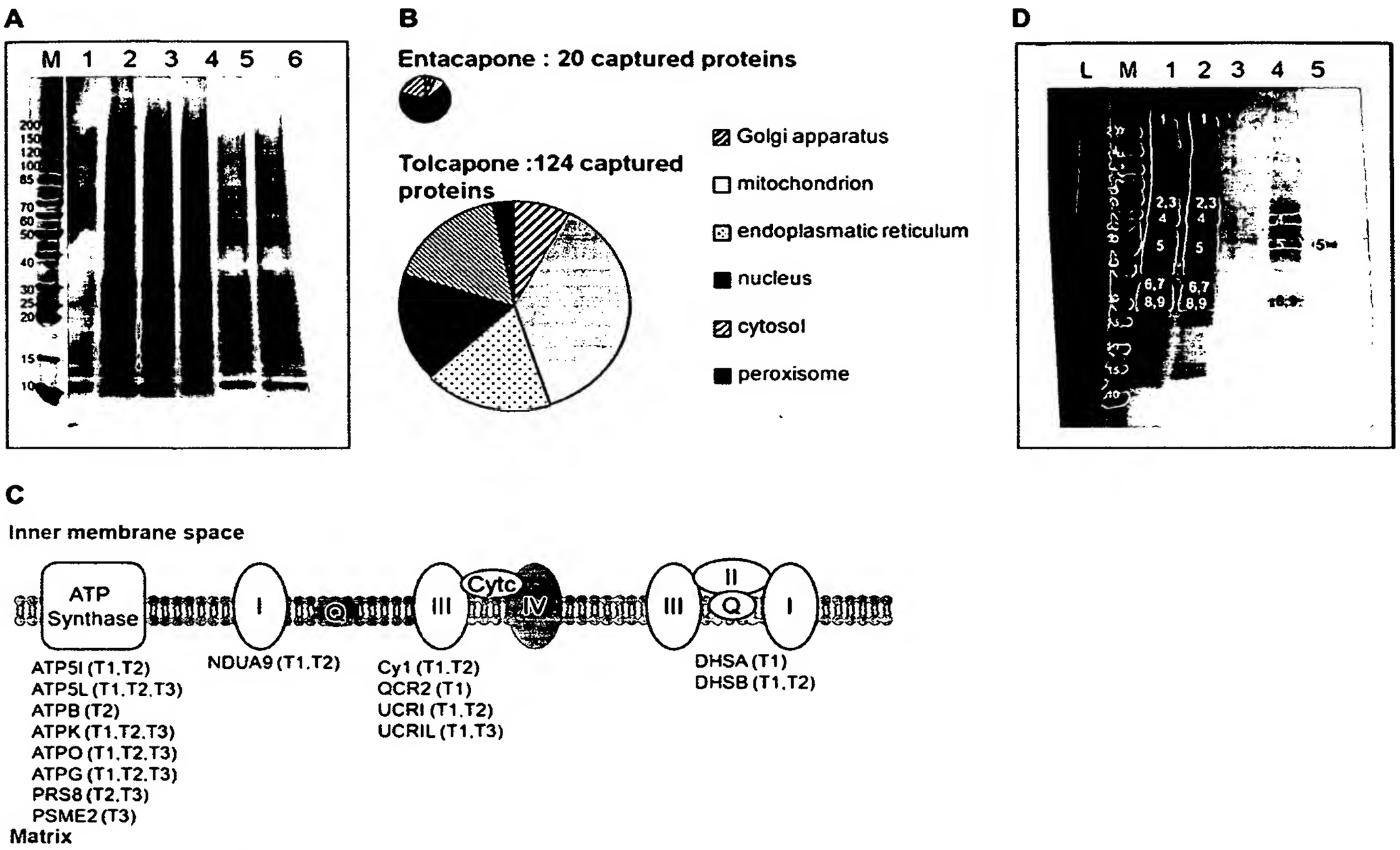

FIG. 5. Tolcapone interacts with components of the respiratory chain and fatty acid β-oxidation. (A) Capturing in HepG2 lysate shows high number of proteins interacting with tolcapone (lanes 2–4) compared to entacapone Capture Compounds (lanes 5 and 6) and even less for the Capture Compound scaffold (lane 1). Each capture experiment was carried out starting from 0.4 mg material, the capture experiments with the different Capture Compounds were carried out in parallel, and all proteins captured in one experiment were loaded onto the gel. (B) Mapping of gene ontologies revealed the localization to interacting proteins in the cellular compartments. A large proportion of proteins interacting with tolcapone is located in the mitochondria and includes members of the respiratory chain (C). (D) Capturing in rat liver mitochondrial fraction enables the identification of tolcapone off targets in fatty acid β-oxidation. Each capture experiment was carried out starting from 0.4 mg material, the capture experiments with the different Capture Compounds were carried out in parallel, and the entire eluate of one experiment was loaded onto the gel. L, mitochondrial lysate. The identification of the proteins corresponding to the numbers indicating the bands in the gel is given in Table 2. M, marker. Description of the gel lanes: The name of the Capture Compound and the number referring to the compound's structure (bold) in Figure 2 are given in brackets. 1, Tolcapone with free benzylic group (Tcp-Ct-CC1, 2); 2, tolcapone with free catechol group (Tcp-Bz-CC2, 5); 3, no selectivity function (scaffold, 1); 4, entacapone with free amide group (Ecp-Ct-CC1, 6); 5, entacapone with free catechol group (Ecp-Am-CC1, 7).

rat liver. In both preparations, we again found that tolcapone Capture Compounds capture significantly more proteins than the respective entacapone compounds. Consistent with the results described above, we identified key enzymes of the fatty acid β-oxidation pathway, such as peroxisomal multifunctional enzyme type 2, peroxisomal acyl-coenzyme A oxidase 3, and the long chain fatty acid-CoA ligase 1, which is found both in the mitochondrial and peroxisomal membranes as specific interaction partners of tolcapone with the potential to induce side effects (Fig. 5D, Table 2).

DISCUSSION

Tolcapone and entacapone are potent inhibitors of COMT for the treatment of Parkinson's disease (Schapira *et al.*, 2000). Although these two drugs are similar, and even structurally identical with respect to the COMT-binding moiety, they show a number of pharmacological differences and thus different clinical effectiveness (Deane *et al.*, 2004). A recent Cochrane meta-analysis of 14 studies in 2566 patients (Deane *et al.*, 2004) found both drugs to be statistically superior to placebo in increasing "on" time and decreasing "off" time. Furthermore, tolcapone was found to have an approximately twice as long therapeutic effect compared to entacapone. This difference is reflected by the pharmacological profile, where tolcapone is characterized by greater bioavailability and higher COMT affinity. Tolcapone increases the half-life of the dopamine precursor levodopa by 80 versus 40% for entacapone (Factor, 2008). However, a significant number of patients treated with

TABLE 2
Proteins Captured by Tolcapone and Entacapone in Solubilized Mitochondrial and Microsomal Fractions of Rat Liver. Corresponding Protein Bands are Depicted in Figure 5D. Processes are Given as Retrieved from SwissProt Annotation via http://www.expasy.org

Gel band	Abbreviation	Name	Molecular weight (kDa)	Accession	Cellular process
1	CLH	Clathrin heavy chain 1	193	P49951	Endocytosis
2	DHB4	Peroxisomal multifunctional enzyme type 2	80	P97852	Fatty acid β-oxidation
3	ACSL1	Long chain fatty acid-CoA ligase 1	79	P18163	Fatty acid metabolism
4	ACOX3	Peroxisomal acyl-coenzyme A oxidase 3	79	Q63448	Fatty acid β-oxidation
5	DHE3	Glutamate dehydrogenase 1, mitochondrial	62	P10860	Glutamate catabolism
6	ARHL1	Protein ADP-ribosylarginine hydrolase-like protein 1	40	Q5XIB3	Protein-amino acid deribolysation
7	DHB13	17-beta hydroxysteroid dehydrogenase 13	34	Q5M875	Oxidation/reduction
8	AUHM	Methylglutaconyl-CoA hydratase, mitochondrial	34	Q9JLZ3	Branched amino acid catabolism
9	ECHM	Enoyl-CoA hydratase, mitochondrial	32	P14604	Fatty acid β-oxidation

tolcapone show disturbed levels of liver enzymes, and in 1998, even three patient fatalities attributed to tolcapone-induced hepatotoxicity were reported (Deane *et al.*, 2004).

In this study, we have used the CCMS technology to elucidate the molecular basis of the difference in the protein-binding profiles between Capture Compounds of tolcapone and entacapone. We have used protein fractions obtained from rat liver as well as lysates of the human hepatocyte cell line HepG2 and obtained consistent results. The conditions used in the preparation of the lysates were chosen to ensure that the membrane protein complexes were solubilized but still native, i.e., nondenaturing conditions were chosen. The application of the CCMS technology reproducibly and unambiguously demonstrated that besides binding the actual target (COMT), tolcapone Capture Compounds interact with a large number of proteins carrying out essential functions in the respiratory chain, fatty acid β-oxidation, and bile acid synthesis. In the liver, fatty acids are metabolized by β-oxidation in mitochondria and peroxisomes and by ω-oxidation in microsomes. Peroxisomal β-oxidation is responsible for the metabolism of very long chain fatty acids. Impairment of correct peroxisomal function may lead to the accumulation of long fatty acids or of hydrogen peroxide through the peroxisomal oxidative reactions. Both mechanisms might contribute to the hepatotoxicity of tolcapone and help explain the side effects observed in animals and humans. Further studies including *in vivo* experiments are necessary to establish the connection between human toxicological events and the results of CCMS experiments.

ACOX3 belongs to the family of fatty acyl-CoA oxidases. It has been shown that mice lacking fatty acyl-CoA oxidases developed steatohepatitis, demonstrating the importance of this class of enzymes for proper liver function (Yu *et al.*, 2003). Peroxisomal multifunctional enzyme type 2 (MFP-2, also D-bifunctional protein, DHB4) has been described previously (Adamski *et al.*, 1995). It plays a central role in peroxisomal β-oxidation as it handles most, if not all, peroxisomal β-oxidation substrates (Huyghe *et al.*, 2006a). In humans, deficiency of this enzyme causes a severe developmental syndrome with abnormalities in several organs, leading to death within the first year of life (Huyghe *et al.*, 2006a). Accumulation of branched long chain fatty acids and very long chain fatty acids as well as a disturbed synthesis of bile acids were documented for these patients. Moreover, lack or mutations of DHB4 are a cause of D-bifunctional protein deficiency. The clinical manifestations of this deficiency are similar to those of disorders of peroxisomal assembly, including X-linked adrenoleukodystrophy, Zellweger cerebro-hepatorenal syndrome, and neonatal adrenoleukodystrophy (Wanders *et al.*, 1990; Watkins *et al.*, 1989). Premature death is observed in one-third of MFP-2 knockout mice, accompanied by more severe aberrations in bile acid metabolism and excessive accumulation of very long chain fatty acids in brain and liver (Baes *et al.*, 2000; Huyghe *et al.*, 2006b).

Besides potential interference with β-oxidation, our results show that tolcapone Capture Compounds interact with proteins of the inner mitochondrial membranes and with components of the respiratory chain. Although insertion of tolcapone into the mitochondrial membrane was not shown directly, the results demonstrate that tolcapone interacts with proteins localized within the membrane. A molecular mechanism in which tolcapone compromises the function of the respiratory chain is in accordance with cell physiological data reporting a decrease in membrane potential in the presence of tolcapone (Haasio *et al.*, 2002a), similar to the *bona fide* decoupling agent 2,4-dinitrophenol. A toxicological study (Haasio *et al.*, 2002b) in which rats were treated with either entacapone or tolcapone reported that no treatment-related findings were observed in entacapone-treated rats; however, animals treated with tolcapone showed increased respiration, decreased activity and drowsiness, and elevation of the rectal body temperature. Although the publications did not address liver toxicity

directly, our results shed light on the reported clinical and cell physiological observations in the study. Mitochondrial and peroxisomal proteins in the liver were identified as off-target proteins bound by tolcapone Capture Compounds. Indeed, the malfunction of the respiratory chain, fatty acid β-oxidation, or bile acid synthesis alone would likely lead to hepatotoxicity (Jaeschke *et al.*, 2002; Pessayre *et al.*, 1999).

After the first launch of tolcapone in Europe (EU) in 1997, three cases of fatal hepatic toxicity were found during postmarketing surveillance (Assal *et al.*, 1998). For this reason, marketing authorization for tolcapone was suspended in the EU in 1998 and labeling was tightened in the United States. Only in 2002, two studies by Haasio *et al.* (2002a,b) described *in vitro* and *in vivo* experiments in rats that point to a decoupling activity of tolcapone in the respiratory chain as explained above. By the application of CCMS technology, we could now, nearly 10 years after three patient fatalities, elucidate the molecular interactions underlying tolcapone's hepatotoxic potential and would certainly have triggered guided safety tests at the preclinical stage.

Several other hypotheses exist on the mechanism of tolcapone's hepatotoxicity. In particular, a correlation of elevated levels of liver transaminase in patients with single nucleotide polymorphisms in the UDP-glucoronidyl transferase 1A gene complex, an enzyme that contributes to the metabolization of tolcapone in the liver, has been reported (Acuna *et al.*, 2002). The authors suggested that impaired activity of UDP-glucoronidyl transferase rendered patients susceptible to hepatotoxic events caused by tolcapone. While this could be of value for the risk prediction for administration of tolcapone to individual patients, this finding does not explain the hepatotoxic potential of tolcapone in the first place. Rather, according to our findings, the primary cause for tolcapone's hepatotoxic potential may be at the level of off-target binding of the drug to proteins identified in our study. Another hypothesis is that tolcapone elicites idiosyncratic drug reactions through reactive metabolites formed from the original drug. They may involve the formation of reactive metabolites and may involve responses of the immune system (Dieckhaus *et al.*, 2002). This has been relatively well characterized in the case of the antiepileptic drug felbamate. Indeed, the formation of reactive metabolites from tolcapone *in vitro* under the experimental conditions chosen has been observed (Smith *et al.*, 2003), leading to the formation of covalent metabolite-glutathione adducts, which may cause glutathione depletion. However, in the study by Smith *et al.*, the formation of reactive metabolites was artificially favored. Although other modes of toxicity cannot be ruled out completely, in our study, we observed a direct binding of the drug to off-target proteins, which can be linked to the adverse effects observed in tolcapone-treated rats and in patients.

Proteins involved in drug side effects cannot be *a priori* predicted. Typical established tests for drug specificity and safety are restricted (1) to profiling the selectivity *in vitro* on a set of recombinantly expressed members of the protein family to which the desired drug target belongs. Or (2) safety assessments are only conducted with respect to an available range of phenotypic cell-based assays. Both approaches cannot cover all possible drug-protein interactions potentially leading to side effects and in particular fail to reveal the molecular identity of unanticipated off-target binders. CCMS provides a unique solution to fill exactly this vital technological gap in a direct, unbiased, and straightforward way. Although drug-protein interaction data do not directly prove that the physiological function of the proteins is compromised, the data directly define and guide further safety assessments. Furthermore, CCMS can be applied to native endogenous proteins from virtually any biological or clinical sample. The application of CCMS in preclinical drug development will help reducing costs by enabling faster GO/NO-GO decisions and will elucidate drug safety by pinpointing interactions that might lead to unwanted toxicological side effects at early stages.

SUPPLEMENTARY DATA

Supplementary data are available online at http://toxsci.oxfordjournals.org/.

ACKNOWLEDGMENTS

We thank Andrew Feinberg and Ernst Mutschler for fruitful discussions and critical reviews of the manuscript. The authors are employees of caprotec bioanalytics GmbH. Capture Compounds(TM) are a proprietary technology of caprotec bioanalytics GmbH.

REFERENCES

Acuna, G., Foernzler, D., Leong, D., Rabbia, M., Smit, R., Dorflinger, E., Gasser, R., Hoh, J., Ott, J., Borroni, E., *et al.* (2002). Pharmacogenetic analysis of adverse drug effect reveals genetic variant for susceptibility to liver toxicity. *Pharmacogenomics J.* **2,** 327–334.

Adamski, J., Normand, T., Leenders, F., Monte, D., Begue, A., Stehelin, D., Jungblut, P. W., and de Launoit, Y. (1995). Molecular cloning of a novel widely expressed human 80 kDa 17 beta-hydroxysteroid dehydrogenase IV. *Biochem. J.* **311**(Pt 2), 437–443.

Aoki, K. F., and Kanehisa, M. (2005). Using the KEGG database resource. *Curr. Protoc. Bioinformatics* Chapter 1, Unit 1.12.

Ashburner, M., Ball, C. A., Blake, J. A., Botstein, D., Butler, H., Cherry, J. M., Davis, A. P., Dolinski, K., Dwight, S. S., Eppig, J. T., *et al.* (2000). Gene ontology: tool for the unification of biology. The Gene Ontology Consortium. *Nat. Genet.* **25,** 25–29.

Assal, F., Spahr, L., Hadengue, A., Rubbia-Brandt, L., and Burkhard, P. R. (1998). Tolcapone and fulminant hepatitis. *Lancet* **352,** 958.

Axelrod, J., and Tomchick, R. (1958). Enzymatic O-methylation of epinephrine and other catechols. *J. Biol. Chem.* **233,** 702–705.

Baes, M., Huyghe, S., Carmeliet, P., Declercq, P. E., Collen, D., Mannaerts, G. P., and Van Veldhoven, P. P. (2000). Inactivation of the

peroxisomal multifunctional protein-2 in mice impedes the degradation of not only 2-methyl-branched fatty acids and bile acid intermediates but also of very long chain fatty acids. *J. Biol. Chem.* **275,** 16329–16336.

Bonifacio, M. J., Palma, P. N., Almeida, L., and Soares-da-Silva, P. (2007). Catechol-O-methyltransferase and its inhibitors in Parkinson's disease. *CNS Drug Rev.* **13,** 352–379.

Bradford, M. M. (1976). A rapid and sensitive method for the quantitation of microgram quantities of protein utilizing the principle of protein-dye binding. *Anal. Biochem.* **72,** 248–254.

Deane, K. H., Spieker, S., and Clarke, C. E. (2004). Catechol-O-methyltransferase inhibitors for levodopa-induced complications in Parkinson's disease. *Cochrane Database Syst. Rev.* **18,** CD004554.

Dennis, G., Jr., Sherman, B. T., Hosack, D. A., Yang, J., Gao, W., Lane, H. C., and Lempicki, R. A. (2003). DAVID: database for annotation, visualization, and integrated discovery. *Genome Biol.* **4,** P3.

Dieckhaus, C. M., Thompson, C. D., Roller, S. G., and Macdonald, T. L. (2002). Mechanisms of idiosyncratic drug reactions: the case of felbamate. *Chem. Biol. Interact.* **142,** 99–117.

Emig, S., Schmalz, D., Shakibaei, M., and Buchner, K. (1995). The nuclear pore complex protein p62 is one of several sialic acid-containing proteins of the nuclear envelope. *J. Biol. Chem.* **270,** 13787–13793.

Factor, S. A. (2008). Current status of symptomatic medical therapy in Parkinson's disease. *Neurotherapeutics* **5,** 164–180.

Haasio, K. (2003). Comparison of the hepatic safety of catechol-O-methyltransferase inhibitors entacapone and tolcapone with special reference to uncoupling of oxidative phosphorylation. Ph. D. Dissertation, University of Helsinki,Helsinki, Finland.

Haasio, K., Koponen, A., Penttila, K. E., and Nissinen, E. (2002a). Effects of entacapone and tolcapone on mitochondrial membrane potential. *Eur. J. Pharmacol.* **453,** 21–26.

Haasio, K., Nissinen, E., Sopanen, L., and Heinonen, E. H. (2002b). Different toxicological profile of two COMT inhibitors in vivo: the role of uncoupling effects. *J. Neural Transm.* **109,** 1391–1401.

Huyghe, S., Mannaerts, G. P., Baes, M., and VanVeldhoven, P. P. (2006a). Peroxisomal multifunctional protein-2: the enzyme, the patients and the knockout mouse model. *Biochim. Biophys. Acta* **1761,** 973–994.

Huyghe, S., Schmalbruch, H., Hulshagen, L., Veldhoven, P. V., Baes, M., and Hartmann, D. (2006b). Peroxisomal multifunctional protein-2 deficiency causes motor deficits and glial lesions in the adult central nervous system. *Am. J. Pathol.* **168,** 1321–1334.

Jaeschke, H., Gores, G. J., Cederbaum, A. I., Hinson, J. A., Pessayre, D., and Lemasters, J. J. (2002). Mechanisms of hepatotoxicity. *Toxicol. Sci.* **65,** 166–176.

Jain, A. N. (2003). Surflex: fully automatic flexible molecular docking using a molecular similarity-based search engine. *J. Med. Chem.* **46,** 499–511.

Jorga, K., Fotteler, B., Heizmann, P., and Gasser, R. (1999). Metabolism and excretion of tolcapone, a novel inhibitor of catechol-O-methyltransferase. *Br. J. Clin. Pharmacol.* **48,** 513–520.

Koster, H., Little, D. P., Luan, P., Muller, R., Siddiqi, S. M., Marappan, S., and Yip, P. (2007). Capture compound mass spectrometry: a technology for the investigation of small molecule protein interactions. *Assay Drug Dev. Technol.* **5,** 381–390.

Laemmli, U. K. (1970). Cleavage of structural proteins during the assembly of the head of bacteriophage T4. *Nature* **227,** 680–685.

Learmonth, D. A., Palma, P. N., Vieira-Coelho, M. A., and Soares-da-Silva, P. (2004). Synthesis, biological evaluation, and molecular modeling studies of a novel, peripherally selective inhibitor of catechol-O-methyltransferase. *J. Med. Chem.* **47,** 6207–6217.

Nowell, S., and Falany, C. N. (2006). Pharmacogenetics of human cytosolic sulfotransferases. *Oncogene* **25,** 1673–1678.

Olson, H., Betton, G., Robinson, D., Thomas, K., Monro, A., Kolaja, G., Lilly, P., Sanders, J., Sipes, G., Bracken, W., *et al.* (2000). Concordance of the toxicity of pharmaceuticals in humans and in animals. *Regul. Toxicol. Pharmacol.* **32,** 56–67.

Pessayre, D., Mansouri, A., Haouzi, D., and Fromenty, B. (1999). Hepatotoxicity due to mitochondrial dysfunction. *Cell Biol. Toxicol.* **15,** 367–373.

Schapira, A. H., Obeso, J. A., and Olanow, C. W. (2000). The place of COMT inhibitors in the armamentarium of drugs for the treatment of Parkinson's disease. *Neurology* **55,** S65–S71.

Schuster, D., Laggner, C., and Langer, T. (2005). Why drugs fail—a study on side effects in new chemical entities. *Curr. Pharm. Des.* **11,** 3545–3559.

Smedley, D., Haider, S., Ballester, B., Holland, R., London, D., Thorisson, G., and Kasprzyk, A. (2009). BioMart—biological queries made easy. *BMC Genomics* **10,** 22.

Smith, K. S., Smith, P. L., Heady, T. N., Trugman, J. M., Harman, W. D., and Macdonald, T. L. (2003). In vitro metabolism of tolcapone to reactive intermediates: relevance to tolcapone liver toxicity. *Chem. Res. Toxicol.* **16,** 123–128.

Tervo, A. J., Nyronen, T. H., Ronkko, T., and Poso, A. (2003). A structure-activity relationship study of catechol-O-methyltransferase inhibitors combining molecular docking and 3D QSAR methods. *J. Comput. Aided Mol. Des.* **17,** 797–810.

Unger, M. M., Reese, J. P., Oertel, W. H., and Eggert, K. M. (2008). Real-life evaluations of compliance with mandatory drug safety monitoring exemplified with tolcapone in Parkinson's disease. *Eur. Neurol.* **60,** 122–126.

Wanders, R. J., van Roermund, C. W., Schelen, A., Schutgens, R. B., Tager, J. M., Stephenson, J. B., and Clayton, P. T. (1990). A bifunctional protein with deficient enzymic activity: identification of a new peroxisomal disorder using novel methods to measure the peroxisomal beta-oxidation enzyme activities. *J. Inherit. Metab. Dis.* **13,** 375–379.

Watkins, P. A., Chen, W. W., Harris, C. J., Hoefler, G., Hoefler, S., Blake, D. C., Jr., Balfe, A., Kelley, R. I., Moser, A. B., Beard, M. E., *et al.* (1989). Peroxisomal bifunctional enzyme deficiency. *J. Clin. Invest.* **83,** 771–777.

Yu, S., Rao, S., and Reddy, J. K. (2003). Peroxisome proliferator-activated receptors, fatty acid oxidation, steatohepatitis and hepatocarcinogenesis. *Curr. Mol. Med.* **3,** 561–572.